

AD-A085 861 VON KARMAN INST FOR FLUID DYNAMICS RHODE-SAINTE-GENESE--ETC F/6 18/9
NUMERICAL STUDY OF FORMATION OF THERMAL NON UNIFORMITIES IN ACT--ETC(U)
JUN 78 M HILL, J BUCHLIN AFOSR-78-3584

UNCLASSIFIED VKI-1978-12

EOARD-TR-79-1

NL

1 or 1
200-400

END
DATE FILMED
8-80
DTIC

ADA 085861

REPORT DOCUMENTATION PAGE		READ INSTRUCTIONS BEFORE COMPLETING FORM
1. Report Number (8) FOARD TR-79-1	2. Govt Accession No. ADA083-861	3. Recipient's Catalog Number
4. Title (and Subtitle) NUMERICAL STUDY OF FORMATION OF THERMAL NON UNIFORMITIES IN ACTIVE PACKED BEDS.		5. Type of Report & Period Covered Final Report.
		6. Performing Org. Report Number (14) VKI-1978-12
7. Author(s) (10) Myron Hill and J-M Buchlin		8. Contract or Grant Number (15) AFOSR-78-3584
9. Performing Organization Name and Address von Karman Institute for Fluid Dynamics Chaussée de Waterloo, 72 1640 Rhode Saint Genese Belgium		10. Program Element, Project, Task Area & Work Unit Numbers 61102F (16) 2301-D1
11. Controlling Office Name and Address European Office of Aerospace Research and Development Box 14 FPO New York 09510		12. Report Date (11) June 1978
14. Monitoring Agency Name and Address European Office of Aerospace Research and Development Box 14 FPO New York 09510		15. THIS WORK WAS SPONSORED BY THE UNITED STATES AIR FORCE THE WORK WAS PERFORMED BY THE VON KARMAN INSTITUTE FOR FLUID DYNAMICS THIS WORK WAS NOT SPONSORED BY THE UNITED STATES AIR FORCE
16. & 17. Distribution Statement Approved for public release; distribution unlimited.		
18. Supplementary Notes		
19. Key Words Heat Transfer Mass Flow Heat Exchangers Fluid Dynamics		
20. Abstract: The purpose of this work was to mathematically model the heat transfer in an active packed bed heat exchanger and to develop an appropriate numerical scheme for the solution of the temperature field. As active packed beds are being considered for use in nuclear reactors, concern is generated as to whether regions of relatively high temperatures will develop. Such concern is the impetus behind the application of the program to two applications concerning heat transfer in packed beds assuming (i) variable porosity of the Brosilow type and (ii) the existence of blockages.		
The results show that for the case of a packed bed with the porosity distribution the so-called hot spot occurs near the wall of the bed. Its magnitude and position were seen to be strongly affected by the assumed velocity profile and wall boundary conditions. In addition, as the proposed mathematical equations		
(Continued on reverse)		

include axial conduction as opposed to a previously developed program which excluded axial conduction and as the results of the two programs approached one another as the Re increased, it is reasonable that the previous program (as it is based on parabolic, not elliptic equations as in the present case) could be implemented with little error expected due to the lack of axial conduction.

In the case of the blockage, however, because of small mass flow in the blocked region, the axial conduction is important and the present program must be used. Effects of variable or constant eddy diffusivity, wall boundary conditions, position of blockage and effective thermal conductivity of the solid are investigated.

Only copies available

This report has been reviewed by the Information Office (EOARD/CMI) and is releasable to the National Technical Information Service (NTIS). At NTIS it will be releasable to the general public, including foreign nations.

This technical report has been reviewed and is approved for publication.

John T. Milton

JOHN T. MILTON
Scientific and Technical Information
Officer

Robert D. Powell

ROBERT D. POWELL
Major, USAF
Flight Vehicles Liaison Officer

FOR THE COMMANDER

Michael A. Greenfield

MICHAEL A. GREENFIELD, Ph.D.
Deputy Director

VON KARMAN INSTITUTE FOR FLUID DYNAMICS
CHAUSSEE DE WATERLOO, 72
B - 1640 RHODE SAINT GENESE, BELGIUM

PROJECT REPORT 1978-12 JUNE 1978

NUMERICAL STUDY OF FORMATION OF THERMAL
NON UNIFORMITIES IN ACTIVE PACKED BEDS

MYRON HILL

SUPERVISOR : J-M BUCHLIN

Project Report	
NTIS Serial	100-115
DOC 145	
Unpublished	
Classification	CONFIDENTIAL
Prepared by	
Approved by	
Reviewed by	
Supervised by	
Editorial by	
Entered by	
File No.	
Date	

A 23

79 05 11 016

DISCLAIMER NOTICE

**THIS DOCUMENT IS BEST QUALITY
PRACTICABLE. THE COPY FURNISHED
TO DTIC CONTAINED A SIGNIFICANT
NUMBER OF PAGES WHICH DO NOT
REPRODUCE LEGIBLY.**

Abstract

The purpose of this work was to mathematically model the heat transfer in an active packed bed heat exchanger and to develop an appropriate numerical scheme for the solution of the temperature field. As active packed beds are being considered for use in nuclear reactors, concern is generated as to whether regions of relatively high temperatures will develop. Such concern is the impetus behind the application of our program to two applications concerning heat transfer in packed beds assuming (i) variable porosity of the Brosilow type and assuming (ii) the existence of blockages.

The results show that for the case of a packed bed with the porosity distribution the so-called hot spot occurs near the wall of the bed. Its magnitude and position were seen to be strongly affected by the assumed velocity profile and wall boundary conditions. In addition as the proposed mathematical equations include axial conduction as opposed to a previously developed program which excluded axial conduction and as the results of the two programs approached one another as the Re increased, it is reasonable that the previous program, (as it is based on parabolic, not elliptic equations as in the present case), could be implemented with little error expected due to the lack of axial conduction.

In the case of the blockage, however, because of small mass flow in the blocked region, the axial conduction is important and the present program must be used. Effects of variable or constant eddy diffusivity, wall boundary conditions, position of blockage and effective thermal conductivity of the solid are investigated.

79 05 11 016

Table of Contents

List of Appendices and Figures	i
Momenclature	ii
Chapter 0: Introduction	1
1: Mathematical Statement of the Problem	2
2: Numerical Treatment of the Problem	4
3: Optimization and Verification of the Numerical Method	6
4: Study of the Formation of Hot Spots Due to Variations in the Porosity Distribution	8
5: Study of the Formation of Hot Spots Due to the Presence of Blockages	12
6: Summary and Conclusions	14
References	16
Appendix A: Development of Differential Equations	17
B. Analytical Solution	21
C1. Nusselt Number Relationship	22
C2. Superficial Velocity Profiles	22
D. Velocity Gradient Model for Eddy Diffusivity	24
E. Program Listings and Sample Outputs	.
Figures	53

List of Appendices and Figures

- Appendix A. Development of differential equations
B. Analytical solution
C1. Experimental Nusselt number relationship
C2. Superficial velocity profiles
D. Velocity gradient model for eddy diffusivity
- Figure 1. Illustration of packed bed
2. Porosity as a continuous function of x and r
3. Form of matrix equation
4. Optimization of numerical procedure
5. Comparison of numerical procedures
6. Reynolds number dependence of the relative error
7. Error as a function of position
8. Second derivatives as functions of position
9. Velocity profiles
10. Porosity and Nusselt number distributions
11. Effect of porosity on temperature profile I
12. " " " " " II
13. " " " " " III
14. Effect of boundary conditions
15. Comparison to experimental results
16. Effect of Peclet number on temperature profile
16.5 Porosity distribution for blockage
17. Velocity field for blockage
18. Radial and axial temperature profiles
19. Eddy diffusivitie variations in x and r
20. Effect of ks^* on temperature profiles
21. Effect of boundary conditions and position of blockage

Nomenclature

C_p ($\frac{\text{Btu}}{\text{lbm} \cdot ^\circ\text{F}}$) specific heat capacity at constant pressure

D_p (ft) diameter of spherical particles of packed bed

E (ft^2/sec) eddy diffusivity

h ($\text{Btu}/\text{ft}^2 \cdot \text{hr} \cdot ^\circ\text{F}$) heat transfer coefficient between packed bed spheres and gas; based on unit area

h_v ($\text{Btu}/\text{ft}^3 \cdot \text{hr} \cdot ^\circ\text{F}$) as above except it is based on unit volume

h_{sw} , h_{gg} ($\text{Btu}/\text{ft}^2 \cdot \text{hr} \cdot ^\circ\text{F}$) heat transfer coefficients at the wall for the solid and gas

H_T (ft) height of packed bed

k_s , k_g ($\text{Btu}/\text{ft} \cdot \text{hr} \cdot ^\circ\text{F}$) molecular thermal conductivities for the solid and gas

k_s^* , k_g^* ($\text{Btu}/\text{ft} \cdot \text{hr} \cdot ^\circ\text{F}$) effective thermal conductivities for the solid and gas

Nu (\emptyset) Nusselt number; $\frac{h \cdot D_p}{k_g}$

Pe' (\emptyset) modified Peclet number; $\frac{V_o \cdot D_p}{E}$

Pr (\emptyset) Prandtl number; $\frac{\mu \cdot C_p}{k_g}$

Q' (Btu/ft^3) rate of heat production per unit solid volume

r (ft) position in radial direction

r^* (\emptyset) non-dimensionalized radial position; r/R_T

R_T (ft) radius of packed bed

Re (\emptyset) Reynolds number; $\frac{V_o \cdot R_T}{\nu}$

T_s , T_g ($^\circ\text{F}$) temperature of solid and gas

T (\emptyset) non-dimensionalized gas temperature; T_g/T_o

T_a ($^\circ\text{F}$) ambient, wall temperature

T_o ($^\circ\text{F}$) inlet gas temperature

U (ft/sec) axial velocity

U^*	(ϕ)	non-dimensional axial velocity; U/V_0
V	(ft/sec)	radial velocity
V^*	(ϕ)	non-dimensional radial velocity; V/V_0
V_0	(ft/sec)	mean inlet gas velocity
x	(ft)	longitudinal position
x^*	(ϕ)	non-dimensional longitudinal position; x/HT
ϵ	(ϕ)	porosity; $\frac{(\text{voidage volume})}{(\text{unit volume})}$
ρ	(lbm/ft ³)	density of the flowing medium
θ	(ϕ)	non-dimensional temperature of the solid
τ	(lbm/ft·sec ²)	viscous stresses
μ	(lbm/ft·sec)	dynamic viscosity
ν	(ft ² /sec)	kinematic viscosity;

1. Introduction

Heat exchangers have diversified uses in industry. The transfer of heat to a flowing medium; the storage of heat; and chemical regeneration are a few such uses. More specifically, packed bed heat exchangers offer the advantage that large rates of heat/chemical transfer can take place in a relatively small volume. A packed bed is typically a collection of small spheres, (however various shapes are possible), housed in a cylindrical tube in such a manner that the spheres' positions are stationary; see figure 1. Small, tightly packed particles are what yield the high surface to volume ratio, $6 \cdot (1 - \epsilon) / D_p$; thereby resulting in good heat transfer properties. Such an advantage is why packed beds, with elements coated with fissionable material; were considered as likely candidates for use as nuclear reactor cores. In fact, plants using such packed beds as reactor cores, are in operation presently.

One concern, however, with the application of packed beds in nuclear reactors, is the existence of regions where temperatures can achieve significantly higher levels than the rest of the field. Such concern stems from the fear that greater-than-designed-for temperatures can arise in these regions and may impare the safe operation of the facility. These regions of relatively high temperatures arise from two principle causes: (i) because of the nonuniformity of the porosity distribution, ϵ , regions of relative minima in ϵ develope where relatively large heat transfer rates occur between solid and gas, (thereby resulting in higher temperatures), and (ii) because of blockages that may develope as a result of a) the retention of dust or foreign matter or b) of the breakage of particles due to possible thermal stresses, higher temperatures may result as well.

It would therefore be useful to be able to mathematically model the problem of heat transfer in a bed of active particles where variations in the porosity occur or blockages exist, and subsequently develope a numerical technique for distributions. Such is the purpose of this work.

The paper will be divided into six chapters: the mathematical statement of heat exchange in an active packed bed; numerical approach used for the solution; optimization and verification of numerical approach; study of the formation of hot spots due to variations in the porosity distribution; study of formation of hot spots due to blockages; and summary of

important results and conclusions.

1. Mathematical Statement of the Problem

The first choice that must be made in modeling heat transfer in a packed bed is whether to enforce the conservation of energy by considering the gas/solid mixture or by considering the gas and solid separately; i.e., to consider a one phase or two phase system. A two phase approach is chosen for this work. In addition, as variations in the θ direction are assumed to be zero, an axis-symmetric, two-dimensional system is used.

The pair of differential equations, conserving energy in the gas and solid state respectively, are derived in appendix A. The results are:

(1) conservation of energy in the gas:

$$(1.) (\rho_u C_p) \frac{\partial T_g}{\partial x} + (\rho_v C_p) \frac{\partial T_g}{\partial r} - \frac{\partial}{\partial x} (k_g^* \frac{\partial T_g}{\partial x}) - \frac{1}{r} \cdot \frac{\partial}{\partial r} (r k_g^* \frac{\partial T_g}{\partial r}) = h_v \cdot (T_s - T_g)$$

(2) conservation of energy in the solid:

$$(2.) - \frac{\partial}{\partial x} (k_s^* \frac{\partial T_s}{\partial x}) - \frac{1}{r} \frac{\partial}{\partial r} (r \cdot k_s^* \frac{\partial T_s}{\partial r}) = h_v \cdot (T_g - T_s) + Q' \cdot (1 - \epsilon)$$

The basic assumptions are enumerated in appendix A. k_s^* and k_g^* are effective thermal conductivities. It is left to express these quantities in terms of their molecular counterparts k_s and k_g . k_g^* is given as in reference (1): $k_g^* = \epsilon \cdot k_g + \rho \cdot C_p \cdot E$. This form is identical, save for the factor ϵ , to what the effective thermal conductivity becomes when one assumes an eddy diffusivity, associated with the Reynolds stresses in the averaged turbulent momentum equation, that is defined analogously as is defined for the viscous stresses τ in the Navier-Stokes equations.

k_g^* has an additional term, $\rho \cdot C_p \cdot E$, which takes account of the heat dissipated by the turbulent fluctuations. We take k_s^* as: $k_s^* = (1 - \epsilon) \cdot k_s$. However, this form for k_s^* only takes account of the gross effect that porosity may have on the effective thermal conductivity. It fails to consider that heat conducted through the solid phase really depends upon the number of contact points between spheres in a given region. Given that conductivity based on the number of contact points is hard to define, we use the above-mentioned expression for k_s^* . It is important to notice that these expressions for k_g^* and k_s^* take account of the fact that not all of the surface of any given face of V (the differential volume in appendix A.), is entirely available to either

the conductive energy flux of the gas phase or of the solid phase. This is expressed by the terms ϵk_g and $(1 - \epsilon) \cdot k_s$.

In the construction of the differential equations, we make the assumption that the porosity "at a point", based on an infinitesimal volume element, is the same as what would be given if the porosity were based on any planar side of the infinitesimal volume element; i.e., at a given point, ϵ based on volume, is equal to ϵ based on area. However talking about porosity defined at a point is rather misleading; for, given a point at r, θ, x , strictly speaking the porosity is either zero or one. Therefore the porosity is discontinuous and the application of partial differential equations is invalid. But, as our partial differential equations do not incorporate variations in the θ direction, we may, hypothetically anyway, average out the variations of ϵ in the θ direction. Assuming such a function could be experimentally derived, this yields a continuous function in x and r . See figure 2. for a clarifying illustration. A function in r that we use in much of our calculations is as given in reference (3):

$$(3.) \epsilon = 0.4 + 0.3 \exp\left(-3.5 \frac{RT}{D_p} \left(1 - \frac{r}{RT}\right)\right) + \cos\left(6.28 \frac{RT}{D_p} \left(1 - \frac{r}{RT}\right)\right) \cdot \exp\left(-0.8 \frac{RT}{D_p} \left(1 - \frac{r}{RT}\right)\right)$$

Equations (1.) and (2.) form a coupled elliptic system for the unknown temperatures T_g and T_s . Therefore Dirichlet, Neumann and/or mixed boundary conditions must be specified for both the solid and gaseous temperatures, completely around the boundary. The boundary conditions used are:

$$(4.) \begin{aligned} (x = 0, r): T_g &= T_0; \frac{\partial T_s}{\partial x} = 0, \text{ or } T_s = T_0 \\ (x, r = RT): -k_g * \frac{\partial T_g}{\partial r} &= h_{gw} \cdot (T_g - T_a); -k_s * \frac{\partial T_s}{\partial r} = h_{sw} \cdot (T_s - T_a) \\ (x = HT, r): \frac{\partial T_g}{\partial x} &= \frac{\partial T_s}{\partial x} = 0 \\ (x, r = 0): \frac{\partial T_g}{\partial r} &= \frac{\partial T_s}{\partial r} = 0 \end{aligned}$$

In passing, the other parameters used in (1.) and (2.) include h_v , the volumetric heat transfer coefficient which governs the rate of heat transfer between solid and gas, and Q' the rate of heat production per unit solid volume.

The boundary conditions at the inlet reflect (i) that the gas enters at a known temperature and (ii) that the solid could also maintain this temperature or could assume, as the gas and solid temperature fields do

at the exit, what we believe the more realistic condition that the normal derivative of the temperature is zero. The boundary conditions at the longitudinal axis simply reflect an assumed symmetry property. The boundary condition at the wall is a mixed one. Setting h_{gw}/kg^* and h_{sw}/ks^* equal to zero or a very large number, an adiabatic or an isothermal wall condition, respectively, is enforced.

2. Numerical Treatment of the Problem

In preparing (1.) , (2.) and (4.) for numerical treatment, it is convenient to non-dimensionalize them beforehand. Using the expressions:

$$x^* = x/HT, r^* = r/RT, U^* = U/Vo, V^* = V/Vo, T = Tg/To, \theta = Ts/To,$$

$$\Pr = \mu \cdot Cp/kg, Re = Vo \cdot RT / \nu, Nu = h \cdot Dp/kg, ks^* = (1 - \epsilon) \cdot ks,$$

$$kg^* = \epsilon \cdot kg + \rho \cdot Cp \cdot E$$

we get the following non-dimensional equations and boundary conditions:

$$(5.) \quad \frac{-1}{Re \cdot Pr} \cdot \frac{RT}{HT^2} \cdot (\epsilon + Pr \cdot (E/\nu)) \frac{\partial^2 T}{\partial x^{*2}} - \frac{-1}{Re \cdot Pr} \cdot \frac{RT}{RT^2} \cdot (\epsilon + Pr \cdot (E/\nu)) \frac{\partial^2 T}{\partial r^{*2}} +$$

$$\left(\frac{U^*}{HT} - \frac{-1}{Re \cdot Pr} \cdot \frac{RT}{HT^2} \cdot \left(\frac{\partial \epsilon}{\partial x^*} + Pr \cdot \frac{\partial}{\partial x^*} (E/\nu) \right) \right) \frac{\partial T}{\partial x^*} +$$

$$\left(\frac{V^*}{RT} - \frac{-1}{Re \cdot Pr} \cdot \frac{RT}{RT^2} \cdot \left(\frac{\partial \epsilon}{\partial r^*} + Pr \cdot \frac{\partial}{\partial r^*} (E/\nu) \right) - \frac{1}{r^*} \cdot \frac{(\epsilon + Pr \cdot (E/\nu)) \cdot RT}{Re \cdot Pr \cdot RT^2} \right) \frac{\partial T}{\partial r^*} =$$

$$\frac{6 \cdot (1 - \epsilon) \cdot Nu \cdot RT}{Re \cdot Pr} \cdot \frac{RT}{Dp^2} \cdot (\theta - T)$$

$$(6.) \quad \frac{-RT}{HT^2} \cdot \frac{(1 - \epsilon)}{Re \cdot Pr} \cdot (ks/kg) \frac{\partial^2 \theta}{\partial x^{*2}} - \frac{RT}{RT^2} \cdot \frac{(1 - \epsilon)}{Re \cdot Pr} \cdot (ks/kg) \frac{\partial^2 \theta}{\partial r^{*2}} +$$

$$\frac{RT}{HT^2 \cdot Re \cdot Pr} \cdot ((ks/kg) \frac{\partial \epsilon}{\partial x^*} - (1 - \epsilon) \cdot \frac{\partial (ks/kg)}{\partial x^*} \frac{\partial \theta}{\partial x^*} +$$

$$\frac{RT}{RT^2 \cdot Re \cdot Pr} \cdot \left(\frac{\partial \epsilon}{\partial r^*} - \frac{(1 - \epsilon)}{r^*} \right) (ks/kg) - (1 - \epsilon) \frac{\partial (ks/kg)}{\partial r^*} \frac{\partial \theta}{\partial r^*} =$$

$$\frac{6 \cdot (1 - \epsilon)}{Dp^2} \cdot Nu \cdot \frac{RT}{Re \cdot Pr} \cdot (T - \theta) + \frac{RT \cdot Q \cdot (1 - \epsilon)}{Re \cdot Pr \cdot kg \cdot To}$$

$$(7.) \quad (x^* = 0, r^*): T = 1, \frac{\partial \theta}{\partial x^*} = 0 \text{ or } \theta = 1$$

$$(x^*, r^* = 1): -\frac{\partial T}{\partial r^*} = (h_{gw} \cdot RT/kg^*) \cdot (T - Ta/To)$$

$$-\frac{\partial \theta}{\partial r^*} = (h_{sw} \cdot RT/ks^*) \cdot (\theta - Ta/To)$$

$$(x^* = 1, r^*): \frac{\partial T}{\partial x^*} = \frac{\partial \theta}{\partial x^*} = 0$$

$$(x^*, r^* = 0): \frac{\partial T}{\partial r^*} = \frac{\partial \theta}{\partial r^*} = 0$$

Such a system of equations and boundary conditions must in general be solved numerically. A constant space grid that is used is indexed below:

writing (5.) and (6.) symbolically as

$$-AA1 \frac{\partial^2 T}{\partial x^*} - CC1 \frac{\partial^2 T}{\partial r^*} + U1 \frac{\partial T}{\partial x^*} + V1 \frac{\partial T}{\partial r^*} + H \cdot T = H \cdot \Theta$$

$$-AA2 \frac{\partial^2 \Theta}{\partial x^*} - CC2 \frac{\partial^2 \Theta}{\partial r^*} + U2 \frac{\partial \Theta}{\partial x^*} + V2 \frac{\partial \Theta}{\partial r^*} + H \cdot T = Q$$

and given the finite difference expressions,

$$\frac{\partial^2 T}{\partial r^*} ij = (T_{ij+1} - 2 T_{ij} + T_{ij-1})/DR^2$$

$$\frac{\partial^2 T}{\partial x^*} ij = (T_{i+1j} - 2 T_{ij} + T_{i-1j})/DX^2$$

$$\frac{\partial T}{\partial x^*} ij = (T_{ij} - T_{i-1j})/DX$$

$\frac{\partial T}{\partial r^*} ij = (T_{ij+1} - T_{ij-1})/2 \cdot DR$, similarly for Θ , one can derive

the following difference equations for T and Θ :

$$(8.) \quad T_{ij-1} \left(\frac{-CC1}{DR^2} - \frac{V1}{2 \cdot DR} \right) + T_{ij} \left(2 \left(\frac{AA1}{DX^2} + \frac{CC1}{DR^2} \right) + \frac{U1}{DX} + H \right) + T_{ij+1} \left(\frac{-CC1}{DR^2} + \frac{V1}{2 \cdot DR} \right) - \\ \Theta_{ij} (H) = T_{i-1j} \left(\frac{AA1}{DX^2} + \frac{U1}{DX} \right) + T_{i+1j} \left(\frac{AA1}{DX^2} \right)$$

$$(9.) \quad \Theta_{ij-1} \left(\frac{-CC2}{DR^2} - \frac{V2}{2 \cdot DR} \right) + \Theta_{ij} \left(2 \left(\frac{AA2}{DX^2} + \frac{CC2}{DR^2} \right) + \frac{U2}{DX} + H \right) + \Theta_{ij+1} \left(\frac{-CC2}{DR^2} + \frac{V2}{2 \cdot DR} \right) - \\ T_{ij} (H) = \Theta_{i-1j} \left(\frac{AA2}{DX^2} + \frac{U2}{DX} \right) + \Theta_{i+1j} \left(\frac{AA2}{DX^2} \right) + Q_{ij}$$

One could consider, in the solution of (8.) and (9.), that temperatures at all nodal points are unknown values. But as this would lead to the inversion of an extremely large, sparse matrix, an alternate method should be found. The problem in employing any alternate scheme is the existence of the terms in (8.) and (9.) contributed by the axial conduction; namely T_{i+1j} and Θ_{i+1j} . If the temperatures along row i are to be solved for, then guessed values must be assumed for these terms. An iterative procedure is clearly called for. This is the complication introduced by the elliptic nature of the equations.

Assuming that all temperatures are known in the k^{th} iteration at all grid points up to and including the $(i-1)^{st}$ row and in the $(k-1)^{st}$ iteration in the i^{th} row and above, the coupled difference equations (8.) and (9.) are applied to the temperatures in the i^{th} row of grid points for all j . A special type of matrix equation is obtained whose form is shown in figure 3. Employing an efficient subroutine to solve this matrix system for T_{ij} and Θ_{ij} along row i , these values are subsequently "over-relaxed" by the use of a method which employs the

following formulas:

$$(T_{ij})_k = (T_{ij})_{k-1} + WS \cdot ((T_{ij})_{\text{matrix}} - (T_{ij})_{k-1})$$

$$(\Theta_{ij})_k = (\Theta_{ij})_{k-1} + WS \cdot ((\Theta_{ij})_{\text{matrix}} - (\Theta_{ij})_{k-1})$$

This procedure is termed relaxation by lines and is used to accelerate the convergence of the solution method. WS is called the over-relaxation factor, whose value is typically between 1 and 2. As we proceed to the next row, we can use the newly updated values of the i₁ row in our calculation of the values in the (i+1)st row as given by the matrix equation. Proceeding in this manner through the bed one can check whether the largest error between iterations satisfies some error criterion. If not, one must start the process again, repeating as many iterations as necessary so as to obtain convergence.

As a final note, it may have been observed that the finite difference expressions used for $\frac{\partial T}{\partial x}$ in deriving (3.) was a first order, one-sided difference expression; unlike the central difference equation for $\frac{\partial T}{\partial r}$. The reasoning for this lies in the assertion that for high enough Re the first derivative term in equations (5.) is significantly greater in magnitude than other terms, and, according to reference (4), to avoid numerical instabilities in the solution as well as enhance the accuracy of the solution, the one-sided, or upwind, differencing scheme should be employed to $\frac{\partial T}{\partial x}$. Unfortunately the upwind differencing scheme was also applied to $\frac{\partial \Theta}{\partial x}$. As no relative weighting with respect to Re exists between the first and second derivative terms in equation (2.), the rational for using the upwind scheme for $\frac{\partial T}{\partial x}$ was inappropriate for use on $\frac{\partial \Theta}{\partial x}$. Therefore it was inconsistent to apply upwind differencing to $\frac{\partial \Theta}{\partial x}$ and it is possible that the solutions obtained were not as accurate as could have been obtained using central differencing on $\frac{\partial \Theta}{\partial x}$; however the discrepancy would be small and would have no implications on conclusions to be drawn.

3. Optimization and Verification of Numerical Method

This chapter concerns itself with the actual implementation of the numerical method in obtaining solutions with the purpose of minimizing the number of iterations necessary for convergence and the comparison of the actual results with those generated by a previously established numerical procedure which ignores axial conduction. Besides the usual

geometric and physical/thermal properties of the gas and solid, the porosity, the velocity field, the Nusselt number and eddy diffusivity, E, must be specified in order to generate a solution. Using a reasonable value for Nu ; setting E to zero; and as required by the analytical solution, assuming the velocity and porosity are constants, ($U/U_0 = 1$ and $\phi = 0.4$), the numerical procedure as presented in this paper was applied. As for boundary condition, the gas and solid were assumed at a given temperature at a given temperature at the inlet as well as at the wall.

Although the discretization method as described by equations (8.) and (9.) was found to be quite satisfactory, in our first attempts to achieve a solution, an alternate method was also considered. This alternate method is equivalent to employing (8.) and (9.) except that the nodal temperatures multiplying the coefficients U_1 , U^2 , V_1 , V^2 , were considered at the $(k-1)^{st}$ iteration. The obvious superiority of the method represented by (8.) and (9.) is reflected in figure 4 . The advantages are shown in two ways: (i) a much lower number of iterations is necessary for convergence and (ii) the first method is less sensitive to changes in WS than the second. What may also be seen in figure 4. is an agreement with the assertion that for an elliptic equation with constant coefficients, the WS that results in the minimum number of iterations, lies between 1 and 2. This is seen to hold even for a variety of Re.

The method of calculation having been established, it remains, as a further check, to compare the results of the numerical solution presented here, (assuming constant porosity, velocity and an isothermal wall condition), to those results given by an associated numerical solution which has already been developed and which ignores axial conduction. This numerical procedure is based on the parabolic mathematical equations which one obtains when axial conduction is ignored. Such a system has the numerical advantage that the solution can be found directly without iteration. The results of the numerical solutions for a Re of five thousand are shown in figure 5. In addition, the results of the previous numerical solution ignoring axial conduction; are compared to an analytical solution which ignores axial conduction by construction as well and which can be generated in terms of Bessel functions. This comparison is almost exact. As the difference between the numerical procedures is the inclusion of axial conduction, it follows that the difference in the num-

erical results is due to the conduction of heat in opposition to the direction of the flow. Looking at the non-dimensional equation (5.), one sees that the product $Re \cdot Pr$ determines the relative importance of the convective terms relative to the conductive terms. Therefore as the Re increases, one would expect that the diffusive terms play an increasingly less significant role and as figure 6. shows, that the numerical solutions should approach one another. Thus for $Re \cdot Pr$ down to about 150 the solution given by the numerical procedure including axial conduction should approximate the numerical solution excluding axial conduction to within 1%. This implies that there exists, for given parameters, a Re , above which the simpler parabolic system of equations can be used; and below which the more complex elliptic system must be employed. However, as seen in figure 7., this relative error does not exhibit a uniform distribution, but is a function of the position of the bed. The result that the relative maxima of error occur near the exit and near the wall of the bed, can be explained by figure 8.. Figure 8. shows that the second derivative of the gas temperature is highest near the bed exit and near the bed wall; and therefore one would expect that in these regions the relative discrepancy between the numerical solutions would be greatest.

It is seen, therefore, that the numerical procedure described in this paper can be optimized in the sense that the number of iterations are minimized, by keeping WS between 1 and 1.2. In addition, the agreement between the results of the numerical approach presented here and the results of the numerical procedure which ignored axial conduction, being shown to become better as the Re increases, serves to justify that the program is operating properly.

4. Study of the Formation of Hot Spots Due to Variations in the Porosity Distribution

In order to better simulate the local properties of a packed bed and its heat transfer characteristics, experimental expressions for the porosity, given as equation (3.), for the local Nusselt number, given in appendix C1, and expressions for parabolic and turbulent superficial velocity profiles are used. The expressions used for the velocity profiles are given in appendix C2 and are graphed along with the porosity and Nusselt number distributions in figures 9. and 10. respectively. The

oscillatory variation of the porosity is a result of the influence of the wall containing the packed bed. The porosity is 1 by definition at the wall and as the center is approached the porosity becomes a constant value, (typically 0.4 for a lightly packed random bed). Figure 11. shows the gas temperature obtained at the exit of the bed for a constant velocity profile and type (i) boundary conditions; (see below). The oscillatory variations observed are due to the variations in the porosity distribution. This can be explained by realizing that regions of relatively low porosity are regions of high spherical density and therefore regions where high heat transfer rates between the solid and the gas exist. The dashed line in figure 11., is the numerical solution given by the program that ignores axial conduction. It shows good agreement with the present solution.

Figures 12. and 13. show the solution obtained at the bed exit for assumed turbulent and laminar velocity profiles respectively. Type (i) boundary conditions are used here also. Again the oscillatory variations are due to the local variation in porosity; but, in addition, due to the fact that the velocity is greater than the mean, up to a certain distance from the center, and is less than the mean nearer the wall, the cooling affects of the fluid are more efficient nearer the center than nearer the wall. Therefore the relative maxima in the temperature profiles are due to both the relative minima of porosity that occur near the wall and to the inefficient cooling in this region. It should be mentioned that E was assumed zero in these cases involving figures 11., 12., 13. .

Assuming a turbulent velocity profile, figure 14. presents the resulting gas temperature distributions for a variety of boundary conditions. The boundary conditions used are defined as follows:

type (i): $T_s(0,r) = T_0, T_s = T_g(x,RT) = T_a$

type (ii): $\frac{\partial T_s}{\partial x}(0,r) = 0, T_s = T_g(x,RT) = T_a$

type (iii): $\frac{\partial T_s}{\partial x}(0,r) = 0, \frac{\partial T_s}{\partial r} = \frac{\partial T_g}{\partial r}(x,RT) = 0 ;$

other boundary conditions remain as previously described and are the same for each of these cases.

It can be seen that by changing from a type (i) to a type (ii) boundary condition, the temperature profile of the gas increases yet keeps the general shape of the isothermal case and that the position of the hot spot has kept the same position. With the introduction of the type (iii)

boundary condition, the opportunity for heat to be passed through the wall is lost. Therefore, as expected, the temperature profile is raised even further. In addition, the hot spot is moved significantly closer to the wall.

It should be mentioned in passing, that as with the results in figures 11., 12., and 13. the dashed line in figure 14., is calculated using a Nusselt number based on the mean Re; whereas the other curves in figure 14. are calculated using a Nusselt number based on the local Re. The shift to a local Nu slightly raises the temperature profile due to the fact that the local Re (and therefore the local Nu), is greater than the mean Re, (mean Nu), for most of the radial dimension. This allows a larger heat transfer between the solid and the gas which raises the resulting temperature profile.

Earlier, the results of the numerical technique developed in this paper compared to a previously established numerical technique, (ignoring axial conduction), which in turn was seen to be identical to an associated analytical solution. The results of the numerical procedures were seen to approach one another as the Re increased. This implied that the numerical procedure including axial conduction was implemented properly. To attempt to justify the numerical results, one must compare them with experimental ones. Such experimental work was done at the Von Karman Institute and is discussed in reference (5). Using their given data, numerical calculations were made. The experimental and numerical results appear in figure 15.. As the temperatures are scaled with respect to the hot spot temperature, only the prediction of the position of the hot spot can be made and not its magnitude. Considering that the experimental data was in the form of a temperature map of the bed exit and that one necessarily must choose the radial profile to compare his numerical results with, (the radial profile through the hot spot of the bed exit was taken) and that one cannot expect the porosity of the experimental packed bed to be the same as that used in the numerical program, that the numerical results rather successfully predicted the radial position of the hot spot as well as the profiles' general shape, can be inferred. An additional point should be mentioned concerning figure 15.. As the bed height is increased, the level of temperature at the exit is raised and therefore the greater the heat loss through the wall. This accounts for the inward movement of the hot spot.

It is seen, then, that the variation in porosity introduces hot spot regions that exist close to the wall of the packed bed and that assumed parabolic or turbulent velocity profiles amplify the magnitude of these hot spots. In addition, the effect of employing adiabatic wall conditions tends to increase even more the temperature of these regions.

As a final point, the results presented in figures 14. and 15., unlike figures 11., 12., 13., were calculated using a value of 20 for the modified Peclet number, Pe' . This value, dependent upon the Re and the ratio D_p/RT , is obtained from the experimental data given in reference (1). Because, (i) the value of Pe' determines the eddy diffusivity, E , which in turn contributes to the effective thermal conductivity kg^* , and (ii) the greater the value of kg^* , the greater the dissipative capacity of the gas is to damp out rapid temperature variations, it is important to be able to represent Pe' satisfactorily if one wants to predict the magnitude of hot spots. As an example, the calculated curve of figure 15., for $HT/D_p = 10$, is repeated in figure 16. and compared to a solution calculated from the same data save that the Pe' is very large, (therefore implying $E = 0$).

As the assumed axial velocity profile, or for that matter the "true" local mean axial velocity profile, would not be expected to show great variations in the radial direction, which would cause relatively large eddy diffusivities to arise, the use of a constant E seems reasonable. However if one assumes a blockage exists, large perturbations in the flow field would result; thereby causing large gradients and therefore larger eddy diffusivities. In addition, as there would be little mass flow in the vicinity of the blockage, the conductive terms would become the main heat transfer process, whatever the bulk Re . Therefore only the application of the numerical procedure including axial conduction, as presented here, would be justified.

5. Study of the Formation of Hot Spots Due to the Presence of Blockages

In the operation of a packed bed heat exchanger, a blockage conceivably might result from the retention of dust/foreign matter being convected by the gas. In the region of the blockage, both the inefficient cooling by the gas and the heating of the dust surrounding the active spheres, would lead to the formation of a hot spot. The blockage, itself, is introduced into the program as a region of the relatively low porosity of 0.1. Outside the blocked region the porosity is 0.4. To avoid large gradients, a linear variation in the porosity between the blockage and the rest of the bed is used. See figure 16. for a clarifying illustration. The local velocity vector, (axial and radial components), is calculated by a program that solves the non-dimensional form of the Ergun equation. Refer to reference (6) for the equation and examples of its applications. The velocity field, for the case of the blockage, is shown in figure 17. As expected the flow tends to be diverted around the blockage, thereby leaving the blocked region with little mass flow through it.

Unlike the previous cases where E was assumed constant over the entire field, we would expect relatively large velocity gradients in the case of the blockage and therefore regions of higher eddy diffusivities. A velocity gradient model relating E to the velocity field is used and is explained in appendix D.

Using the velocity gradient model for eddy diffusivity, the above definition for porosity, the Nusselt number expression in appendix C1 and the calculated velocity field, temperature distributions were obtained for a variety of cases.

Figure 13. shows axial and radial gaseous temperature curves for constant as well as variable E , using an isothermal wall condition. It must be mentioned that in calculating the variable eddy diffusivity distribution from the velocity field, an arbitrary constant multiplying the vector components of E , E_x and E_r , was adjusted so that the vectoral sum of the average E_x and the average E_r over the entire bed mesh, was such that the effective Pe' calculated from this mean value, matched the Pe' given in reference (1). As figure 18. shows, the presence of a blockage causes a significant temperature peak in the radial profile and effects an acceleration in the, what would otherwise be a linear temperature profile.

The variable E solution gave larger estimates of peak temperatures than the constant E solution. This can be explained by noting in figure 19. that in the region of the peak of the radial temperature curve, the E estimated by the variable model is much lower than the mean bed value. Hence less turbulence and less efficient cooling is the result and therefore the variable E model will give greater temperatures. Identical arguments can explain the discrepancy between the axial temperature profiles of figure 18. when one notes that as with the upper curve in figure 19., the lower one shows that the variable E is much less than the mean value in the region of interest.

As mentioned in chapter , the expression $ks^* = (1 - \epsilon) \cdot ks$, does not take into account that ks^* really depends on the number of contact points between spheres rather than exclusively on the porosity. One would expect, then, that ks^* would in reality be somewhat less than that given by the above expression. Figure 20. shows the radial temperature at the bed exit for the same blockage case as treated before, (given as dots (•)), and compares this result with those profiles calculated by assuming subsequently lower values of ks . Because of increasing resistance to conductive heat flow, the model predicts subsequently larger peak temperature values as ks decreases.

The affect of employing a type (iii), adiabatic, wall condition as opposed to an isothermal one, has virtually no affect on the characteristics of the mid-bed radial profile, as exemplified by the upper curve in figure 21. . Not only is this ineffectuality in changing peak temperature values true at the mid-bed position, but it is true for the entire bed.

The lower curve in figure 21. shows that as the blockage is moved closer to the bed exit, the temperature peak at the bed rises accordingly. This brings up the immediate concern that temperature peaks may develop inside a packed bed with a blockage that may exceed the temperatures realized at the bed exit; and as it is difficult to determine temperatures inside an operating packed bed heat exchanger, these temperatures may go undected. The results from which the lower curve in figure 21. was derived, justify this concern; for as the blockage is in either the lower, middle, or upper position, the maximum gaseous temperature in the blocked region attains 89.5%, (at $x = 0.47$ HT), 95.5%, (at $x = 0.63$ HT) and 99.9%, (at $x = 0.20$ HT), of the maximum value of the exit temperature respectively.

It is therefore seen, then, that the introduction of blockages into packed beds, result in large peaks in the temperature field distribution. By using a velocity gradient model for the eddy diffusivity, E , the temperature peaks have been higher than might have otherwise been expected had a constant E been used. These hot spots may attain higher values, still, if one assumes that the effective thermal conductivity of the solid is lower than that given by the assumed expression. The magnitude of these peaks, in addition, are functions of the position of the blocked region; and it was seen that the possibility definitely exists that the magnitude of hot spots may be greatest inside the bed, itself, and therefore difficult to detect.

6. Summary and Conclusions

Envisioning the use of an active packed bed in a nuclear reactor, the concern of hot spot development due to porosity variation or due to the presence of blockages, is raised. It would be useful, therefore, to be able to calculate the resulting temperature field assuming that these porosity variations or blockages occur. To that end, a two phase axis-symmetric mathematical model for heat transfer in an active packed bed was proposed. As axial conduction is considered, the resulting equations are elliptic and if calculations are to be done efficiently, these equations must be solved by an iteration procedure. A method of over-relaxation by lines was employed and whose arbitrary coefficient of relaxation was chosen so as to approximately minimize the number of iterations needed for convergence. A numerical procedure, which ignores axial conduction, which was shown essentially identical with an associated analytical solution, gave results which approached the numerical values of the present program as the Reynolds number increased. As the relative difference between the two solutions was on the order of 3-4% for low Re and decreased to approximately 1% for moderate Re , the results of the numerical solution were verified.

Concerning the case where variable porosity is assumed, it was seen that temperature peaks developed close to the bed wall. The position and magnitude of these hot spots was seen to be a strong function of the assumed velocity profile, the bed height, as well as the boundary conditions at the wall. The present solution was also seen to be in close agreement with the results of the previous program which ignores axial conduction. It is

in this respect that the following is proposed. For as most industrial uses insure Re of sufficient magnitude to assure that the inclusion of axial conduction would give temperatures of 90-95% of the ones given by the program excluding axial conduction and as the elliptic equations involve more complicated, time-consuming methods, it would perhaps be more efficient to base a design method on a mathematical model ignoring axial conduction, keeping in mind that the results are to some degree an upper limit to the "actual temperatures". This concept of the questionable usefulness of the inclusion of the axial conduction, however, cannot be applied to the case where blockages are present.

As demonstrated, even for relatively large bulk Re , the mass flow inside the blockage itself was small and therefore, in the blocked region, heat transfer by conduction will play the major role. The blockage introduced a substantial peak in the radial temperature profile through the blockage itself. The overall maximum temperature, however, was still at the bed exit; even though it was approached by the maximum blockage temperature as the blockage moved downstream. It bears looking into the possibility that the maximum blockage temperature may exceed the maximum exit temperature by effecting changes in the position and size of a blockage.

As a final point, it was mentioned that the actual ks^* may be lower than assumed. It was demonstrated that by lowering ks^* the peak of the radial exit temperature profile was raised. It would therefore be useful to investigate the true nature of ks^* so as one could place more certainty on whether a proposed design for the operation of an active packed bed is acceptable if one assumes the presence of a blockage.

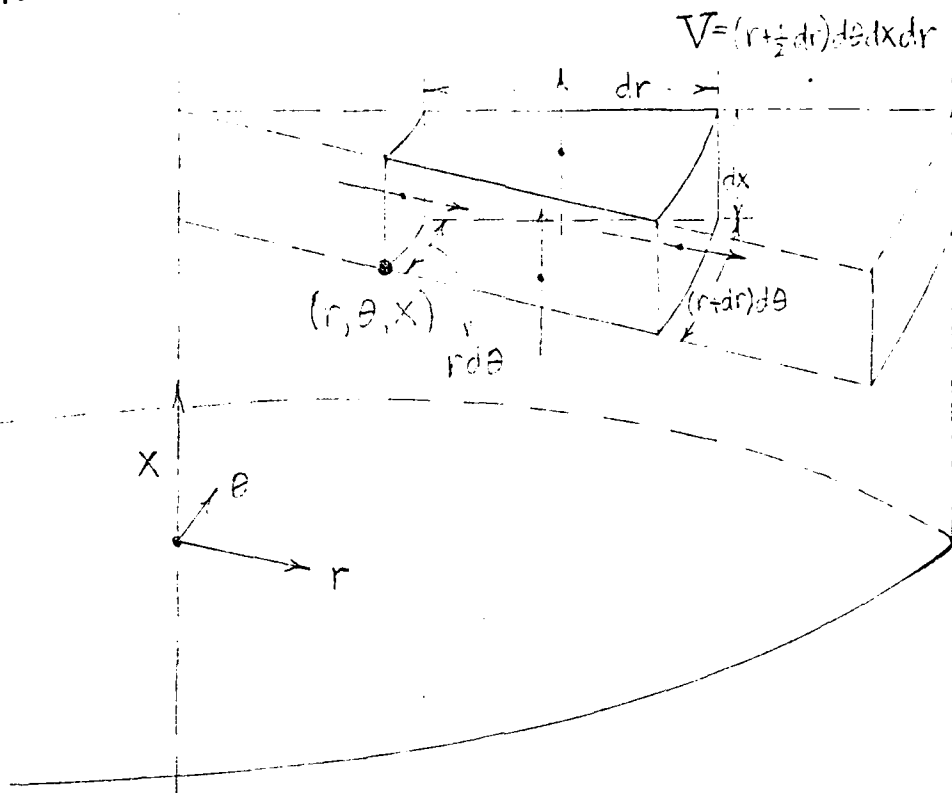
References

1. Singer, E., Wilhelm, R. H., Chemical Engineering Progress, "Heat Transfer in Packed Beds; Analytical solution and Design Method", No. 7, July 1950, vol. 46.
3. Benenati, R. F., Brosilow C. B., A.J.che.E. J., "Void Fraction Distribution in beds of spheres", July 1962, No. 3, vol. 8.
4. Spalding, D. B., International Journal for Numerical Methods in Engineering, "A Novel Finite Difference Formulation for Differential Expressions Involving Both First and Second Derivatives", 1972, vol. 4.
5. Buchlin, J. W., Ginoux J. J., "Experimental Study of Hot Spot in Active Packed Beds", March 1975, Von Karman Inst. Technical Note # 108
6. Stanek, V., Szekely, J., The Canadian Journal of Chemical Engineering, "The Effect of Non-uniform Porosity in Causing Flow Maldistributions in Isothermal Packed Beds", Feb. 1972, vol. 50.

APPENDICES

THE EFFECT OF DIFFERENTIAL ELEMENTS

A.



SUPPOSE WE WANT TO CONSERVE THE QUANTITY Q IN THE INFINITESIMAL VOLUME V . TAKING THE OUTWARD NORMAL AS POSITIVE, AND IGNORING VARIATIONS IN THE θ DIRECTION, THE NET FLUX OUT OF V OF Q , IS GIVEN BY THE FOLLOWING EQUATION.

$$\text{FLUX} = Q_{r+dr} f_{r+dr} - Q_r f_r + Q_{x+dx} f_{x+dx} - Q_x f_x \\ = Q_{r+dr} (r+dr) d\theta dx - Q_r r d\theta dx + (Q_{x+dx} - Q_x) (r + \frac{1}{2}dr) d\theta dr \Rightarrow$$

$$\frac{\text{FLUX}}{V} = \frac{(Q_{r+dr} - Q_r)r}{(r + \frac{1}{2}dr)dr} + \frac{Q_{x+dx} - Q_x}{dx}; \text{ let } dx = dr \rightarrow \\ = \frac{\frac{dQ_r}{dr}r + \frac{Q_r}{r}}{r} + \frac{\frac{dQ_x}{dx}x}{dx} = \frac{1}{r} \frac{d}{dr}(r \cdot Q_r) + \frac{1}{dx} \frac{dQ_x}{dx}$$

HEAT TRANSFER IN AN ACTIVE PACKED BED
 THERE ARE TWO TYPES OF ENERGY FLUXES ACCROSS
 THE SPHERES OF V THAT SHALL BE CONSIDERED:
 CONVECTIVE AND CONDUCTIVE FLUXES FOR THE GAS
 AND CONDUCTIVE FLUXES FOR THE SOLIDS (SINCE THE PARTICLES
 DO NOT MOVE).

- c) FOR THE GAS THERE MUST BE A BALANCE BETWEEN
 THE NET FLUX OUT OF V WITH THAT WHICH IS
 DELIVERED TO THE GAS ACROSS THE SURFACE OF THE
 SPHERES:

$$\text{CONVECTIVE FLUX} \left\{ \begin{array}{l} Q_x = \rho u C_p T_g \\ Q_r = \rho v C_p T_g \end{array} \right.$$

$$\text{CONDUCTIVE FLUX} \left\{ \begin{array}{l} Q_x = -k_{g,x}^* \cdot \frac{\partial T_g}{\partial x} \\ Q_r = -k_{g,r}^* \cdot \frac{\partial T_g}{\partial r} \end{array} \right.$$

$$\text{FLUX ACROSS SPHERES SURFACE} \left\{ h_v \cdot (T_s - T_g) ; \quad \therefore \right.$$

$$-\frac{\partial}{\partial x} (k_{g,x}^* \cdot \frac{\partial T_g}{\partial x}) - \frac{1}{r} \cdot \frac{\partial}{\partial r} (r \cdot k_{g,r}^* \cdot \frac{\partial T_g}{\partial r}) + \rho u C_p \frac{\partial T_g}{\partial x} + \rho v C_p \frac{\partial T_g}{\partial r} + \rho C_o T_g \frac{\partial u}{\partial x} + \rho C_o T_g \frac{\partial v}{\partial r} + \rho v C_o T_g / r = h_v (T_s - T_g)$$

ASSUMING INCOMPRESSIBLE FLOW:

$$\nabla \cdot (\underline{v}) = \frac{\partial u}{\partial x} + \frac{1}{r} \cdot \frac{\partial}{\partial r} (r v) = 0 \Rightarrow$$

$$-\frac{\partial}{\partial x} \left(k_{\text{g}}^* \cdot \frac{\partial T_g}{\partial x} \right) - \frac{1}{r} \cdot \frac{\partial}{\partial r} \left(r \cdot k_{\text{sr}}^* \cdot \frac{\partial T_s}{\partial r} \right) + \rho u c_p \frac{\partial T_g}{\partial x} + \rho v c_p \frac{\partial T_s}{\partial r}$$

$$= h_g (T_g - T_s)$$

b) FOR THE SOLID THE PROCESS IS ANISOTROPIC. AGAIN ONE MUST TAKE ACCOUNT OF THE CONDUCTIVE FLUXES AND BALANCE THEM WITH THE FLUX ACROSS THE SPHERICAL SURFACE FROM THE GAS AND THE ENERGY PER UNIT SOLID VOLUME, Q' , PRODUCED IN THE SPHERES THEMSELVES.

$$\text{CONDUCTIVE FLUX} \left\{ \begin{array}{l} Q_x = -k_{sx}^* \frac{\partial T_s}{\partial x} \\ Q_r = -k_{sr}^* \frac{\partial T_s}{\partial r} \end{array} \right.$$

$$\text{FLUX ACROSS SPHERICAL SURFACE} \left\{ \begin{array}{l} f_g \cdot (T_g - T_s) \end{array} \right.$$

$$\text{ENERGY PRODUCED} \left\{ \begin{array}{l} Q' \cdot (1-\epsilon) ; \quad \therefore \\ \text{PER UNIT VOLUME} \\ \text{PER SECOND} \end{array} \right.$$

$$-\frac{\partial}{\partial x} \left(k_{sx}^* \cdot \frac{\partial T_s}{\partial x} \right) - \frac{1}{r} \cdot \frac{\partial}{\partial r} \left(r \cdot k_{sr}^* \cdot \frac{\partial T_s}{\partial r} \right)$$

$$= h_g (T_g - T_s) + Q' \cdot (1-\epsilon).$$

WHERE k_{g}^* AND k_{sr}^* ARE EFFECTIVE THERMAL CONDUCTIVITIES.

ASSUMPTIONS

- (i) STEADY STATE INCOMPRESSIBLE FLOW
- (ii) ρ , C_p , k_g , k_s , h_v , μ , Q' ARE INDEPENDENT OF TEMPERATURE
- (iii) POROSITY BASED ON VOLUME EQUALS POROSITY BASED ON AREA.
- (iv) POROSITY IS A CONTINUOUS FUNCTION
- (v) THERMAL PROPERTIES WHOSE EXPERIMENTAL CORRELATIONS ARE BASED ON BULK POROSITY OR VELOCITY ARE STILL VALID WHEN LOCAL POROSITY OR VELOCITY IS USED.
- (vi) VISCOUS DISSIPATION AND HEAT TRANSFER DUE TO RADIATION ARE NEGLECTED.

B. ANALYTICAL SOLUTION

$$T_o = T_w + \sum_n \left\{ \frac{2 \cdot (T_o - T_w)}{\lambda_n \cdot J_1(\lambda_n)} \cdot \exp\left(-\frac{P_n}{\alpha_n} \cdot x\right) + \frac{\sigma_n}{P_n} \cdot \left(1 - \exp\left(-\frac{P_n}{\alpha_n} \cdot x\right)\right) \right\} \cdot J_0(\lambda_n)$$

$$T_s = T_w + \sum_n \left\{ \frac{H}{(H + \lambda_n^2 \cdot K)} \cdot \left[\frac{2 \cdot (T_o - T_w)}{\lambda_n \cdot J_1(\lambda_n)} \cdot \exp\left(-\frac{P_n}{\alpha_n} \cdot x\right) + \frac{\sigma_n}{P_n} \cdot \left(1 - \exp\left(-\frac{P_n}{\alpha_n} \cdot x\right)\right) \right] \right.$$

$$\left. + \frac{2 \cdot S_o}{\lambda_n \cdot J_1(\lambda_n) \cdot (H + \lambda_n^2 \cdot K)} \right\} \cdot J_0(\lambda_n \cdot r)$$

$$\text{WIT-} \quad \frac{\sigma_n}{P_n} = \frac{\lambda_n^2 \cdot H \cdot D_o}{R T^2} \cdot \left\{ \frac{\epsilon}{Re \cdot Pr} + \frac{1}{Pe} + \frac{1}{K_s / K_g + \frac{\lambda_n^2}{6 \cdot (1-\epsilon) \cdot Nu} \cdot \left(\frac{D_o}{R T} \right)^2 \cdot \left(\frac{Re \cdot Pr}{Nu} \right)} \right\}$$

$$\frac{\sigma_n}{P_n} = \frac{2 \cdot S_o \cdot R T^2}{\lambda_n^2 \cdot J_1(\lambda_n) \cdot K_s} \cdot \left\{ \frac{1}{1 + \left[\frac{\lambda_n^2}{6 \cdot (1-\epsilon) \cdot Nu} \cdot \left(\frac{D_o}{R T} \right)^2 + \frac{1}{K_s / K_g} \right] \cdot \left[\epsilon + \frac{Re \cdot Pr}{Pe} \right]} \right\}$$

$$\text{WHERE } \lambda_n: J_0(\lambda_n) = 0$$

$$Re' = D_p \cdot Re / RT$$

$$Pe = V_o \cdot D_p / E$$

$$K_s / K_g = (1-\epsilon) \cdot (K_s / K_g)$$

$$S_o / K_s = Q'' / \dot{m}_s$$

$$H = (6 \cdot (1-\epsilon) \cdot Nu \cdot (RT/D_p)^2) / (\epsilon + \frac{Re \cdot Pr}{Pe} \cdot (D_p/RT))$$

$$K = (1-\epsilon) \cdot (F_c \cdot K_g) / (\epsilon + \frac{Re \cdot Pr}{Pe} \cdot (D_p/RT))$$

$$S_o = S_o \cdot K \cdot R^2 / K_s$$

C1. NUCSELT NUMBER RELATIONSHIP

if $\gamma = 1 - \epsilon$

$\beta = (\alpha)^{1/3}$

$$\gamma = 2 - 3\cdot\beta + 3\cdot(\beta)^5 - 2\cdot(\beta)^6$$

THEN

$$Nu = 1.6 \cdot \left\{ \frac{Re_{\infty} \cdot Pr}{6.8} \cdot [1 - (\alpha)^{5/3}] \right\}^{1/3}$$

C2. SUPERFICIAL VELOCITY PROFILES

if $us = u/\%$, THEN FOR

(i) CONSTANT VELOCITY: $us = 1$.

(ii) TURBULENT VELOCITY PROFILE:

if $FLD = 0.079 / (RE_{RT})^{1/4}$

$$RFLD = [FLD/2]^{1/2}$$

$$REF = RE_{RT} \cdot RFLD$$

$$YP = REF \cdot (1 - r/RT)$$

$$RA = 1 - 30/REF$$

$$RE = 1 - 5/REF$$

THEN

(continued)

FOR $C \leq r/RT < R_A$

$$U_S = R_{FLD} \cdot \left\{ 5.5 + 2.5 \cdot \log \left[Y_P \cdot \frac{1.5 \cdot (1 + r/RT)}{1 + 2 \cdot (r/RT)^2} \right] \right\}$$

FOR $R_A \leq r/RT < R_B$

$$U_S = R_{FLD} \cdot \left\{ -3.05 + 5 \cdot \log (Y_P) \right\}$$

FOR $R_B \leq r/RT \leq 1$

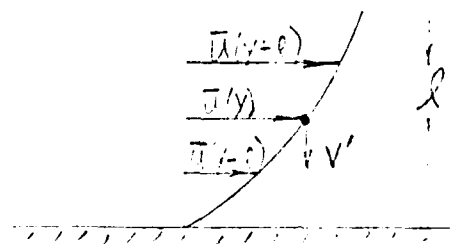
$$U_S = R_{FLD} \cdot Y_P.$$

(iii) LAMINAR VELOCITY PROFILE

$$U_S = 2 \cdot (1 - (r/RT)^2)$$

D. VELOCITY/GRADIENT MODEL FOR EDDY DIFFUSIVITY

$$\text{REYNOLDS STRESS} = -\rho \overline{u'v'} \equiv \tau_{app}$$



$$|u'| = |\bar{u}(y) - \bar{u}(y-\Delta y)| ; \text{ REPLACE } l \text{ BY } \Delta y$$

$$\frac{|u'|}{\Delta y} = \frac{|\bar{u}(y) - \bar{u}(y-\Delta y)|}{\Delta y} ; \text{ TAKE LIMIT } \Delta y \rightarrow 0$$

$|u'| = \lambda \cdot \left| \frac{\partial \bar{u}}{\partial y} \right|$. THIS MAKES THE ASSUMPTION
THAT THE MIXING LENGTH, λ ,
IS OF INFINITECIAL ORDER.

$$\begin{aligned} \text{ASSUME} \quad |v'| &= C_1 \cdot |u'| \\ \overline{u'v'} &= -C_2 \cdot \overline{|u'|} \cdot \overline{|v'|} \\ \tau_{app} &\equiv \rho \cdot E_y \frac{\partial \bar{u}}{\partial y} \end{aligned}$$

$$\begin{aligned} \text{THEN } \tau_{app} &= -\rho \overline{u'v'} \\ &= -\rho \cdot [-C_2 \cdot \overline{|u'|} \cdot C_1 \cdot \overline{|u'|}] \\ &= \rho \cdot C_1 \cdot C_2 \cdot \lambda^2 \cdot \left| \frac{\partial \bar{u}}{\partial y} \right|^2 \Rightarrow \end{aligned}$$

$$E_y = \lambda^2 \cdot \left| \frac{\partial \bar{u}}{\partial y} \right| \quad \text{WHERE } \lambda^2 = C_1 \cdot C_2 \cdot l^2.$$

$$\text{SIMILARLY: } E_x = \lambda^2 \cdot \left| \frac{\partial \bar{u}}{\partial x} \right|$$

Appendix E.

Program Listings and Sample Outputs

Program code for calculating the temperature field assuming variable velocity and porosity distributions	26
Corresponding output	29
Velocity field calculation for the case of a blockage	33
Program code for calculating the temperature field for the case of a blockage; using the velocity data above	42
Corresponding output	47

```
      DEFINE FILE B=108=M(L0
      COMMON/BLKE/A1(41),B1(41),C1(41),D1(41),E1(41)
      COMMON/BLKE/A2(41),B2(41),C2(41),D2(41),E2(41)
      COMMON/F2/Z(43),A3(43),M3UP,M3UP
      DIMENSION W1(31,31),W2(31,31),SOLN1(31),SOLN2(31),EP(31),EPR(31),
      IPNC(31),USA(31)
C
      READ (105,100) RT,HT,RE,PR,PNU,TKG,TKR
      FORMAT(7F10.0)
      READ(105,200)MMAX,NMAX,J99MAX,EPS,WS,DP,TA,QP,POR
  200  FORMAT(315,5F10.0,F7.5)
      READ (105,150) PE,T0,VIS,M9,RNGU,RNSQ,RNSO,ALPHA,BETA
  150  FORMAT (3(E10.4),13,3(E10.4),2(F4.1))
C
      WRITE (108,600) RT,HT,RE,PR,PNU,TKG,TKR,POR,PE,VIS
      WRITE (108,600) MMAX,NMAX,J99MAX,EPS,WS,DP,TA,T0,QP,M9
  600  FORMAT (1X,10(E12.4),/)
      WRITE (108,601) RNGU,RNSW,RNSO,ALPHA,BETA
  601  FORMAT (1X,5(E10.4),//)
C
C INITIALIZATION OF TEMPERATURES
      DO 5 I=1,NMAX
      DO 5 J=1,NMAX
      W1(I,J)=ALPHA
      W2(I,J)=BETA
  5 CONTINUE
      US=1.
      VS=0.
      E=DP*RE*VIS/(RT*PE)
      POR=0.
      M1=MMAX-1
      N1=NMAX-1
      DX=1./FLOAT(M1)
      DR=1./FLOAT(N1)
  (   J99=0
      G=FLOAT(M1-1)*FLOAT(N1-1)
C DETERMINATION OF COEFFICIENTS IN DISCRETIZED EQUATIONS
  7   J99=J99+1
      DT1=0.
      DT2=0.
      DER1=0.
      DER2=0.
      DO 10 I=2,M1
      IP1=I+1
      IM1=I-1
      DO 20 J=2,N1
      CALL DATSW(1,ISW)
      GO TO (627,629),ISW
  629  CONTINUE
      IF (I .EQ. 2) GO TO 625
      POR=EP(J)
      PORR=EPR(J)
      PNU=PNC(J)
      US=USA(J)
  625  R=FLOAT(J-1)*DR
      IF (I .GT. 2) GO TO 630
C
C FIND E(R)
      ZP=PT*(1.-R)/DP
      POP =0.4+0.3*(EXP(-3.5*ZR)+COS(6.28*ZR)*EXP(-0.8*ZR))
      PORP1=1.05*EXP(-3.5*ZR)
      PORP2=1.384*SIN(6.28*ZR)*EXP(-0.8*ZR)
```

```
PORR3=0.24*COS(8.28*ZR)*EXP(-0.8*ZR)
PORR=RT*(PORR1+PORR2+PORR3)/DP
EPOR(J)=POR
EPRI(J)=PORR
C 627 R= FLDAT(J-1)+DP
C
IF (MR .EQ. 1) GO TO 90
IF (MR .EQ. 3) GO TO 85
US=2.+(1.-R**2.)
GO TO 90
85 FLD=C.078/(RE*(3.25))
REF=SQRT(FLD/2.)
REF=REF*PFLD
YP=REF***(1.-R)
C
PA=1.-3./REF
RB=1.-5./REF
C
IF (R .LT. RA) GO TO 86
US=REFL*D(5.5+2.5*ALOG(YP)*(1.5*(1.+R))/(1.+2.*R*R)))
GO TO 90
86 IF (R .LT. RB) GO TO 87
US=REFL*D(-3.05+5.*ALOG(YP))
GO TO 90
C 87 US=REFL*YP
90 USAK(J)=US
REB=RE*DP*US/RT
C FIND NU(RE,E(R))
C
C=1.-POR
D2=C**0.33333
D1=2.-3.*D2+3.*D2**5.-2.*D2**6.
PNH=1.6*((REB+PR/(POR*D1))***(1.-C**1.66667))**0.33333
C
PN(J)=PNH
C CALCULATE COEFFICIENTS IN EQUATIONS
C
630 AA1=RT*(POR+PR*E/VIS)/(RE*PR*HT*HT)
AA2=RT*(1.-POR)*TKR/(RE*PR*HT*HT)
CC1=RT*(POR+PR*E/VIS)/(RE*PR*RT*RT)
CC2=RT*(1.-POR)*TKR/(RE*PR*RT*RT)
H=6*(1.-POR)*EN0*RT/(RE*PR*DP*DP)
D=RT*TP*(1.-POR)/(RE*PR*TKG*T0)
V1=-CC1/R-RT*POR/(RE*PR*RT*RT)+VS/RT
V2=-CC2/R+RT*POR/(RE*PR*RT*RT)
U1=US/HT
U2=0.
C
A1(J)=-CC1/DR/DR-V1/DR/2.
B1(J)=2.*(AA1/DX/DX+CC1/DR/DR)+H+U1/DX
C1(J)=-CC1/DR/DR+V1/DR/2.
D1(J)=H
E1(J)=W1(IM1,J)*(AA1/DX/DX+U1/DX)+W1(IP1,J)*(AA1/DX/DX)
C
A2(J)=-CC2/DR/DR-V2/DR/2.
B2(J)=2.*(AA2/DX/DX+CC2/DR/DR)+H+U2/DX
C2(J)=-CC2/DR/DR+V2/DR/2.
D2(J)=H
E2(J)=W2(IM1,J)*(AA2/DX/DX+U2/DX)+W2(IP1,J)*(AA2/DX/DX)+R
C
20 CONTINUE
C ADJUST COEFFICIENTS SO AS TO SATISFY BOUNDARY CONDITIONS
C
B1(2)=B1(2)+A1(2)
B2(2)=B2(2)+A2(2)
B1(N1)=B1(N1)+C1(N1)/(1.+DR*RT*RNGW)
E1(N1)=E1(N1)-C1(N1)+DR*RT*RNGW*TA/(T0*(1.+DR*RT*RNGW))
B2(N1)=B2(N1)+C2(N1)/(1.+DR*RT*RNSW)
E2(N1)=E2(N1)-C2(N1)+DR*RT*RNSW*TA/(T0*(1.+DR*RT*RNSW))
C EXECUTE SOLUTION TECHNIQUE TO SOLVE COUPLED TRIDIAGONAL SYSTEM
C
CALL TRISLU (NMAX,SOLN1,SOLN2)
C EXECUTE RELAXATION TECHNIQUE IN ORDER TO UPDATE UNKNOWN VALUES
```

```
DO 30 J=2,N1
  SN1=W1(I,J)+WE*(SOLN1(I,J)-W1(I,J))
  SN2=W2(I,J)+WE*(SOLN2(I,J)-W2(I,J))
  ER1=ABS(SN1-SOLN1(I,J))
  ER2=ABS(SN2-SOLN2(I,J))
  DT1=DT1+ER1/5
  DT2=DT2+ER2/5
  FIND MAXIMUM ERROR IN THE NET AND ITS POSITION
  CALL CONVZ(I,J,ER1,ER2,L11,L12,LJ1,LJ2,DER1,DER2)
  W1(I,J)=SN1
  W2(I,J)=SN2
  30 CONTINUE
  T1(I,1)=W1(I,1)
  W2(I,1)=W2(I,1)
  W1(I,NMAX)=W1(I,N1)+DR*RT*RNG0*TA/T0/(1.+DR*RT*RNG0)
  W2(I,NMAX)=W2(I,N1)+DR*RT*RNG0*TA/T0/(1.+DR*RT*RNG0)
  10 CONTINUE
  DO 35 J=1,NMAX
  W1(NMAX,J)=W1(N1,J)
  W2(NMAX,J)=W2(N1,J)
  W1(I,J)=1.
  W2(I,J)=(DX+HT*RNG0+W2(2,J))/((1.+DX+HT*RNG0))
  35 CONTINUE
  IF (J99 .LE. 30) GO TO 38
  GO TO 39
  38 WRITE(108,300) J99,L11,LJ1,DER1,L12,LJ2,DER2
  39 FORMAT(1X,2HE, 13,3H X=, 12,3H R=, 12, 3H ERMAX1=, E12.6,
  1 2X,2HE=, 12,3H R=, 12, 3H ERMAX2=, E12.6,/)
  400 FORMAT(1X,3HE,RAYG1=, E12.6,10H ERAYGE=, E12.6,/)
  39 CONTINUE
  IF (J99 .GT. J99MAX) GO TO 40
  IF (DT1 .GT. EPS) GO TO 7
  IF (DT2 .GT. EPS) GO TO 7
  40 CONTINUE
  IF (J99 .LE. 30) GO TO 45
  WRITE(108,300) J99,L11,LJ1,DER1,L12,LJ2,DER2
  WRITE(108,400) DT1,DT2
  45 CONTINUE
  WRITE(108,500) (USA(J),J=2,N1)
  WRITE(108,500) (EP(J),J=2,N1)
  WRITE(108,500) (PN(J),J=2,N1)
  THE SOLUTION FOLLOWS
  450 WRITE(108,450)
  FORMAT(7,12,47HTEMPERATURE DISTRIBUTIONS FOR THE GAS AND SOLID,/7)
  DO 55 K=1,NMAX
  L=NMAX-K+1
  WRITE(108,500) (W1(L,J),J=1,NMAX)
  WRITE(108,500) (W2(L,J),J=1,NMAX)
  500 FORMAT(2X,11F9.4,/7)
  800 FORMAT(1X,1H+,11F0.4,/7)
  55 CONTINUE
  2
  460 WRITE(108,460)
  FORMAT(1H1)
  MSUP=NMAX+1
  NSUP=NMAX+1
  DO 948 I=2,MSUP
  DO 943 J=2,NSUP
  Z(I,J)=W1(I-1,J-1)
  948 CONTINUE
  CALL BUNIV
  DO 950 I=2,MSUP
  DO 950 J=2,NSUP
  Z(I,J)=W2(I-1,J-1)
  950 CONTINUE
  CALL BUNIV
  END
```

HOT

-29-

RT	HT	Re	Fr	Nu	KF	KB/KG	1000E+00	1000E+00	Le'	kin. vis.
5000E-01	1000E+00	.5000E+04	.7200E+00	5144E+02	.2500E-01	1000E+03	487081	2000E+02	1532E-04	
.3100E+02	2100E+02	1.0E+03	2030E+02	1000E+03	.1100E+01	1000E+01	2000E+02	1500E+02	4000E+06	3000E+01
1000E+11	1000E+11	1000E+11	1000E+01	1000E+01						

K= 1 X=30 R=20 EPPMAX1= 227570E-01 X=30 R=20 EPPMAX2= 192099E-01
EPPAVG1= 67349PE-02 EPPAVG2= 113569E-01
K= 2 X=30 R=18 EPPMAX1= 962830E-02 X=30 R=19 EPPMAX2= 122167E-01
EPPAVG1= 499500E-02 EPPAVG2= 887595E-02
K= 3 X=30 R=15 EPPMAX1= 789356E-02 X=30 R=16 EPPMAX2= 101500E-01
EPPAVG1= 378989E-02 EPPAVG2= 700379E-02
K= 4 X=30 R=15 EPPMAX1= 64792EE-02 X=30 R=14 EPPMAX2= 86450EE-02
EPPAVG1= 293180E-02 EPPAVG2= 555242E-02
K= 5 X=30 R=15 EPPMAX1= 525570E-02 X=30 R=17 EPPMAX2= 737190E-02
EPPAVG1= 222050E-02 EPPAVG2= 440557E-02
K= 6 X=30 R=15 EPPMAX1= 422668E-02 X=30 R=13 EPPMAX2= 621414E-02
EPPAVG1= 177619E-02 EPPAVG2= 319762E-02
K= 7 X=30 R=11 EPPMAX1= 343132E-01 X=30 R=12 EPPMAX2= 513894E-01
EPPAVG1= 133924E-02 EPPAVG2= 2772E0E-02
K= 8 X=30 R=11 EPPMAX1= 219712E-02 X=30 R=12 EPPMAX2= 430393E-02
EPPAVG1= 109493E-02 EPPAVG2= 210334E-02
K= 9 X=30 R=11 EPPMAX1= 226794E-02 X=30 R=10 EPPMAX2= 356102E-02
EPPAVG1= 948227E-02 EPPAVG2= 124735E-02
K= 10 X=30 R=11 EPPMAX1= 182915E-02 X=30 R=10 EPPMAX2= 293064E-02
EPPAVG1= 163450E-03 EPPAVG2= 178472E-02
K= 11 X=30 R=11 EPPMAX1= 145981E-02 X=30 R= 9 EPPMAX2= 240421E-02
EPPAVG1= 518972E-03 EPPAVG2= 109641E-02
K= 12 X=30 R=11 EPPMAX1= 117697E-02 X=30 R= 9 EPPMAX2= 19e26eE-02
EPPAVG1= 405937E-03 EPPAVG2= 867278E-03
K= 13 X=30 R=11 EPPMAX1= 924389E-03 X=30 R= 9 EPPMAX2= 159454E-02
EPPAVG1= 717429E-03 EPPAVG2= 665192E-03
K= 14 X=30 R=11 EPPMAX1= 747691E-03 X=30 R= 9 EPPMAX2= 129032E-02
EPPAVG1= 246707E-03 EPPAVG2= 941550E-03
K= 15 X=30 R=11 EPPMAX1= 594132E-03 X=30 R= 9 EPPMAX2= 104237E-02
EPPAVG1= 194202E-03 EPPAVG2= 427185E-03
K= 16 X=30 R= 7 EPPMAX1= 473022E-03 X=30 R= 6 EPPMAX2= 840187E-03
EPPAVG1= 151744E-03 EPPAVG2= 336746E-03
K= 17 X=30 R= 7 EPPMAX1= 377655E-03 X=30 R= 6 EPPMAX2= 676155E-03
EPPAVG1= 118594E-03 EPPAVG2= 265216E-03
K= 18 X=30 R= 7 EPPMAX1= 302407E-03 X=30 R= 5 EPPMAX2= 543594E-03
EPPAVG1= 926772E-04 EPPAVG2= 308727E-03
K= 19 X=30 R= 7 EPPMAX1= 232419E-03 X=30 R= 5 EPPMAX2= 435829E-03

ERRAVOL = 1E4163E-03
X=20 RF = 5 ERMAX1= 103812E-03 X=20 RF = 5 ERMAX2= 349045E-03
EFFAVOL= 544071E-04 ERRAVOL= 103005E-03
ERRAVOL = 103005E-04 ERRAVOL= 103005E-03
EFFAVOL= 439734E-04 ERRAVOL= 101260E-03
X=20 RF = 5 ERMAX1= 11825CE-03 X=20 RF = 5 ERMAX2= 22220CE-03
EFFAVOL= 543599E-04 ERRAVOL= 704771E-04

1 4452	1 4414	1 4251	1 4263	1 4152	1 4020	1 3966	1 3891	1 3495	1 3273	1 3017	
1 2271	1 2475	1 2141	1 1757	1 1303	1 0737	0 9963	0 7646	0 4172	0 3997	0 3534	0 4005
0 3838	0 3918	0 4061	0 4122	0 3998	0 3818	0 4002	0 4172	0 3997	0 3534	0 4005	
0 4619	0 4693	0 5112	0 4042	0 5439	0 4213	0 2510	0 5253	0 4256	64 5041	58 6477	
0 5307	0 5321	0 5462	0 4451	0 5277	0 3235	0 3818	0 4017	0 4256	64 5041	58 6477	
17 2076	15 1572	73 5594	54 1422	37 4112	50 0517	87 2457	34 2975				

* TEMPERATURE DISTRIBUTIONS FOR THE GAS AND SOLID

1 5711	1 5781	1 5807	1 5816	1 5819	1 5838	1 5961	1 5969	1 6114	1 6240		
1 6214	1 6171	1 6320	1 6448	1 6179	1 5842	1 5699	1 5443	1 4449	1 3733		
1 5810	1 5610	1 5619	1 5847	1 8682	1 8710	1 8742	1 8799	1 8860	1 8894		
*	1 5975	1 5943	1 8848	1 6696	1 8562	1 8236	1 7609	1 6996	1 5279	1 3733	
*	1 5711	1 5781	1 5807	1 5816	1 5819	1 5838	1 5961	1 5969	1 6114	1 6240	
*	1 5214	1 6171	1 6320	1 6448	1 6179	1 5842	1 5699	1 5443	1 4449	1 3733	
*	1 5810	1 5610	1 5619	1 5847	1 8682	1 8710	1 8742	1 8799	1 8860	1 8894	
*	1 3925	1 2943	1 8848	1 6696	1 8562	1 8236	1 7609	1 6996	1 5279	1 3733	
*	1 5615	1 5615	1 5631	1 5629	1 5641	1 5709	1 5782	1 5908	1 5934	1 6063	
*	1 6017	1 5292	1 6155	1 6225	1 6036	1 5716	1 5601	1 5378	1 4415	1 3333	
*	1 8512	1 8522	1 8531	1 6559	1 8594	1 8622	1 8653	1 8711	1 8773	1 8807	
*	1 2871	1 2887	1 2770	1 6623	1 8496	1 8132	1 7566	1 6961	1 5255	1 3733	
*	1 5416	1 5413	1 5452	1 5429	1 5441	1 5508	1 5581	1 5587	1 5604	1 5731	1 5861
*	1 5816	1 5795	1 5565	1 6118	1 5871	1 5570	1 5486	1 5300	1 4375	1 3333	
*	1 8301	1 6381	1 8330	1 6418	1 8453	1 8430	1 8511	1 8570	1 8632	1 8657	1 8668
*	1 8715	1 2737	1 8646	1 6525	1 8391	1 8024	1 7497	1 6906	1 6215	1 3333	
*	1 5211	1 5211	1 5227	1 5223	1 5234	1 5301	1 5373	1 5378	1 5394	1 5521	1 5651
*	1 5618	1 5591	1 5766	1 5971	1 5697	1 5416	1 5364	1 5216	1 4331	1 3333	
*	1 8210	1 8210	1 8220	1 6247	1 8282	1 8309	1 9340	1 8398	1 8461	1 8486	1 8500
*	1 8551	1 2579	1 8495	1 6362	1 8261	1 7986	1 7412	1 6838	1 6165	1 3333	
*	1 5004	1 5004	1 5019	1 5015	1 5025	1 5091	1 5162	1 5166	1 5181	1 5307	1 5438
*	1 5405	1 5381	1 5563	1 5729	1 5518	1 5257	1 5238	1 5128	1 4285	1 3333	
*	1 3023	1 3023	1 8032	1 6059	1 8094	1 8120	1 8151	1 8210	1 8273	1 8299	1 8314
*	1 9319	1 8403	1 8728	1 6204	1 8118	1 7865	1 7317	1 6762	1 6110	1 3333	
*	1 4766	1 4796	1 4311	1 4806	1 4815	1 4890	1 4950	1 4952	1 4966	1 5091	1 5223
*	1 5120	1 5169	1 5356	1 5542	1 5333	1 5093	1 5106	1 5036	1 4237	1 3333	
*	1 7826	1 7926	1 7835	1 7862	1 7894	1 7922	1 7952	1 8011	1 8074	1 8101	1 8178
*	1 3177	1 3218	1 8150	1 6077	1 7965	1 7736	1 7215	1 6680	1 6050	1 3333	
*	1 4587	1 4587	1 4601	1 4596	1 4504	1 4638	1 4736	1 4737	1 4749	1 4874	1 5005
1 4972	1 4952	1 5146	1 5342	1 5144	1 4924	1 4970	1 4941	1 4187	1 3333		

*	1 7624	1 7624	1 7632	1 7659	1 7693	1 7718	1 7747	1 7806	1 7870	1 7898	1 7916
*	1 7979	1 8025	1 7960	1 7863	1 7805	1 7601	1 7108	1 6594	1 5987	1 3222	1 4786
*	1 4777	1 4377	1 4391	1 4325	1 4392	1 4455	1 4522	1 4521	1 4532	1 4656	1 4786
*	1 4752	1 4734	1 4933	1 5137	1 4951	1 4751	1 4829	1 4842	1 4175	1 3223	1 7710
*	1 7418	1 7418	1 7427	1 7453	1 7486	1 7510	1 7540	1 7598	1 7662	1 7690	1 7710
*	1 7776	1 7823	1 7777	1 7684	1 7641	1 7461	1 6997	1 6505	1 5921	1 3222	1 4561
*	1 4117	1 4167	1 4191	1 4174	1 4181	1 4242	1 4308	1 4305	1 4315	1 4437	1 4561
*	1 4572	1 4514	1 4716	1 4923	1 4753	1 4572	1 4684	1 4739	1 4090	1 3223	1 7501
*	1 7211	1 7211	1 7219	1 7245	1 7279	1 7301	1 7317	1 7388	1 7452	1 7480	1 7501
*	1 7570	1 7622	1 7584	1 7580	1 7472	1 7316	1 6882	1 6412	1 5952	1 3222	1 4345
*	1 3227	1 3957	1 3971	1 3963	1 3969	1 4029	1 4092	1 4089	1 4096	1 4217	1 4345
*	1 4310	1 4281	1 4493	1 4717	1 4551	1 4338	1 4537	1 4637	1 4624	1 3223	1 7291
*	1 7003	1 7003	1 7011	1 7036	1 7066	1 7091	1 7119	1 7176	1 7240	1 7269	1 7291
*	1 7352	1 7424	1 7388	1 7313	1 7300	1 7168	1 6763	1 6316	1 5782	1 3222	1 4122
*	1 7317	1 3747	1 3761	1 3752	1 3756	1 3815	1 3878	1 3972	1 3998	1 4122	
*	1 4016	1 4067	1 4276	1 4502	1 4344	1 4199	1 4377	1 4521	1 3965	1 3223	1 7078
*	1 4774	1 6784	1 6902	1 6826	1 6958	1 6880	1 6907	1 6963	1 7026	1 7055	1 7078
*	1 7151	1 7213	1 7189	1 7123	1 7123	1 7016	1 6640	1 6217	1 5709	1 3222	1 3900
*	1 3539	1 3539	1 3550	1 3541	1 3544	1 3602	1 3663	1 3655	1 3658	1 3775	1 3900
*	1 3841	1 3842	1 4052	1 4223	1 4132	1 4004	1 4215	1 4405	1 3903	1 3323	1 6844
*	1 4575	1 6585	1 6592	1 6616	1 6647	1 6668	1 6694	1 6750	1 6812	1 6840	1 6844
*	1 6478	1 7010	1 6987	1 6929	1 6943	1 6860	1 6514	1 6114	1 5633	1 3223	1 3678
*	1 3329	1 3329	1 3340	1 3381	1 3332	1 3398	1 3448	1 3438	1 3439	1 3553	1 3678
*	1 3635	1 3614	1 3926	1 4061	1 3916	1 3803	1 4047	1 4283	1 3828	1 3223	1 6646
*	1 6375	1 6375	1 6382	1 6406	1 6436	1 6456	1 6481	1 6535	1 6587	1 6624	1 6646
*	1 6724	1 6793	1 6781	1 6731	1 6759	1 6700	1 6383	1 6008	1 5554	1 3223	1 3452
*	1 3119	1 3119	1 3130	1 3120	1 3120	1 3175	1 3232	1 3221	1 3220	1 3331	1 3452
*	1 3409	1 3386	1 3597	1 3835	1 3695	1 3596	1 3872	1 4156	1 3769	1 3333	1 6431
*	1 6156	1 6163	1 6172	1 6195	1 6224	1 6243	1 6267	1 6320	1 6381	1 6408	1 6431
*	1 6508	1 6586	1 6573	1 6530	1 6571	1 6535	1 6248	1 5897	1 5472	1 3223	1 3227
*	1 2908	1 2908	1 2920	1 2909	1 2909	1 2961	1 3017	1 3004	1 3000	1 3109	1 3227
*	1 3161	1 3156	1 3366	1 3696	1 3470	1 3393	1 3689	1 4021	1 3696	1 3333	1 6212
*	1 5956	1 5956	1 5962	1 5984	1 6012	1 6030	1 6053	1 6105	1 6164	1 6190	1 6212
*	1 6230	1 6370	1 6362	1 6326	1 6379	1 6366	1 6109	1 5782	1 5387	1 3333	1 3001
*	1 2639	1 2699	1 2710	1 2698	1 2697	1 2748	1 2802	1 2786	1 2780	1 2886	1 3001
*	1 2953	1 2925	1 3133	1 3373	1 3239	1 3163	1 3498	1 3879	1 3618	1 3333	1 5993
*	1 5746	1 5746	1 5751	1 5773	1 5800	1 5817	1 5838	1 5889	1 5946	1 5971	1 5993
*	1 6071	1 6153	1 6148	1 6118	1 6183	1 6192	1 5964	1 5662	1 5298	1 3333	1 2775
*	1 2489	1 2489	1 2500	1 2488	1 2485	1 2535	1 2587	1 2569	1 2561	1 2664	1 2775
*	1 2724	1 2693	1 2998	1 3138	1 3005	1 2936	1 3298	1 3729	1 3534	1 3333	1 5772
*	1 5535	1 5535	1 5541	1 5562	1 5588	1 5603	1 5623	1 5672	1 5728	1 5751	1 5772
*	1 5850	1 5933	1 5931	1 5906	1 5982	1 6013	1 5813	1 5536	1 5204	1 3333	1 2549
*	1 2260	1 2280	1 2291	1 2278	1 2274	1 2321	1 2371	1 2352	1 2341	1 2441	1 2549
*	1 2495	1 2460	1 2661	1 2899	1 2765	1 2703	1 3089	1 3568	1 3444	1 3333	1 5549
*	1 5325	1 5325	1 5330	1 5350	1 5375	1 5389	1 5407	1 5455	1 5508	1 5530	1 5549

*	1.5617	1.5710	1.5711	1.5691	1.5776	1.5628	1.5655	1.5404	1.5106	1.3333	1.2217	1.2322
*	1.2251	1.2071	1.2081	1.2068	1.2063	1.2108	1.2156	1.2135	1.2122	1.3333	1.2217	1.2322
*	1.2256	1.2227	1.2423	1.2657	1.2521	1.2463	1.2869	1.3395	1.3345	1.3333	1.5307	1.5325
*	1.5117	1.5113	1.5118	1.5138	1.5162	1.5174	1.5190	1.5236	1.5238	1.5307	1.5325	
*	1.5432	1.5485	1.5487	1.5471	1.5566	1.5676	1.5491	1.5265	1.5002	1.3333	1.1994	1.2095
*	1.1992	1.1962	1.1972	1.1859	1.1852	1.1895	1.1941	1.1919	1.1903	1.3333		
*	1.2076	1.1993	1.2183	1.2412	1.2275	1.2216	1.2638	1.3209	1.3237	1.3333	1.5083	1.5093
*	1.4901	1.4901	1.4905	1.4924	1.4947	1.4958	1.4973	1.5017	1.5066	1.5083		
*	1.5125	1.5257	1.5260	1.5246	1.5349	1.5438	1.5318	1.5117	1.4891	1.3333	1.1771	1.1868
*	1.1603	1.1653	1.1663	1.1649	1.1642	1.1683	1.1727	1.1703	1.1685	1.3333		
*	1.1807	1.1760	1.1942	1.2164	1.2024	1.1965	1.2394	1.3006	1.3116	1.3333		
*	1.4686	1.4686	1.4690	1.4709	1.4730	1.4739	1.4753	1.4795	1.4842	1.4856	1.4870	
*	1.4944	1.5025	1.5027	1.5016	1.5126	1.5231	1.5135	1.4959	1.4772	1.3333	1.1548	1.1640
*	1.1445	1.1445	1.1455	1.1441	1.1433	1.1471	1.1512	1.1487	1.1467	1.3333		
*	1.1578	1.1529	1.1700	1.1913	1.1771	1.1708	1.2138	1.2783	1.2979	1.3333	1.4625	1.4636
*	1.4488	1.4468	1.4472	1.4489	1.4510	1.4517	1.4528	1.4569	1.4613	1.4625		
*	1.4708	1.4787	1.4793	1.4729	1.4894	1.5013	1.4939	1.4787	1.4643	1.3333	1.1251	1.1326
*	1.1237	1.1237	1.1247	1.1233	1.1225	1.1259	1.1298	1.1273	1.1251	1.3333		
*	1.1350	1.1293	1.1457	1.1660	1.1517	1.1450	1.1869	1.2537	1.2821	1.3333	1.4385	1.4394
*	1.4243	1.4243	1.4246	1.4263	1.4282	1.4288	1.4297	1.4335	1.4377	1.4385		
*	1.4463	1.4549	1.4539	1.4529	1.4650	1.4781	1.4727	1.4599	1.4499	1.3333	1.1105	1.1183
*	1.1030	1.1030	1.1040	1.1027	1.1018	1.1049	1.1084	1.1060	1.1038	1.3333		
*	1.1124	1.1071	1.1215	1.1403	1.1263	1.1191	1.1587	1.2262	1.2638	1.3333	1.4131	1.4137
*	1.4004	1.4004	1.4007	1.4023	1.4040	1.4044	1.4052	1.4087	1.4126	1.4131		
*	1.4203	1.4277	1.4272	1.4262	1.4386	1.4527	1.4491	1.4387	1.4337	1.3333	1.0886	1.0956
*	1.0816	1.0826	1.0935	1.0824	1.0814	1.0841	1.0872	1.0850	1.0827	1.3333		
*	1.0900	1.0849	1.0975	1.1145	1.1011	1.0935	1.1294	1.1953	1.2419	1.3333	1.3851	1.3853
*	1.3740	1.3740	1.3742	1.3757	1.3773	1.3775	1.3780	1.3813	1.3849	1.3851		
*	1.3916	1.3985	1.3977	1.3965	1.4090	1.4239	1.4219	1.4140	1.4144	1.3333	1.0671	1.0731
*	1.0626	1.0626	1.0634	1.0624	1.0615	1.0638	1.0664	1.0644	1.0623	1.3333		
*	1.0681	1.0634	1.0738	1.0895	1.0765	1.0689	1.0994	1.1605	1.2151	1.3333	1.3520	1.3519
*	1.3426	1.3426	1.3428	1.3442	1.3456	1.3457	1.3460	1.3490	1.3522	1.3520		
*	1.3577	1.3640	1.3629	1.3615	1.3739	1.3890	1.3886	1.3834	1.3903	1.3333	1.0464	1.0511
*	1.0433	1.0433	1.0440	1.0432	1.0425	1.0441	1.0462	1.0446	1.0428	1.3333		
*	1.0472	1.0432	1.0511	1.0627	1.0523	1.0450	1.0694	1.1214	1.1816	1.3333	1.3096	1.3092
*	1.3021	1.3021	1.3023	1.3035	1.3047	1.3046	1.3047	1.3073	1.3100	1.3333		
*	1.3142	1.3197	1.3193	1.3168	1.3284	1.3431	1.3444	1.3425	1.3570	1.3333	1.0273	1.0305
*	1.0255	1.0255	1.0260	1.0254	1.0249	1.0260	1.0273	1.0262	1.0250	1.3333		
*	1.0277	1.0249	1.0300	1.0379	1.0310	1.0259	1.0409	1.0787	1.1383	1.3333	1.2494	1.2489
*	1.2442	1.2442	1.2443	1.2453	1.2462	1.2460	1.2460	1.2501	1.2501	1.3333		
*	1.2529	1.2572	1.2556	1.2541	1.2639	1.2768	1.2797	1.2817	1.3054	1.3333	1.0110	1.0125
*	1.0103	1.0103	1.0105	1.0103	1.0100	1.0105	1.0111	1.0106	1.0100	1.3333		
*	1.0112	1.0098	1.0121	1.0158	1.0125	1.0099	1.0164	1.0353	1.0803	1.3333	1.1561	1.1556
*	1.1534	1.1534	1.1534	1.1539	1.1545	1.1543	1.1554	1.1566	1.1566	1.3333		
*	1.1580	1.1605	1.1593	1.1581	1.1643	1.1727	1.1759	1.1810	1.2113	1.3333	1.0000	1.0000
*	1.0000	1.0000	1.0000	1.0000	1.0000	1.0000	1.0000	1.0000	1.0000	1.3333		

DP = 0.0050000 RT = 0.0500000 HT = 0.1000000
 DENS = .1211E+01 VISC0 = .1940E-04 RET = 4000.00 PR = 0.72
 GK = 0.02500 SK = 0.75000 Q = 399999 98
 TEX = 20.0 T0=15.00
 M= 31 N= 31 NF= 100 NG= 20
 OVER RELAXATION FACTOR= 1.40 TEST= 0.01
 NJNG = ***** QNG = 0.00
 NJNS = ***** QNS = 0.00
 BLOKAGE 1*
 PMINAO = 0.100 PMAXAO = 0.400
 I11AO = 11 I22AO = 21 J11AO = 11 J4AO = 21
 BLOKAGE 2*
 PMINAI = 0.100 PMAXAI = 0.400
 I11AI = 50 I22AI = 50 J11AI = 50 J4AI = 50

N= 1 DT =	.736E-02	DER =	.665E-01	POUR I = 20 ET J = 25
N= 2 DT =	.362E-02	DER =	.162E-01	POUR I = 18 ET J = 27
N= 3 DT =	.213E-02	DER =	.729E-02	POUR I = 16 ET J = 28
N= 4 DT =	.161E-02	DER =	.819E-02	POUR I = 19 ET J = 19
N= 5 DT =	.144E-02	DER =	.921E-02	POUR I = 18 ET J = 20
N= 6 DT =	.127E-02	DER =	.787E-02	POUR I = 17 ET J = 20
N= 7 DT =	.113E-02	DER =	.741E-02	POUR I = 16 ET J = 20
N= 8 DT =	.102E-02	DER =	.695E-02	POUR I = 16 ET J = 20
N= 9 DT =	.930E-03	DER =	.651E-02	POUR I = 15 ET J = 20
N= 10 DT =	.860E-03	DER =	.611E-02	POUR I = 15 ET J = 20
N= 11 DT =	.804E-03	DER =	.579E-02	POUR I = 14 ET J = 20
N= 12 DT =	.756E-03	DER =	.554E-02	POUR I = 13 ET J = 20
N= 13 DT =	.715E-03	DER =	.532E-02	POUR I = 13 ET J = 20
N= 14 DT =	.678E-03	DER =	.510E-02	POUR I = 13 ET J = 20
N= 15 DT =	.644E-03	DER =	.486E-02	POUR I = 13 ET J = 20
N= 16 DT =	.612E-03	DER =	.462E-02	POUR I = 13 ET J = 20
N= 17 DT =	.592E-03	DER =	.437E-02	POUR I = 13 ET J = 20
N= 18 DT =	.553E-03	DER =	.422E-02	POUR I = 12 ET J = 20
N= 19 DT =	.526E-03	DER =	.409E-02	POUR I = 12 ET J = 20
N= 20 DT =	.501E-03	DER =	.397E-02	POUR I = 12 ET J = 20
N= 21 DT =	.479E-03	DER =	.386E-02	POUR I = 12 ET J = 20
N= 22 DT =	.460E-03	DER =	.376E-02	POUR I = 12 ET J = 20
N= 23 DT =	.307E-03	DER =	.219E-02	POUR I = 11 ET J = 21
N= 24 DT =	.211E-03	DER =	.142E-02	POUR I = 11 ET J = 22
N= 25 DT =	.210E-03	DER =	.174E-02	POUR I = 10 ET J = 20
N= 26 DT =	.197E-03	DER =	.910E-03	POUR I = 10 ET J = 20
N= 27 DT =	.160E-03	DER =	.741E-03	POUR I = 12 ET J = 20
N= 28 DT =	.161E-03	DER =	.781E-03	POUR I = 16 ET J = 19
N= 29 DT =	.154E-03	DER =	.697E-03	POUR I = 15 ET J = 19
N= 30 DT =	.142E-03	DER =	.637E-03	POUR I = 14 ET J = 19
N= 31 DT =	.136E-03	DER =	.636E-03	POUR I = 13 ET J = 19
N= 32 DT =	.132E-03	DER =	.592E-03	POUR I = 15 ET J = 19
N= 33 DT =	.126E-03	DER =	.547E-03	POUR I = 14 ET J = 19
N= 34 DT =	.121E-03	DER =	.564E-03	POUR I = 13 ET J = 19
N= 35 DT =	.117E-03	DER =	.507E-03	POUR I = 12 ET J = 19
N= 36 DT =	.113E-03	DER =	.468E-03	POUR I = 14 ET J = 19
N= 37 DT =	.109E-03	DER =	.478E-03	POUR I = 13 ET J = 19
N= 38 DT =	.106E-03	DER =	.451E-03	POUR I = 13 ET J = 16
N= 39 DT =	.102E-03	DER =	.420E-03	POUR I = 13 ET J = 16
N= 40 DT =	.983E-04	DER =	.415E-03	POUR I = 13 ET J = 19

VITESSE AXIALE

1 4530420	1 4524543	1 4506978	1 4477825	1 4437258	1 4385521	1 4322889	1 4249676	1 4166164	1 4072627
1 3969344	1 3956447	1 3734072	1 3602191	1 3460634	1 3309163	1 3147211	1 2974054	1 2788594	1 2589341
1 2374218	1 2140512	1 1884165	1 1599341	1 1278266	1 0907173	1 0664109	0 9616390	0 8187643	0 5745172
0 0030169	1 2708390	1 2708390	1 2693318	1 2669766	1 2636840	1 2594956	1 2544310	1 2485200	1 2417889
1 2259922	1 2170089	1 2073404	1 1970443	1 1861688	1 1747807	1 1629802	1 1508889	1 1387509	1 1268586
1 115331	1 1062765	1 0997820	1 0984880	1 1060476	1 1285460	1 1731845	1 0722443	0 9033707	0 8336806
0 0020000	1 223070	1 2230700	1 2218362	1 2199414	1 2133337	1 2140238	1 2100331	1 2034002	1 2001362
1 1943424	1 1980364	1 1912079	1 1739957	1 1664426	1 1596237	1 1506176	1 1420332	1 1344993	1 1265454
1 1121595	1 1058742	1 1003476	1 0954249	1 0904026	1 0833615	1 0697509	1 0427028	1 0129136	0 9948704
0 0030000	1 1942108	1 1942108	1 1842228	1 1819506	1 1798924	1 1773002	1 1741877	1 1796007	1 1665905
1 1622027	1 1575127	1 1525571	1 1474150	1 1421478	1 1366823	1 1313123	1 1262691	1 1211473	1 1161975
1 1114233	1 1068499	1 1024010	1 0979480	1 0932684	1 0880309	1 0918356	1 0743856	1 0659297	1 0583035
0 0030000	1 1527836	1 1527836	1 1522311	1 1511022	1 1494339	1 1472976	1 1447493	1 1418569	1 1386859
1 1353059	1 1317950	1 1282194	1 1246699	1 1212446	1 1179113	1 1148101	1 1119479	1 1093456	1 1070013
1 1046824	1 1028416	1 1010969	1 0992491	1 0975012	1 0951746	1 0928249	1 0903102	1 0878307	1 085117
1 0843146	0 0000000	1 1290234	1 1290234	1 1279231	1 1266077	1 1248636	1 1226928	1 1201632	1 1173582
1 1113322	1 1083394	1 1050598	1 1029577	1 1007929	1 0990870	1 0979033	1 0972750	1 0971963	1 0976398
1 0935379	1 0927665	1 1012042	1 1026937	1 1041021	1 1053216	1 1062860	1 1065727	1 1074054	1 1076450
1 1072613	0 0000000	1 1113244	1 1113244	1 1098035	1 1090052	1 1065304	1 1034593	1 1000204	1 0962284
1 0922837	1 0883963	1 0847491	1 0815638	1 0790479	1 0773814	1 0767090	1 0771370	1 0767308	1 0814869
1 0900766	1 0255013	1 1012840	1 1070307	1 1126119	1 1176097	1 1219245	1 1254501	1 1281598	1 1300582
1 1311718	0 0000000	1 1031473	1 1031473	1 1025792	1 10302672	1 0965139	1 0916126	1 0857832	1 0792601
1 0723378	1 0653930	1 0589151	1 0530984	1 0468633	1 0459602	1 0452187	1 0466509	1 0505372	1 0568076
1 0654060	1 0760272	1 0680956	1 0606516	1 1129534	1 1242771	1 1341810	1 1424506	1 1490405	1 1539984
1 1534069	0 0000003	1 1142159	1 1142159	1 1113822	1 1073273	1 1033258	1 0932624	1 0831255	1 0712177
1 0577202	1 0432768	1 0288250	1 0156059	1 0049134	0 9976622	0 9943343	0 9953857	1 0011959	1 0122573
1 0228543	1 0506469	1 0757971	1 1013108	1 1246490	1 1445034	1 1605805	1 1730945	1 1824834	1 1592223
1 1936938	1 1962336	0 0000000	1 1498487	1 1498487	1 1469853	1 1415040	1 1334342	1 1222047	1 1071384
1 0625869	1 0321908	0 9974039	0 9623960	0 93361224	0 9141794	0 9028546	0 8993519	0 8048650	0 9221041
1 0544805	1 0349075	1 9644829	1 1176362	1 1582106	1 1873472	1 2076998	1 2216985	1 2311688	1 2774657
1 2413979	1 2432663	0 0000030	1 2114096	1 2114096	1 2114155	1 2085302	1 2032092	1 1949188	1 1822881
1 1633334	1 1737137	1 06669295	1 0554684	0 8849590	0 7902928	0 783137	0 7219319	0 7033351	0 6983524
0 7879730	0 9442774	1 1146879	1 2075931	1 2523288	1 2749231	1 2665841	1 2926400	1 2957525	1 2973052
1 2920318	1 2983292	0 0000030	1 2866479	1 2866479	1 2898338	1 2959164	1 3000500	1 3059156	
1 3142234	1 3268566	1 3463492	1 3771641	0 8975745	0 3886543	0 3279743	0 3070248	0 2842963	0 2722265
1 2934785	0 3766772	1 0165805	1 5222681	1 4619160	1 4240682	1 3992548	1 3824224	1 3707459	1 3625842
1 35322960	1 35122113	0 0000000	1 3472176	1 3472176	1 3515747	1 3565600	1 3629067	1 3711959	1 3821487
1 3967520	1 4164275	1 4431775	1 4798868	1 0484922	0 3228217	0 0378934	0 0408711	0 0393838	0 0342552
0 0197931	0 3505821	1 1488914	1 5674912	1 51363736	1 4792327	1 4520884	1 4321387	1 4174718	1 4067948
1 3932357	1 3942164	1 3913572	0 0000000	1 3825226	1 3825226	1 3967819	1 3910705	1 3960898	1 4020979
1 4173849	1 4264488	1 4359312	1 442670	0 9935176	0 3025085	0 0465074	0 0434403	0 0408112	0 0385976
0 0370443	1 3221169	1 0629755	1 5026414	1 1681112	1 3228916	1 4590245	1 4469445	1 4369404	1 428386
1 9229198	1 4186272	1 163810	0 0000000	1 3981074	1 3951074	1 4018142	1 4051563	1 4085350	1 4122368
1 4161825	1 4201194	1 0239203	1 4268905	1 4288282	0 99793160	0 2976760	0 0468582	0 0442009	0 0418371
0 03320243	0 3147304	1 0407037	1 4778566	1 4719868	1 4649487	1 4575815	1 4505053	1 4441264	1 4387053
1 4344064	1 4313139	1 4294541	0 0000000	1 409064	1 409064	1 4041340	1 40706424	1 4099610	1 4129780
1 1157617	1 4186668	1 4207757	1 4224321	1 4231795	0 9751367	0 2961941	0 0466993	0 0442277	0 0419426
0 0359509	0 0379138	0 3130436	1 0358238	1 4719743	1 4677811	1 4526378	1 4570558	1 4514983	1 4463222
1 4331534	1 4354919	1 4339636	0 0000000	1 3932359	1 3932359	1 3963482	1 3997823	1 4032590	1 4070070
1 4109534	1 4149332	1 4186658	1 4217675	1 4232320	0 9759974	0 2963227	0 0465920	0 0439921	0 0416851
0 0333699	0 0379769	0 3149192	1 0414201	1 4785093	1 4730865	1 4661008	1 4587879	1 4517605	1 4454257

1	4400470	1	4257805	1	4327133	1	4308703	0	0000000	1	3724315	1	3724315	1	3762593	1	3805592	1	3955575	1	7916314
1	3327714	1	4069374	1	4161092	1	4255345	1	4340210	0	3863068	0	3001906	0	0459999	0	0420222	0	0406049		
0	0354545	0	0370524	0	3225043	1	0642392	1	3046223	1	432243	1	4732626	1	4614403	1	4494735	1	4393668		
1	321692	1	4237562	1	4216340	1	4192247	0	0000000	1	3322270	1	3322270	1	3364476	1	3412394	1	3475757		
1	3357873	1	3667463	1	3913794	1	4010543	1	4277601	1	4643461	1	0374802	0	3191739	0	0371053	0	0401182	0	0358402
0	0339856	0	01688291	0	3513977	1	1507308	1	5704280	1	5195990	1	4826965	1	4557457	1	4356357	1	4214420		
1	4138831	+1	4024123	+1	3984621	1	3956469	0	0000009	1	2677974	1	2677974	1	2704766	1	2730520	1	2762737		
1	1285038	1	2584381	1	2959242	1	3078243	1	3274336	1	3592975	0	8953388	0	3836028	0	3243636	0	3041073		
0	2821720	0	2718285	0	2903633	0	3776993	1	0190380	1	3260732	1	4661187	1	4285958	1	4040593	1	3874692	1	3760000
1	3680255	1	3625573	1	3589942	1	3569939	0	0000000	1	1887725	1	1987729	1	1880696	1	1853778	1	1804879		
1	1727220	1	1608271	1	1425716	1	1140225	1	0677785	0	8721716	0	7804468	0	7494507	0	7157722				
0	6988621	0	6956242	0	7197251	0	7882258	0	9467916	1	1193673	1	2120771	1	2574740	1	2807796	1	2927026		
1	2931446	1	3025649	1	3043654	1	3052690	1	3056737	0	0000000	(1226904	1	1226904	1	1203873	+1	11562134	1	1081922
1	0976629	+1	0873159	+1	0650134	+1	0415471	+1	0128850	0	9801596	0	9473441	+0	9209521	+0	9037250	0	8945397		
0	8931539	0	9027358	0	92201571	+0	9545184	+0	0058244	1	05629209	+1	1222821	+1	1632196	+1	1938120	+1	2143615		
1	2235832	1	2395704	+1	2462151	+1	2503988	+1	2526834	0	0020000	+1	0934819	+1	0834819	+1	0815626	+1	0775764		
1	0722864	1	0650458	1	0563733	+1	0455132	1	0336703	+1	0211259	+1	0087812	0	9978331	0	9895205	0	9847133	0	1818784
0	3873939	0	9356729	1	0091556	1	0260645	1	0520095	1	0791004	1	1063051	1	1311024	1	1522102	1	1697752		
1	1827250	1	1528265	1	2001026	1	2049682	1	2072415	0	0000000	1	0672504	1	0672504	1	0661737	1	0641079		
1	0611647	1	0574514	1	0531014	1	0483205	1	0433805	1	0396264	1	0344660	1	0313308	1	0296458	1	0297596		
0	0313263	1	0363369	1	0431135	1	0522538	1	0636264	1	0768783	1	0913438	1	10161525	1	1204451	1	1235219	1	1449450
1	1145116	1	1121648	1	1679572	1	1719769	1	1743224	0	0000000	(0645926	1	0645926	1	0642720	+1	0637773		
1	0621639	+1	0606923	+1	0590585	+1	0573594	+1	0558480	+1	0546100	+1	0538639	+1	0537910	+1	0545683	+1	0563762		
1	0592032	+1	0632259	+1	0684174	+1	0747242	+1	0820282	+1	0501242	+1	0987204	+1	1074769	+1	1160386	+1	1240773		
1	1313218	+1	1376347	+1	1427927	+1	1466190	+1	1496812	+1	1513793	0	0000000	+1	0680836	+1	0680836	+1	0681043	+1	0679376
1	0676700	1	0773684	1	0670918	1	0669148	1	0669184	1	0671884	1	0678166	1	0689722	1	0704509	1	0721594		
1	0752821	1	0786143	1	0825336	1	0869302	1	0919076	1	0971642	1	1026222	1	1081159	1	1124702	1	1185223		
1	1231214	1	1271667	1	1305593	1	1332262	1	1351335	1	1362731	0	0000000	1	0733527	1	0733527	1	0735215		
1	0737111	1	0738385	1	0741293	1	0744637	1	0749328	1	0755742	1	0764253	1	0775262	1	0789031	1	0805933	1	0826194
1	0849702	1	0376405	1	0906142	1	0938549	1	0973012	1	1008912	1	1045398	1	1081630	1	1116660	1	1149585		
1	1179570	1	1205933	1	1229120	1	1245698	1	1258346	1	1265934	0	0000000	(0782111	1	0782111	1	0785091		
1	0752932	+1	0791606	+1	0796225	+1	0801925	+1	0809106	+1	0817719	+1	0827988	+1	0840064	+1	0853994	+1	0863914		
1	0887881	+1	0907773	+1	0929334	+1	0952356	+1	0977095	+1	1002475	+1	1028349	+1	1054218	+1	1073520	+1	1103737	+1	1126357
1	1146939	+1	1164914	+1	1180301	+1	1191940	+1	1200511	+1	1205683	0	0000000)	0817355	+1	0817355	+1	0820562		
1	0842466	+1	0946936	+1	0852605	+1	0859346	+1	0867280	+1	0876429	+1	0886794	+1	0898370	+1	0911119	+1	0924213		
1	0939821	+1	0953530	+1	0972130	+1	0989302	+1	1006868	+1	1024533	+1	1042100	+1	1059225	+1	1075670	+1	1091197		
1	1125479	+1	1178346	+1	1129532	+1	1138964	+1	1146355	+1	1151695	+1	1154920	0	0000000	+1	0835677	+1	0835677		
1	0838842	+1	0942462	+1	0843996	+1	0852605	+1	0865346	+1	0867280	+1	0876429	+1	0886794	+1	0898370	+1	0911119	+1	0924213
1	0979801	+1	0955590	+1	0972130	+1	0989302	+1	1006868	+1	1024535	+1	1042100	+1	1059225	+1	1075670	+1	1091197		
1	1105479	+1	1118346	+1	1129532	+1	1138964	+1	1146355	+1	1151695	+1	1154920	0	0000000						

VITESSE RADIALE

0.0000000	0.0000000	0.0000000	0.0000000	0.0000000	0.0000000	0.0000000	0.0000000	0.0000000	0.0000000	0.0000000	0.0000000	0.0000000	0.0000000	0.0000000	0.0000000	0.0000000	0.0000000	0.0000000	0.0000000	0.0000000	0.0000000		
0.0000000	0.0000000	0.0000000	0.0000000	0.0000000	0.0000000	0.0000000	0.0000000	0.0000000	0.0000000	0.0000000	0.0000000	0.0000000	0.0000000	0.0000000	0.0000000	0.0000000	0.0000000	0.0000000	0.0000000	0.0000000	0.0000000		
0.0000000	0.0000000	0.0000000	0.0000000	0.0000000	0.0000000	0.0000000	0.0000000	0.0000000	0.0000000	0.0000000	0.0000000	0.0000000	0.0000000	0.0000000	0.0000000	0.0000000	0.0000000	0.0000000	0.0000000	0.0000000	0.0000000		
0.0000000	0.0000000	0.0000000	0.0000000	0.0000000	0.0000000	0.0000000	0.0000000	0.0000000	0.0000000	0.0000000	0.0000000	0.0000000	0.0000000	0.0000000	0.0000000	0.0000000	0.0000000	0.0000000	0.0000000	0.0000000	0.0000000		
0.12112276	0.1302322	0.1384399	0.1456407	0.1517007	0.1564729	0.1597732	0.1613813	0.1610271	0.1587902	0.1510320	0.1444769	0.1321090	0.1152142	0.0930094	0.0647259	0.0298550	0.4905426	0.3805502	0.2367059	0.0610502	0.0500000	0.0200000	0.0000000
0.0610502	0.0500000	0.0159138	0.0216271	0.0322809	0.0427171	0.0528827	0.0627273	0.0721636	0.0811722	0.03615428	0.0473319	0.1043964	0.1106500	0.1159931	0.1203306	0.1235550	0.1255681	0.1262949	0.1234656	0.1255681	0.1112227	0.1112227	
0.12114364	0.1161482	0.1113324	0.1069233	0.1045558	0.1070174	0.1189698	0.1466661	0.1136705	0.0903011	0.0800000	0.0800000	0.0800000	0.0800000	0.0800000	0.0800000	0.0800000	0.0800000	0.0800000	0.0800000	0.0800000	0.0800000		
0.0608279	0.0608279	0.089701	0.0917515	0.09481831	0.0903915	0.0448480	0.0947472	0.1012006	0.1029523	0.1036887	0.1027517	0.1010739	0.0998285	0.0967478	0.0930287	0.0886601	0.0843766	0.0794609	0.0733337	0.0636761	0.0461446	0.0241446	0.0241446
0.03614351	0.03614351	0.0624243	0.0717393	0.0767658	0.0812213	0.0850001	0.0980023	0.0901297	0.0912337	0.0914253	0.0914253	0.0914253	0.0914253	0.0914253	0.0914253	0.0914253	0.0914253	0.0914253	0.0914253	0.0914253	0.0914253	0.0914253	
0.03143350	0.03143350	0.0000000	0.0000000	0.0000000	0.0000000	0.0000000	0.0000000	0.0000000	0.0000000	0.0000000	0.0000000	0.0000000	0.0000000	0.0000000	0.0000000	0.0000000	0.0000000	0.0000000	0.0000000	0.0000000	0.0000000	0.0441335	
0.05172653	0.0564182	0.2625044	0.0683996	0.0739464	0.0739795	0.0933147	0.0677650	0.0871447	0.0920203	0.0800000	0.0828253	0.0801706	0.0738563	0.0661338	0.0571788	0.0470748	0.0360246	0.0241572	0.0212115	0.0200000	0.0200000	0.0200000	
0.03121535	0.03121535	0.0296456	0.0473267	0.0544987	0.0632095	0.0715437	0.0796376	0.0871431	0.0926851	0.1022351	0.0980000	0.0998223	0.0981723	0.0934549	0.0866481	0.0806096	0.0713112	0.071054	0.0714918	0.0726325	0.0726325	0.0726325	
0.01557442	0.1028070	0.0994432	0.0937243	0.0838866	0.0762467	0.0651637	0.0529953	0.0400021	0.0267450	0.0200000	0.0270503	0.0219203	0.0217237	0.0434242	0.0566672	0.0709423	0.0935545	0.0949158	0.1132076	0.1244277	0.1317216	0.1382155	
0.01525254	0.01525254	0.0219203	0.0217237	0.02012056	0.02021056	0.1344991	0.1206942	0.1143970	0.1003045	0.0846199	0.0867000	0.0841095	0.0821890	0.0652188	0.0639178	0.0523837	0.0482377	0.0452430	0.0477247	0.0502909	0.0536894	0.0502909	
0.015148130	0.015148130	0.0165553	0.01641035	0.0143425	0.0143425	0.0116754	0.0116754	0.0213016	0.0213016	0.0248500	0.0248500	0.0248500	0.0248500	0.0248500	0.0248500	0.0248500	0.0248500	0.0248500	0.0248500	0.0248500	0.0248500		
0.01520423	0.01520423	0.0169726	0.02120232	0.02021056	0.02021056	0.1846584	0.1628864	0.1390498	0.1145662	0.09402521	0.0965267	0.09402521	0.09402521	0.09402521	0.09402521	0.09402521	0.09402521	0.09402521	0.09402521	0.09402521	0.09402521	0.0875554	
0.009712111	-0.1018752	-0.0969310	-0.0727366	-0.0209127	-0.0375096	-0.0978440	-0.1596398	-0.2224841	-0.2972722	-0.3355048	-0.3676905	-0.2524797	-0.3141530	-0.2637101	-0.2257708	-0.1947421	-0.1472269	-0.1130576	-0.0817844	-0.0257774	-0.0270503	-0.0257774	
-0.0528796	-0.0528796	-0.0257774	-0.0257774	-0.0000000	-0.0000000	-0.0165672	-0.0341998	-0.0531120	-0.0738026	-0.0966761	-0.1237076	-0.1543443	-0.1916716	-0.2374990	-0.2947090	-0.3669370	-0.2159222	-0.0589663	-0.0670903	-0.2269497	-0.3641112	-0.4976325	-0.4976325
0.6222276	0.7188502	0.5515047	0.4323362	0.3397657	0.2676465	0.2093124	0.1623650	0.1221085	0.0871764	0.0555707	0.0270503	0.0257774	0.0257774	0.0257774	0.0257774	0.0257774	0.0257774	0.0257774	0.0257774	0.0257774	0.0257774	0.0257774	
-0.0555707	-0.0555707	-0.0257774	-0.0257774	-0.0000000	-0.0000000	-0.0167737	-0.0167737	-0.0231216	-0.0231216	-0.0274871	-0.0422676	-0.0422676	-0.0422676	-0.0422676	-0.0422676	-0.0422676	-0.0422676	-0.0422676	-0.0422676	-0.0422676	-0.0422676	-0.0422676	
-0.05365556	-0.05365556	-0.1934311	-0.2451639	-0.3154913	-0.4162337	-0.3378375	-0.1364418	-0.0402673	-0.1935786	-0.3466155	-0.4886177	-0.6393789	-0.441830	-0.4782491	-0.3672141	-0.2873992	-0.2267620	-0.1788174	-0.1387534	-0.1048667	-0.0750119	-0.0750119	
-0.0484753	0.0234050	0.0000000	(0.0000000)	-0.0118513	-0.0275084	-0.0262663	-0.0488658	-0.0612287	-0.0753523	-0.0882471	-0.1014581	-0.1132744	-0.1213701	-0.1230176	-0.1452092	-0.0943317	-0.0662170	-0.0472519	-0.0375317	-0.0270503	-0.0270503	-0.0270503	
-0.05172386	-0.05172386	-0.1934311	-0.2451639	-0.3154913	-0.4162337	-0.3378375	-0.1364418	-0.0402673	-0.1935786	-0.3466155	-0.4886177	-0.6393789	-0.441830	-0.4782491	-0.3672141	-0.2873992	-0.2267620	-0.1788174	-0.1387534	-0.1048667	-0.0750119	-0.0750119	
-0.0347276	-0.0347276	-0.0257774	-0.0257774	-0.0000000	-0.0000000	-0.0295148	-0.0222157	-0.0141520	-0.0097313	-0.0079651	-0.0068739	-0.0055221	-0.0047024	-0.0026237	-0.0478761	-0.0645706	-0.0822147	-0.0966840	-0.0461971	-0.0321959	-0.0257774	-0.0257774	
-0.0742158	-0.0742158	-0.0257774	-0.0257774	-0.0000000	-0.0000000	-0.0297615	-0.0200000	-0.0044236	-0.0045260	-0.0065530	-0.0082338	-0.0091310	-0.0152623	-0.0207394	-0.0049472	-0.0003621	-0.0053375	-0.0081595	-0.0075939	-0.0069048	-0.0062191	-0.0055488	
0.0048558	0.0245219	0.0086234	0.0169683	0.0224558	0.0251292	0.0254501	0.0239778	0.0212286	0.0176226	0.0048558	0.0197704	0.0184018	0.0166431	0.0173242	0.0093688	0.0056891	0.0036894	0.0035078	0.0033788	0.0033313	0.0174048	0.0015020	
0.00564457	0.00564457	0.0245219	0.02052312	0.02051926	0.0044793	0.0071173	0.0020218	0.0065518	0.0014223	0.0027195	0.0023045	0.0013491	0.0011711	0.00207333	0.0003602	0.0000000	0.0036270	0.0071168	0.0104676	0.0134911	0.0163295	0.0015020	
0.00533116	0.00533116	0.0197704	0.0184018	0.0166431	0.0000000	-0.0000000	-0.0173242	-0.0056891	-0.0036888	-0.0152623	-0.0188602	-0.0199743	-0.0193365	-0.0174048	-0.00533116	-0.00533116	-0.0193365	-0.0174048	-0.00533116	-0.00533116	-0.00533116	0.0015020	

-0 0146010 -0 0112459 -0 0075811 -0 0087852 -0 0010000 -0 0010000 -0 0077055 -0 0152524 -0 0216021 -0 0295836 -0 0358510
 0 0410520 0 0445471 0 0454674 0 0424302 0 0376765 0 0162956 -0 0001162 0 0033342 0 0043049 0 0045974
 0 0051034 0 0268183 0 0213257 -0 0111792 -0 037047 0 0516932 0 0582947 0 0569631 0 0519729 0 0448234
 0 0164432 -0 0274613 -0 0182423 -0 0020130 0 0000000 0 0000000 0 0124537 0 0261534 0 0356072 0 0337224
 0 0274914 -0 0218892 0 0263513 0 0104332 0 01230671 0 01324675 0 01351113 0 01567592 0 0258270 0 0051243 -0 0361181.
 -0 1057531 -0 1733790 -0 2162858 -0 1687067 -0 1731634 -0 1623522 -0 1439060 -0 1267722 -0 1062523 -0 0865001
 0 0075213 -0 0494254 -0 0322237 -0 017294 0 0000000 0 0070000 0 0174932 0 0338634 0 0552507 0 0767940
 0 0265841 -0 0272224 -0 1561772 0 0289342 0 0217718 0 0215948 0 0218687 0 0440157 0 0440707 0 0316816
 0 01314272 -0 0271063 -0 4792801 0 0306233 0 0261215 0 02726947 0 0302110 0 02111320 0 02212151 0 01737701 -0 1347530
 0 12016511 -0 0276302 0 0445937 -0 0226216 0 0000000 0 0000000 0 0176561 0 0262768 0 0555243 0 0771893
 0 0265842 -0 0274267 0 0389523 -0 0263527 0 0219726 0 0292317 0 03698431 0 0204426 0 0649537 0 0801793
 0 0152413 -0 0262445 -0 0282432 -0 0142328 0 0117225 -0 03470079 0 04232730 0 0331720 0 02617100 -0 0242154
 0 01579337 -0 0195733 -0 0044329 -0 0140172 0 0211822 0 0000000 0 0129796 0 0263228 0 0398478 0 0537146
 0 0671871 -0 0205418 -0 0928332 0 1028694 -0 1073459 -0 1032891 0 0795214 -0 0284795 -0 0292082 -0 0281862
 0 0174446 -0 0231189 -0 2239481 -0 0261155 -0 0264755 -0 3434827 -0 0356006 -0 2617750 -0 0186011 -0 1784501
 0 01412913 -0 0262527 -0 02785459 -0 0507142 -0 0247082 0 0000000 0 0069537 0 0128601 0 0227912
 0 0232436 -0 0310455 0 0342621 0 0352104 0 0330024 0 0253710 0 0148181 0 029456 -0 0261459 -0 0521539 -0 0809270
 0 127515 -0 1278275 -0 1639111 -0 1848915 -0 1522272 -0 1897588 -0 1905019 -0 1279010 -0 1521441 -0 1304693
 0 0212226 -0 0243773 -0 0625553 -0 0405303 -0 012912 -0 0020000 0 0020000 0 0245254 0 0047223 -0 0061276
 0 0214326 -0 0277372 -0 0062953 -0 0044320 -0 0009421 -0 0054055 -0 0150316 -0 0257355 -0 0217256 -0 0812986
 0 0144176 -0 0200424 -0 0932763 -0 0048935 -0 1172754 -0 1143823 -0 1203921 -0 1173555 -0 1101287 -0 0993461 -0 0875238
 -0 07372078 -0 0550982 -0 0441541 -0 0291977 -0 0144187 0 0000000 0 0000000 0 0000418 0 0002084 -0 0001597
 -0 00015419 -0 0228923 -0 0051600 -0 0081375 -0 0120050 -0 0157902 -0 0224563 -0 0288959 -0 0358204 -0 0432743
 -0 01266122 -0 0577372 -0 0641441 -0 0624951 -0 0734222 -0 0753761 -0 0757140 -0 0374742 -0 0697678 -0 0642004
 -0 0517656 -0 0646463 -0 0392526 -0 0278201 -0 0170737 -0 0277443 0 0000000 0 0010676 -0 0021901 -0 0034662
 -0 0019737 -0 0067664 -0 008121 -0 0114278 -0 014356 -0 0176634 -0 0213044 -0 0252079 -0 0222640 -0 0333429
 -0 0017295 -0 009225 -0 0046703 -0 0046544 -0 0482075 -0 0486888 -0 0485010 -0 0470038 -0 0444192 -0 0408249
 -0 0019265 -0 0071144 -0 0253758 -0 0192175 -0 0128352 -0 0052800 0 0000000 0 0000000 0 0012518 -0 0023212 -0 0241296
 -0 0017539 -0 0053331 -0 0069253 -0 00869349 -0 0056444 -0 0126218 -0 0148185 -0 0171222 -0 014838 -0 0213432 -0 0241296
 -0 0282579 -0 0281417 -0 0296879 -0 0308178 -0 0214511 -0 0315244 -0 0309996 -0 0298555 -0 0281034 -0 0257784
 -0 0023943 -0 0236181 -0 0162448 -0 0121667 -0 0811229 -0 0040460 0 0000000 0 0000000 0 0010459 -0 0023952
 -0 0101472 -0 0172724 -0 0182345 -0 0189825 -0 0194717 -0 0196703 -0 0195477 -0 0190866 -0 0182818 -0 0171350 -0 0156693
 -0 0129145 -0 0119133 -0 0097106 -0 0073597 -0 0049180 -0 0024487 -0 0000000 0 0000000 0 0006768 -0 0012291
 -0 0050172 -0 0227124 -0 0034250 -0 0041577 -0 0044902 -0 0056634 -0 0064244 -0 0071770 -0 0079044 -0 0065982
 -0 0023226 -0 0297305 -0 0102313 -0 0105377 -0 0107371 -0 0107959 -0 0106493 -0 0103654 -0 0088916 -0 0092416
 -0 0094320 -0 0074722 -0 0063863 -0 0051983 -0 0039359 -0 0026290 -0 0013073 0 0000000 0 0000000 -0 0004330 -0 0004580
 -0 00266870 -0 009205 -0 0011535 -0 0013998 -0 0016420 -0 0018873 -0 0021304 -0 0023678 -0 0025344 -0 0022085
 -0 0023939 -0 0031650 -0 0032955 -0 0023980 -0 0034395 -0 0034407 -0 0033916 -0 0032897 -0 0031312 -0 0029224
 -0 0022641 -0 0023591 -0 0020138 -0 0016792 -0 0012422 -0 0028300 -0 0004116 0 0000000
 -0 0029939 -0 0031650 -0 0032955 -0 0023980 -0 0034395 -0 0034407 -0 0033916 -0 0032897 -0 0031312 -0 0029224
 -0 0022641 -0 0023591 -0 0020138 -0 0016792 -0 0012422 -0 0028300 -0 0004116 0 0000000

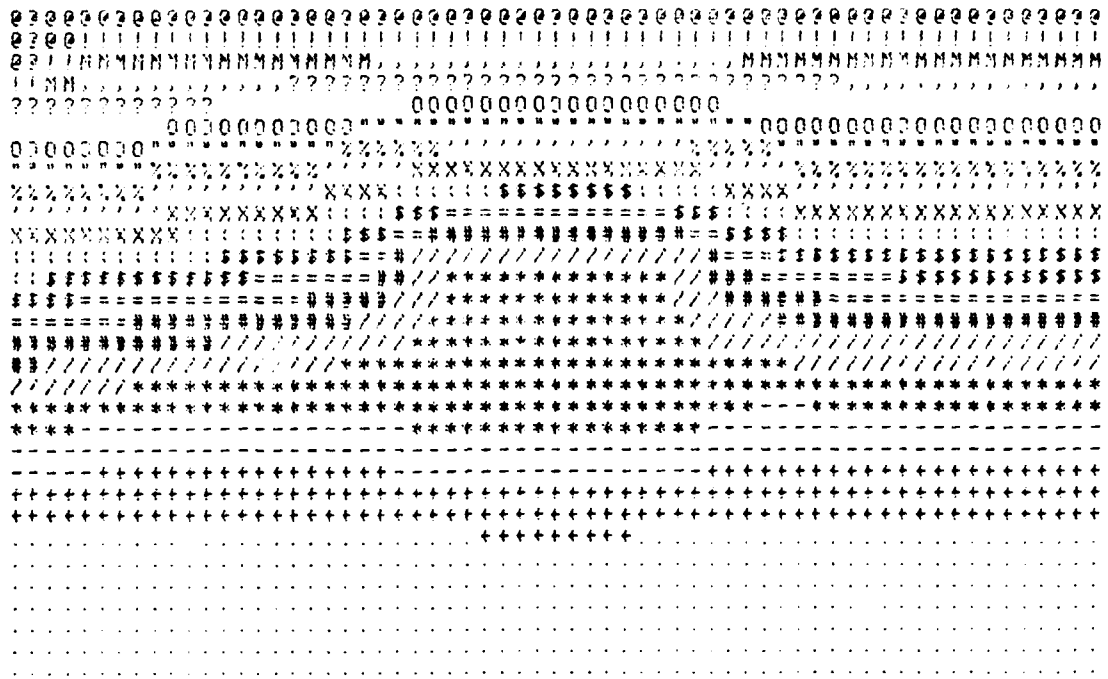
.....
'.....
'.0.....
'.00.....
'.000.....
'.0000.....
'.00000.....
'.000000.....
'.0000000.....
'.00000000.....
'.000000000.....
'.0000000000.....
'.00000000000.....
'.000000000000.....
'.0000000000000.....
'.00000000000000.....
'.000000000000000.....
'.0000000000000000.....
'.00000000000000000.....
'.000000000000000000.....
'.0000000000000000000.....
'.00000000000000000000.....
'.000000000000000000000.....
'.0000000000000000000000.....
'.00000000000000000000000.....
'.000000000000000000000000.....
'.0000000000000000000000000.....
'.00000000000000000000000000.....
'.000000000000000000000000000.....
'.0000000000000000000000000000.....
'.00000000000000000000000000000.....
'.000000000000000000000000000000.....
'.0000000000000000000000000000000.....
'.00000000000000000000000000000000.....
'.000000000000000000000000000000000.....
'.0000000000000000000000000000000000.....
'.00000000000000000000000000000000000.....

MINIMUM = 0.00000E-01 MAXIMUM = 4.00000E-01 CLASSES = 2.000

.	.LT.	2.000E-02	'	.LT.	2.200E-01
+	.LT.	4.000E-02	%	.LT.	2.400E-01
-	.LT.	6.000E-02	*	.LT.	2.600E-01
*	.LT.	8.000E-02	0	.LT.	2.800E-01
/	.LT.	1.000E-01	.	.LT.	3.000E-01
#	.LT.	1.200E-01	?	.LT.	3.200E-01
=	.LT.	1.400E-01	,	.LT.	3.400E-01
\$.LT.	1.600E-01	M	.LT.	3.600E-01
:	.LT.	1.800E-01	!	.LT.	3.800E-01
X	.LT.	2.000E-01	E	.LT.	4.000E-01

DISTRIBUTION DES LIGNES DE COURANT

-79-



MINIMUM = 0.00000E+01 MAXIMUM = 5.52470E-01 CLASSES = 2.762

.	.LT.	2.762E-02	.	.LT.	3.039E-01
+	.LT.	5.525E-02	%	.LT.	3.315E-01
-	.LT.	8.287E-02	"	.LT.	3.591E-01
*	.LT.	1.105E-01	0	.LT.	3.867E-01
/	.LT.	1.381E-01	.	.LT.	4.144E-01
#	.LT.	1.657E-01	?	.LT.	4.420E-01
=	.LT.	1.934E-01	,	.LT.	4.696E-01
\$.LT.	2.210E-01	M	.LT.	4.972E-01
:	.LT.	2.486E-01	!	.LT.	5.248E-01
X	.LT.	2.762E-01	Q	.LT.	5.525E-01

ISOVITESSE RADIALE

- 41 -

MINIMUM = -7.11170E-01 MAXIMUM = 7.18834E-01 CLASSES = 7.150

.	.LT.	-6.397E-01	*	.LT.	7.533E-02
+	.LT.	-5.682E-01	%	.LT.	1.448E-01
-	.LT.	-4.967E-01	"	.LT.	2.183E-01
*	.LT.	-4.252E-01	0	.LT.	2.898E-01
/	.LT.	-3.537E-01	.	.LT.	3.613E-01
#	.LT.	-2.822E-01	?	.LT.	4.328E-01
=	.LT.	-2.107E-01	>	.LT.	5.043E-01
\$.LT.	-1.392E-01	M	.LT.	5.758E-01
:	.LT.	-6.767E-02	!	.LT.	6.473E-01
X	.LT.	3.832E-03	@	.LT.	7.188E-01

STOP
%EOD

```
DEFINE FILE 10=U(1(R:5084,G(1:BN,FI,RW)
DEFINE FILE 5=105=M:SI
DEFINE FILE 8=106=M:LO
COMMON/DPRH/DP,RT,HT
COMMON/FLUIDE/DENS,VIS,RE,PR
COMMON/HEAT/TKG,TKS,BP,TA,TC
COMMON/WALL/RHGW,RUG,RHSW,RWS
COMMON/NTOT/NMAX,NMAX
COMMON/TCALV/NF,NG,W3,TEST
COMMON/DATPOR/PMINAO,PMAXAO,PMINAI,PMAXAI
COMMON/INDPOR/111AO,122AO,J11AO,J4AO,111AI,122AI,J11AI,J4AI
COMMON/IND/I,J
COMMON/PORBUS/POR,PORX,PORR
COMMON/INSP/DR,DX,DR2,DX2,DRDF,DXDX,DXDR
COMMON/BLKK/A1(41),B1(41),C1(41),D1(41),E1(41)
COMMON/BLKE/A2(41),B2(41),C2(41),D2(41),E2(41)
DIMENSION W1(31,31),W2(31,31),SOLN1(31),SOLN2(31),P(31,31)
C
C      CALL LECRIB
C
C      READ (5,500) J99MAX,EPS,Z1,PNS0,ALPHA,BETA
500 FORMAT (15,5(F10.4))
      WRITE (6,700) J99MAX,EPS,Z1,PNS0,ALPHA,BETA
700 FORMAT (5X,8HJ99MAX= ,13,2X,5HEPS= ,F6.4,2X,4HZ1= ,
1 E10.4,2X,6HNS0= ,E10.4,2X,7HALPHA= ,F4.2,2X,6HBTET= ,F4.2,2X)
      READ (10'1) P
C
C      INITIALIZATION OF TEMPERATURES
C
      DO 5 I=1,MMAX
      DO 5 J=1,NMAX
      W1(I,J)=ALPHA
      W2(I,J)=BETA
5 CONTINUE
C
      TKR=TKS/TKG
      M1=MMAX-1
      N1=NMAX-1
      DX=1./FLOAT(M1)
      DR=1./FLOAT(N1)
      J99=0
      G=FLOAT(M1-1)*FLOAT(N1-1)
C
C      DETERMINATION OF COEFFICIENTS IN DISCRETIZED EQUATIONS
C
      7 J99=J99+1
      DT1=0.
      DT2=0.
      DEP1=0.
      DER2=0.
      EXA=0.
      ERA=0.
C
      DO 10 I=2,N1
      IP1=I+1
      IM1=I-1
      IP2=I+2
      IM2=I-2
      DO 20 J=2,M1
      JP1=J+1
      JM1=J-1
      JP2=J+2
      JM2=J-2
      C
```

```
C FIND ECRD
C      CALL SQUEL
C      R= FLOAT(J-1)*DR
C
C      US=(P(I,J,1)-P(I,J,0))/(2.*DR*R)
C      VS=-(P(I,J,1)-P(I,J,0))*RT/(2.*DX*R*HT)
C      VR=SQRT(US*US+VS*VS)
C      REB=RE*DP*VR/RT
C
C THE DETERMINATION OF THE EDDY DIFFUSIVITY,E, AND ITS DERIVATIVES
C USING A MIXING LENGTH MODEL
C
C      VSU=0.
C      VSL=0.
C      USL=US
C      USR=0.
C      IF (I .EQ. M1) GO TO 50
C      VSU=-RT*(P(IF2,J)-P(I,J))/(2.*DX*R*HT)
C 50   IF (I .EQ. 2) GO TO 52
C      VSL=-RT*(P(I,J)-P(IM2,J))/(2.*DX*R*HT)
C 52   IF (J .EQ. 2) GO TO 54
C      USL=(P(I,J)-P(I,JM2))/(2.*DR*E)
C 54   IF (J .EQ. N1) GO TO 56
C      USR=(P(I,JP2)-P(I,J))/(2.*DR*R)
C 56   CONTINUE
C      DVSX=(VSU-VSL)/(2.*DX)
C      DUSR=(USR-USL)/(2.*DR)
C      DDVSX=(VSU-2.*VS+VSL)/(DX*DX)
C      DDUSR=(USR-2.*US+USL)/(DR*DR)
C      Z2=1.
C      Z3=1.
C      IF (DVsx .LT. 0.) Z2=-1.
C      IF (DDUSR .LT. 0.) Z3=-1.
C
C      EX=Z1*DP*DP*RE*VIS*ABS(DVSX)/(RT*HT)
C      ER=Z1*DP*DP*RE*VIS*ABS(DUSR)/(RT*RT)
C      EXX=Z1*Z2*DP*DP*RE*VIS*DDVSX/(RT*HT)
C      ERR=Z1*Z3*DP*DP*RE*VIS*DDUSR/(RT*RT)
C      EXA=EXA+EX/G
C      ERA=ERA+ER/G
C
C FIND NUCRE, ECRD
C
C      C=1.-POR
C      O2=0.*0.33333
C      O1=2.-3.*O2+3.*O2**5.-2.*O2**6.
C      PNU=1.6*((REB+PR/(POR*O1))*(1.-C**1.66667))**0.33333
C
C CALCULATE COEFFICIENTS IN EQUATIONS
C
C      AA1=RT*(POR+PR*EX/VIS)/(RE*PR*HT*HT)
C      AA2=RT*(1.-POR)*TKR/(RE*PR*HT*HT)
C      CC1=RT*(POR*PR*ER/VIS)/(RE*PR*RT*RT)
C      CC2=RT*(1.-POR)*TKR/(RE*PR*RT*RT)
C      H=6*(1.-POR)*PNU*RT/(RE*PR*DP*DP)
C      Q=RT*QP*(1.-MAXAD)/(RE*PR*TKG*T0)
C      Y1=-CC1/R-RT*(PORR+PR*ERR/VIS)/(RE*PR*RT*RT)+VS/RT
C      Y2=-CC2/R+RT*PORR*TKR/(RE*PR*RT*RT)
C      U1=US/HT-RT*(PORX+PR*EXX/VIS)/(RE*PR*HT*HT)
C      U2=RT*TKR*PORX/(RE*PR*HT*HT)
C
C COEFFICIENTS USED IN UPWIND DIFFERENCING
C
C      IF (U1 .LT. 0.) GO TO 60
C      AB=-1.
C      BB=1.
C      CB=0.
C      GO TO 63
C 60   AB=0.
C      BB=-1.
C      CB=1.
C 63   IF (V1 .LT. 0.) GO TO 65
C      AB=-1.
C      BB=1.
C      CB=0.
C      GO TO 67
C 65   AB=0.
C      BB=-1.
```

```
C C9=1.
67 CONTINUE
C
B1(J)= -CC1/DR/DP+V1*A9/DR
B1(J)=2.*(A81/DX/DX+CC1/DR/DR)+H+U1*B8/DX+V1*B9/DR
C1(J)= -CC1/DR/DP+V1*C9/DR
D1(J)=H
E1(J)=A81*(W1(IP1,J)+W1(IM1,J))/DX/DX-U1*(A8*V1(IM1,J)+C8*W1(IP1,
1,J))/DX
C USE CENTRAL DIFFERENCING FOR THETA X AND THETA R
C
B8=0.
B9=0.
C8=0.5
C9=0.5
A8=-0.5
A9=-0.5
C
A2(J)= -CC2/DR/DR+V2*A9/DR
B2(J)=2.*(A82/DX/DX+CC2/DR/DR)+H+U2*B8/DX+V2*B9/DR
C2(J)= -CC2/DR/DR+V2*C9/DR
D2(J)=H
E2(J)=A82*(W2(IP1,J)+W2(IM1,J))/DX/DX-U2*(A8*V2(IM1,J)+C8*W2(IP1,
1,J))/DX+G
C
C 0 CONTINUE
C ADJUST COEFFICIENTS SO AS TO SATISFY BOUNDARY CONDITIONS
C
B1(2)=B1(2)+A1(2)
B2(2)=B2(2)+A2(2)
B1(N1)=B1(N1)+C1(N1)/(1.+DR*RT*RNGWD)
E1(N1)=E1(N1)-C1(N1)*DR*RT*RNGWD*TA/(T0*(1.+DR*RT*RNSWD))
B2(N1)=B2(N1)+C2(N1)/(1.+DR*RT*RNSWD)
E2(N1)=E2(N1)-C2(N1)*DR*RT*RNSWD*TA/(T0*(1.+DR*RT*RNSWD))
C EXECUTE SOLUTION TECHNIQUE TO SOLVE COUPLED TRIDIAGONAL SYSTEM
C
CALL TRISB0 (NMAX,SOLN1,SOLN2)
C EXECUTE RELAXATION TECHNIQUE IN ORDER TO UPDATE UNKNOWN VALUES
C
DO 30 J=2,N1
C
SN1=W1(I,J)+WS*(SOLN1(J)-W1(I,J))
SN2=W2(I,J)+WS*(SOLN2(J)-W2(I,J))
C
ERR1=ABS(SN1-SOLN1(J))
ERR2=ABS(SN2-SOLN2(J))
DT1=DT1+ERR1/G
DT2=DT2+ERR2/G
C
C FIND MAXIMUM ERROR IN THE NET AND ITS POSITION
C
CALL CONVZ(I,J,ERR1,ERR2,L11,L12,LJ1,LJ2,DER1,DER2)
C
W1(I,J)=SN1
W2(I,J)=SN2
30 CONTINUE
W1(I,1)=W1(I,2)
W2(I,1)=W2(I,2)
W1(NMAX)=(W1(I,N1)+DR*RT*RNGWD*TA/T0)/(1.+DR*RT*RNGWD)
W2(I,NMAX)=(W2(I,N1)+DR*RT*RNSWD*TA/T0)/(1.+DR*RT*RNSWD)
10 CONTINUE
DO 35 J=1,NMAX
W1(MMAX,J)=W1(M1,J)
W2(MMAX,J)=W2(M1,J)
W1(1,J)=1.
W2(1,J)=(DX*HT*RNSD+Y2(2,J))/((1.+DX*HT*RNSD)
35 CONTINUE
IF (J99 .LE. 30) GO TO 38
GO TO 39
38 WRITE(103,300) J99,L11,LJ1,DER1,L12,LJ2,DER2
300 FORMAT(1X,2HK=, I3,3H X=, I2,3H R=, I2, 9H ERRMAX1=, E12.6,
I2X,2HX=, I2,3H R=, I2, 9H ERRMAX2=, E12.6,/)
WRITE(103,400) DT1,DT2
400 FORMAT(1X,3HERRAVG1=, E12.6,10H  ERRAVG2=, E12.6,/)
39 CONTINUE
IF (J99 .GT. J99MAX) GO TO 40
```

```
IF (DT1 .GT. EPS) GO TO 7
IF (DT2 .GT. EPS) GO TO 7
40 CONTINUE
IF (J39 .LE. 30) GO TO 45
WRITE(108,300) J39,L11,LJ1,DER1,L12,LJ2,DER2
WRITE(108,400) DT1,DT2
45 CONTINUE
EF=SQRT(EXA*EXA+ERA*ERA)
WRITE(108,425) EF
425 FORMAT (1X,13HEFFECTIVE E= ,E10.4,/)
C THE SOLUTION FOLLOWS
C
450 FORMAT(7,1X,47HTEMPERATURE DISTRIBUTIONS FOR THE GAS AND SOLID,//)
DO 55 K=1,NMAX
L=NMAX-K+1
WRITE(108,500) W1(L,J),J=1,NMAX
WRITE(108,500) W2(L,J),J=1,NMAX
500 FORMAT (2X,11F9.4,/)
800 FORMAT (1X,1H*,11F9.4,/)
55 CONTINUE
C
      WRITE(10'3) W1
      WRITE(10'4) W2
C
LES :
```

**

FR,CL,SL,UL,(HOTBEY)

5508

IPLANTATION DES SEGMENTS***

```
0000
1 R84
2 96
0 9C
DCA
E32
E56
E60
E72
E82
SEC2
F34
F38
F52
F94
598
659C
6592
658H
6644
6648
6654
6658
665E
6652
6656
665C
665E
6724
6B6A
6B6E
```

46

```

DP= 0.0050000      RT= 0.0500000      HT= 0.1000000
DENS= .1211E+01      VISCO= .1530E-04      RET= 4000.00      PR= 0.72
GX= 0.02500      SK= 0.75000      Q= 399999.98
TEX= 20.0      T0=15.00
M= 31      N= 31      NF= 100      NC= 20
OVER RELAXATION FACTOR= 1.05      TEST= 0.01
NJUG = *****      QUS = 0.00
NJUS = *****      QUS = 0.00
BLOCKAGE 1*
PMINA0 = 0.100      PMAXA0 = 0.400
I11A0 = 11      I22A0 = 21      J11A0 = 11      J4A0 = 21

BLOCKAGE 2*
PMINA1 = 0.100      PMAXA1 = 0.400
I11A1 = 50      I22A1 = 50      J11A1 = 50      J4A1 = 50

J99MAX= 200      EPS= 0.0001      Z1= 1427E+00      RNSD= .0000E+00      ALPHA= 1.00      BETA= 1.00
K= 1 X=30 R=26 ERRMAX1= .261211E-01 X=30 R=26 ERRMAX2= .245571E-01
ERRAVG1= .137386E-01      ERRAVG2= .149187E-01
K= 2 X=20 R=15 ERRMAX1= .124416E-01 X=30 R=14 ERRMAX2= .143375E-01
ERRAVG1= .498161E-02      ERRAVG2= .698663E-02
K= 3 X=19 R=15 ERRMAX1= .926781E-02 X=30 R=14 ERRMAX2= .963020E-02
ERRAVG1= .311554E-02      ERRAVG2= .385653E-02
K= 4 X=18 R=16 ERRMAX1= .661278E-02 X=18 R=16 ERRMAX2= .660515E-02
ERRAVG1= .170721E-02      ERRAVG2= .214579E-02
K= 5 X=18 R=16 ERRMAX1= .450993E-02 X=18 R=16 ERRMAX2= .450230E-02
ERRAVG1= .101622E-02      ERRAVG2= .124753E-02
= 6 X=18 R=16 ERRMAX1= .299358E-02 X=18 R=15 ERRMAX2= .300026E-02
ERRAVG1= .611704E-03      ERRAVG2= .743903E-03
K= 7 X=18 R=15 ERRMAX1= .195599E-02 X=18 R=15 ERRMAX2= .196648E-02
ERRAVG1= .376413E-03      ERRAVG2= .453293E-03
K= 8 X=18 R=15 ERRMAX1= .126934E-02 X=18 R=15 ERRMAX2= .127602E-02
ERRAVG1= .234520E-03      ERRAVG2= .280629E-03
K= 9 X=18 R=15 ERRMAX1= .819206E-03 X=18 R=15 ERRMAX2= .823021E-03
ERRAVG1= .147451E-03      ERRAVG2= .175611E-03
K= 10 X=18 R=15 ERRMAX1= .526428E-03 X=18 R=15 ERRMAX2= .529289E-03
ERRAVG1= .932289E-04      ERRAVG2= .110667E-03
K= 11 X=18 R=15 ERRMAX1= .337601E-03 X=18 R=15 ERRMAX2= .339508E-03
ERRAVG1= .592476E-04      ERRAVG2= .701482E-04
EFFECTIVE E= .4695E-03

```

TEMPERATURE DISTRIBUTIONS FOR THE GAS AND SOLID

47

2.0104	2.0104	2.0119	2.0164	2.0255	2.0402	2.0610	2.0984	2.1216	2.1584	2.1949		
2.2252	2.2430	2.2432	2.2235	2.1870	2.1412	2.0933	2.0477	2.0059	1.9682	1.9339		
* 1.9023	1.8712	1.8375	1.7971	1.7447	1.6726	1.5680	1.3945	1.3333	1.2318	2.2644	2.2952	
* 2.1184	2.1184	2.1213	2.1275	2.1380	2.1536	2.1747	2.2012	2.2318	2.2644	2.2952		
* 2.3194	2.3322	2.3300	2.3117	2.2799	2.2394	2.1956	2.1524	2.1115	2.0737	2.0385		
* 2.0048	1.9703	1.9320	1.8855	1.8251	1.7437	1.6333	1.4883	1.3333	2.1216	2.1584	2.1949	
2.0104	2.0104	2.0119	2.0164	2.0255	2.0402	2.0610	2.0884	2.0503	2.0854	2.1252	2.1653	
2.2252	2.2430	2.2432	2.2235	2.1870	2.1412	2.0933	2.0477	2.0059	1.9682	1.9339		
* 1.9023	1.8712	1.8375	1.7971	1.7447	1.6726	1.5680	1.3945	1.3333	1.2318	2.2644	2.2952	
* 2.1184	2.1184	2.1213	2.1275	2.1380	2.1536	2.1747	2.2012	2.2318	2.2644	2.2952		
* 2.3194	2.3322	2.3300	2.3117	2.2799	2.2394	2.1956	2.1524	2.1115	2.0737	2.0385		
* 2.0048	1.9703	1.9320	1.8855	1.8251	1.7437	1.6333	1.4883	1.3333	2.0503	2.0854	2.1252	2.1653
1.9703	1.9703	1.9717	1.9764	1.9855	2.0004	2.0218	2.0503	2.0854	2.1252	2.1653		
2.1933	2.2201	2.2216	2.2009	2.1617	2.1129	2.0631	2.0165	1.9744	1.9367	1.9029		
* 1.8721	1.8424	1.8106	1.7728	1.7235	1.6555	1.5564	1.3916	1.3333	2.2029	2.2377	2.2711	
* 2.0856	2.0856	2.0885	2.0948	2.1054	2.1213	2.1430	2.1705	2.2029	2.2377	2.2711		
* 2.2978	2.3125	2.3111	2.2923	2.2589	2.2166	2.1714	2.1273	2.0861	2.0483	2.0135		
* 1.9805	1.9472	1.9105	1.8661	1.8085	1.7306	1.6245	1.4846	1.3333	2.0462	2.0892	2.1336	
1.9278	1.9278	1.9293	1.9339	1.9430	1.9579	1.9797	2.0091	2.0462	2.0892	2.1336		
2.1719	2.1963	2.1998	2.1782	2.1356	2.0835	2.0314	1.9838	1.9414	1.9038	1.8703		
* 1.8404	1.8122	1.7824	1.7471	1.7012	1.6375	1.5442	1.3985	1.3333	2.1322	2.1665	2.2042	2.2410
* 2.0450	2.0450	2.0479	2.0542	2.0650	2.0812	2.1035	2.1322	2.1665	2.2042	2.2410		
* 2.2711	2.2885	2.2984	2.2691	2.2336	2.1889	2.1419	2.0966	2.0550	2.0172	1.9828		
* 1.9507	1.9183	1.8841	1.8424	1.7881	1.7146	1.6138	1.4801	1.3333	2.0514	2.1006		
1.9848	1.9848	1.8862	1.8907	1.8996	1.9144	1.9362	1.9663	2.0051	2.0514	2.1006		
2.1439	2.1729	2.1791	2.1567	2.1102	2.0541	1.9997	1.9511	1.9084	1.8708	1.8376		
* 1.9085	1.7817	1.7539	1.7213	1.6787	1.6193	1.5317	1.3853	1.3333	2.1276	2.1683	2.2091	
* 2.0025	2.0025	2.0054	2.0117	2.0224	2.0387	2.0615	2.0912	2.1276	2.1683	2.2091		
* 2.2432	2.2640	2.2657	2.2459	2.2081	2.1607	2.1115	2.0651	2.0229	1.9850	1.9309		
* 1.9197	1.8894	1.8567	1.8177	1.7670	1.6979	1.6026	1.4732	1.3333	2.0119	2.0665		
1.8417	1.8417	1.8430	1.8473	1.8559	1.8702	1.9917	1.9220	1.9622	2.0119	2.0665		
2.1154	2.1499	2.1601	2.1374	2.0860	2.0253	1.9683	1.9188	1.8759	1.8382	1.8050		
* 1.7767	1.7513	1.7256	1.6956	1.6565	1.6013	1.5193	1.3922	1.3333	2.1310	2.1761		
* 1.9597	1.9597	1.9625	1.9686	1.9792	1.9953	2.0183	2.0489	2.0870	2.1310	2.1761		
* 2.2149	2.2398	2.2440	2.2240	2.1836	2.1331	2.0816	2.0339	1.9911	1.9531	1.9192		
* 1.8888	1.8598	1.8293	1.7930	1.7458	1.6812	1.5913	1.4704	1.3333	2.0175	1.9703	2.0310	
1.7987	1.7987	1.8000	1.8040	1.8121	1.8257	1.8465	1.8764	1.9175	1.9703	2.0310		
2.0860	2.1270	2.1431	2.1209	2.0635	1.9974	1.9377	1.8873	1.8443	1.8064	1.7730		
* 1.7453	1.7213	1.6977	1.6704	1.6347	1.5838	1.5072	1.3791	1.3333	2.0451	2.0923	2.1422	
* 1.9167	1.9167	1.9195	1.9254	1.9356	1.9314	1.9743	2.0053	2.0451	2.0923	2.1422		

48

*	2.1862	2.2161	2.2240	2.2043	2.1609	2.1066	2.0528	.2.0037	1.9603	1.9219	1.8880
*	1.9582	1.9306	1.8021	1.7686	1.7250	1.6647	1.5802	1.4656	1.3333	1.2710	1.9265
	1.7362	1.7562	1.7573	1.7610	1.7685	1.7812	1.8010	1.8300	1.8710	1.9265	1.9944
	2.0350	2.1034	2.1283	2.1087	2.0435	1.9708	1.9082	1.8572	1.8143	1.7761	1.7419
*	1.7146	1.6919	1.6704	1.6460	1.6138	1.5672	1.4959	1.3763	1.3333	2.0020	2.0524
*	1.9740	1.9740	1.8765	1.8822	1.8920	1.9073	1.9298	1.9610	2.0120	2.1076	
*	2.1571	2.1929	2.2059	2.1877	2.1409	2.0827	2.0259	1.9754	1.9312	1.8922	1.8579
*	1.8223	1.9019	1.7754	1.7447	1.7047	1.6488	1.5696	1.4609	1.3333	1.8240	1.8812
	1.7143	1.7143	1.7154	1.7137	1.7256	1.7374	1.7560	1.7838	1.8240	1.9577	
	2.0224	2.0781	2.1154	2.1026	2.0272	1.9466	1.8810	1.8297	1.7872	1.7486	1.7124
*	1.6849	1.6635	1.6440	1.6226	1.5941	1.5521	1.4859	1.3737	1.3333	1.9586	2.0120
*	1.9314	1.9314	1.8338	1.8392	1.8485	1.8633	1.8853	1.9165	1.9586	2.0729	
*	2.1279	2.1703	2.1903	2.1753	2.1251	2.0622	2.0023	1.9501	1.9049	1.8649	1.8293
*	1.7925	1.7739	1.7493	1.7215	1.6852	1.6338	1.5597	1.4565	1.3333	1.7789	1.8372
	1.6736	1.6736	1.6745	1.6776	1.6840	1.6951	1.7128	1.7395	1.7789	1.9251	
	1.9835	2.0498	2.1028	2.1055	2.0166	1.9267	1.8580	1.8068	1.7658	1.7268	1.6856
*	1.6369	1.6363	1.6198	1.6004	1.5759	1.5386	1.4776	1.3716	1.3333	1.9164	1.9734
*	1.7892	1.7892	1.7915	1.7966	1.8055	1.8199	1.8416	1.8730	1.9164	2.0408	
*	2.1002	2.1486	2.1775	2.1690	2.1157	2.0479	1.9844	1.9301	1.8836	1.8417	1.8031
*	1.7719	1.7468	1.7240	1.6992	1.6667	1.6199	1.5507	1.4525	1.3333	1.8006	1.9100
	1.6345	1.6345	1.6354	1.6332	1.6442	1.6348	1.6720	1.6986	1.7390	1.8006	
	1.9645	2.0210	2.0360	2.1203	2.0161	1.9164	1.9443	1.7939	1.7564	1.7182	1.6628
*	1.6308	1.6104	1.5946	1.5793	1.5588	1.5265	1.4709	1.3698	1.3333	1.9395	2.0160
*	1.7480	1.7480	1.7501	1.7549	1.7634	1.7773	1.7991	1.8312	1.8771	1.9395	
*	2.0770	2.1287	2.1665	2.1695	2.1155	2.0432	1.9732	1.9180	1.8699	1.8256	1.7803
	1.7458	1.7204	1.6992	1.6774	1.6490	1.6068	1.5426	1.4488	1.3333	1.7838	1.9249
	1.5976	1.5976	1.5984	1.6011	1.6067	1.6169	1.6340	1.6618	1.7072	1.7838	
	1.9695	2.0029	2.0662	2.1427	2.0433	1.9401	1.9603	1.8087	1.7800	1.7412	1.6419
*	1.6060	1.5853	1.5714	1.5587	1.5421	1.5148	1.4649	1.3683	1.3333	1.8421	1.9128
*	1.7087	1.7087	1.7107	1.7151	1.7232	1.7368	1.7585	1.7921	1.8421	1.9128	1.9996
*	2.0553	2.1016	2.1461	2.1656	2.1188	2.0448	1.9708	1.9108	1.8655	1.8214	1.7617
*	1.7217	1.6952	1.6754	1.6562	1.6317	1.5912	1.5349	1.4454	1.3333	1.7524	1.9019
	1.5632	1.5632	1.5640	1.5685	1.5718	1.5814	1.5978	1.6253	1.6716	1.7524	
	1.9631	2.0050	2.0557	2.1425	2.0980	2.0029	1.9922	1.8380	1.7984	1.7411	1.6281
*	1.5846	1.5619	1.5482	1.5373	1.5242	1.5019	1.4583	1.3663	1.3333	1.8054	1.8799
*	1.6722	1.6722	1.6740	1.6781	1.6858	1.6989	1.7202	1.7539	1.8054	1.9723	
*	2.0317	2.0681	2.1178	2.1528	2.1260	2.0559	1.9706	1.9056	1.8676	1.8162	1.7473
*	1.7012	1.6722	1.6525	1.6353	1.6141	1.5812	1.5270	1.4420	1.3333	1.6286	1.7044
	1.5306	1.5306	1.5313	1.5335	1.5383	1.5468	1.5615	1.5862	1.6286	1.8522	

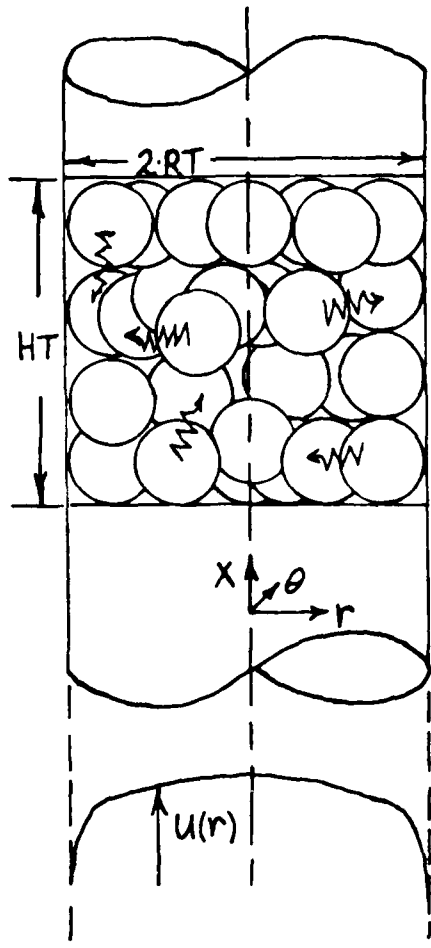
49

*	1.9216	1.9747	2.0421	2.1321	2.1291	2.0747	1.9227	1.8398	1.7844	1.7183	1.6056
*	1.5592	1.5362	1.5234	1.5145	1.5045	1.4871	1.4500	1.3644	1.3333	1.7629	1.8355
*	1.6381	1.6381	1.6397	1.6434	1.6504	1.6624	1.6821	1.7137	1.7629	1.9286	
*	1.9929	2.0355	2.0970	2.1361	2.1314	2.0774	1.9801	1.9058	1.8569	1.7979	1.7257
*	1.6772	1.6476	1.6287	1.6134	1.5954	1.5670	1.5181	1.4382	1.3333	1.6505	1.7863
*	1.4933	1.4992	1.4999	1.5018	1.5058	1.5130	1.5255	1.5467	1.5834	1.6770	1.5725
*	1.3562	1.3120	1.9356	2.0867	2.0921	2.0440	1.8872	1.7993	1.7419	1.6770	
*	1.5293	1.5086	1.4974	1.4905	1.4834	1.4704	1.4399	1.3619	1.3333	1.7164	1.8700
*	1.6058	1.6059	1.6072	1.6104	1.6165	1.6269	1.6442	1.6722	1.7828	1.8700	
*	1.9334	1.9782	2.0346	2.0923	2.0958	2.0469	1.9477	1.8706	1.8204	1.7623	1.6937
*	1.6479	1.6204	1.6233	1.5904	1.5756	1.5516	1.5083	1.4341	1.3333	1.5384	1.7153
*	1.4691	1.4691	1.4696	1.4711	1.4743	1.4803	1.4905	1.5079	1.5954	1.6299	1.5363
*	1.7838	1.8403	1.9172	2.0232	2.0331	1.9890	1.9351	1.7480	1.6915	1.6686	1.7267
*	1.4933	1.4801	1.4708	1.4657	1.4612	1.4523	1.4285	1.3590	1.3333	1.8048	
*	1.5750	1.5750	1.5761	1.5788	1.5839	1.5925	1.6070	1.6307	1.7267	1.8048	
*	1.9647	1.9094	1.9682	2.0301	2.0379	1.9928	1.8963	1.8208	1.7727	1.7189	1.6569
*	1.6159	1.5915	1.5770	1.5665	1.5549	1.5352	1.4976	1.4293	1.3333	1.5410	1.6410
*	1.4398	1.4398	1.4401	1.4413	1.4439	1.4485	1.4566	1.4703	1.4949	1.5799	1.4997
*	1.7054	1.7617	1.9385	1.9456	1.9579	1.9182	1.7726	1.6893	1.6359	1.5799	
*	1.4670	1.4514	1.4440	1.4406	1.4382	1.4331	1.4157	1.3558	1.3333	1.6694	1.7357
*	1.5453	1.5453	1.5462	1.5493	1.5522	1.5592	1.5709	1.5901	1.6212	1.6694	
*	1.7823	1.9319	1.8903	1.9536	1.9639	1.9233	1.8330	1.7620	1.7185	1.6715	1.6179
*	1.5847	1.5620	1.5501	1.5421	1.5334	1.5179	1.4861	1.4247	1.3333	1.4890	1.5655
*	1.4110	1.4110	1.4113	1.4122	1.4142	1.4178	1.4240	1.4347	1.4535	1.5285	1.4629
*	1.6223	1.6744	1.7476	1.8519	1.8603	1.8244	1.6969	1.6238	1.5768	1.5285	
*	1.4356	1.4223	1.4170	1.4151	1.4147	1.4130	1.4019	1.3524	1.3333	1.6124	1.6646
*	1.5165	1.5165	1.5172	1.5198	1.5218	1.5271	1.5361	1.5509	1.5749	1.6646	
*	1.7088	1.7462	1.8020	1.8623	1.8721	1.8368	1.7583	1.6959	1.6398	1.6216	1.5778
*	1.5420	1.5322	1.5230	1.5174	1.5115	1.5001	1.4740	1.4197	1.3333	1.4399	1.4920
*	1.3825	1.3825	1.3927	1.3834	1.3849	1.3877	1.3923	1.4002	1.4141	1.4776	1.4262
*	1.5324	1.5868	1.6441	1.7195	1.7277	1.7109	1.6237	1.5635	1.5199	1.4776	
*	1.4043	1.3941	1.3900	1.3892	1.3905	1.3918	1.3869	1.3488	1.3333	1.5306	1.5573
*	1.4885	1.4885	1.4890	1.4902	1.4924	1.4963	1.5028	1.5134	1.5541	1.5941	
*	1.6275	1.6600	1.7148	1.7600	1.7667	1.7422	1.6848	1.6304	1.6008	1.5709	1.5372
*	1.5150	1.5024	1.4959	1.4925	1.4893	1.4817	1.4614	1.4144	1.3333	1.3903	1.4189
*	1.3536	1.3536	1.3538	1.3544	1.3556	1.3576	1.3609	1.3661	1.3749	1.4212	1.3880
*	1.4440	1.4649	1.4784	1.4929	1.5066	1.5163	1.5129	1.4807	1.4510	1.4212	
*	1.3725	1.3631	1.3626	1.3629	1.3655	1.3696	1.3707	1.3448	1.3333	1.4886	1.5046
*	1.4609	1.4609	1.4613	1.4622	1.4638	1.4666	1.4710	1.4779	1.4886	1.5261	
*	1.5464	1.5736	1.5991	1.6174	1.6236	1.6175	1.5985	1.5686	1.5397	1.5181	1.4959

-50

*	1 4811	1 4729	1 4690	1 4676	1 4667	1 4627	1 4482	1 4090	1 3333	1 3417	1 3502
*	1 3237	1 3437	1 3239	1 3243	1 3252	1 3267	1 3288	1 3318	1 3359	1 3417	1 3502
*	1 3520	1 3643	1 3676	1 3698	1 3700	1 3705	1 3695	1 3658	1 3591	1 3512	1 3436
*	1 3378	1 3345	1 3341	1 3355	1 3394	1 3460	1 3531	1 3405	1 3333	1 3417	1 3502
*	1 4328	1 4328	1 4332	1 4339	1 4353	1 4373	1 4404	1 4448	1 4509	1 4592	1 4698
*	1 4812	1 4927	1 5016	1 5068	1 5078	1 5047	1 4975	1 4868	1 4746	1 4637	1 4543
*	1 4475	1 4435	1 4421	1 4424	1 4436	1 4431	1 4343	1 4032	1 3333	1 3038	1 3074
*	1 2925	1 2925	1 2926	1 2930	1 2937	1 2948	1 2963	1 2983	1 3008	1 3102	1 3070
*	1 3111	1 3127	1 3136	1 3141	1 3150	1 3158	1 3159	1 3152	1 3135	1 3102	1 3070
*	1 3047	1 3036	1 3040	1 3065	1 3117	1 3207	1 3338	1 3357	1 3333	1 4200	1 4250
*	1 4033	1 4033	1 4036	1 4043	1 4053	1 4069	1 4091	1 4120	1 4156	1 4200	1 4250
*	1 4239	1 4340	1 4368	1 4394	1 4390	1 4382	1 4360	1 4324	1 4279	1 4231	1 4188
*	1 4157	1 4141	1 4142	1 4160	1 4192	1 4222	1 4194	1 3969	1 3333	1 2661	1 2676
*	1 2536	1 2596	1 2397	1 2620	1 2605	1 2612	1 2622	1 2633	1 2647	1 2721	1 2714
*	1 2669	1 2699	1 2707	1 2713	1 2720	1 2726	1 2730	1 2730	1 2727	1 2721	1 2714
*	1 2711	1 2715	1 2730	1 2762	1 2824	1 2935	1 3125	1 3304	1 3333	1 3814	1 3836
*	1 3716	1 3716	1 3719	1 3724	1 3731	1 3742	1 3756	1 3772	1 3792	1 3814	1 3836
*	1 3857	1 3873	1 3886	1 3895	1 3899	1 3899	1 3894	1 3884	1 3870	1 3854	1 3840
*	1 3872	1 3837	1 3948	1 3880	1 3931	1 3995	1 4030	1 3899	1 3333	1 2298	1 2306
*	1 2259	1 2259	1 2260	1 2262	1 2265	1 2269	1 2275	1 2282	1 2290	1 2361	1 2364
*	1 2314	1 2322	1 2328	1 2335	1 2342	1 2348	1 2354	1 2358	1 2361	1 2364	1 2368
*	1 2374	1 2386	1 2407	1 2444	1 2511	1 2637	1 2884	1 3244	1 3333	1 3440	1 3452
*	1 3384	1 3384	1 3395	1 3398	1 3393	1 3400	1 3408	1 3418	1 3429	1 3440	1 3452
*	1 3463	1 3472	1 3480	1 3487	1 3493	1 3496	1 3498	1 3498	1 3497	1 3495	1 3496
*	1 3501	1 3513	1 3538	1 3591	1 3649	1 3745	1 3845	1 3820	1 3333	1 1941	1 1953
*	1 1920	1 1920	1 1921	1 1922	1 1924	1 1927	1 1931	1 1936	1 1941	1 1947	1 1953
*	1 1959	1 1965	1 1972	1 1978	1 1985	1 1993	1 1999	1 2006	1 2012	1 2019	1 2027
*	1 2037	1 2052	1 2075	1 2113	1 2180	1 2313	1 2608	1 3175	1 3333	1 3080	1 3087
*	1 3043	1 3043	1 3044	1 3046	1 3050	1 3054	1 3059	1 3065	1 3072	1 3080	1 3087
*	1 3035	1 3102	1 3109	1 3116	1 3122	1 3128	1 3133	1 3138	1 3143	1 3148	1 3156
*	1 3167	1 3185	1 3215	1 3265	1 3347	1 3473	1 3638	1 3730	1 3333	1 1605	1 1610
*	1 1584	1 1584	1 1585	1 1585	1 1587	1 1589	1 1592	1 1596	1 1600	1 1678	1 1688
*	1 1615	1 1621	1 1627	1 1633	1 1640	1 1648	1 1655	1 1663	1 1670	1 1678	1 1688
*	1 1699	1 1715	1 1737	1 1772	1 1835	1 1962	1 2291	1 3094	1 3333	1 2729	1 2735
*	1 2702	1 2702	1 2703	1 2705	1 2707	1 2710	1 2714	1 2718	1 2723	1 2729	1 2735
*	1 2742	1 2748	1 2755	1 2762	1 2769	1 2776	1 2783	1 2790	1 2798	1 2806	1 2817
*	1 2831	1 2851	1 2984	1 2937	1 3027	1 3177	1 3406	1 3627	1 3333	1 1263	1 1270
*	1 1254	1 1254	1 1254	1 1255	1 1256	1 1258	1 1260	1 1266	1 1266	1 1340	1 1350
*	1 1280	1 1285	1 1291	1 1297	1 1303	1 1310	1 1317	1 1324	1 1332	1 1340	1 1350
*	1 1361	1 1375	1 1395	1 1424	1 1476	1 1588	1 1926	1 2999	1 3333	1 2387	1 2392

51

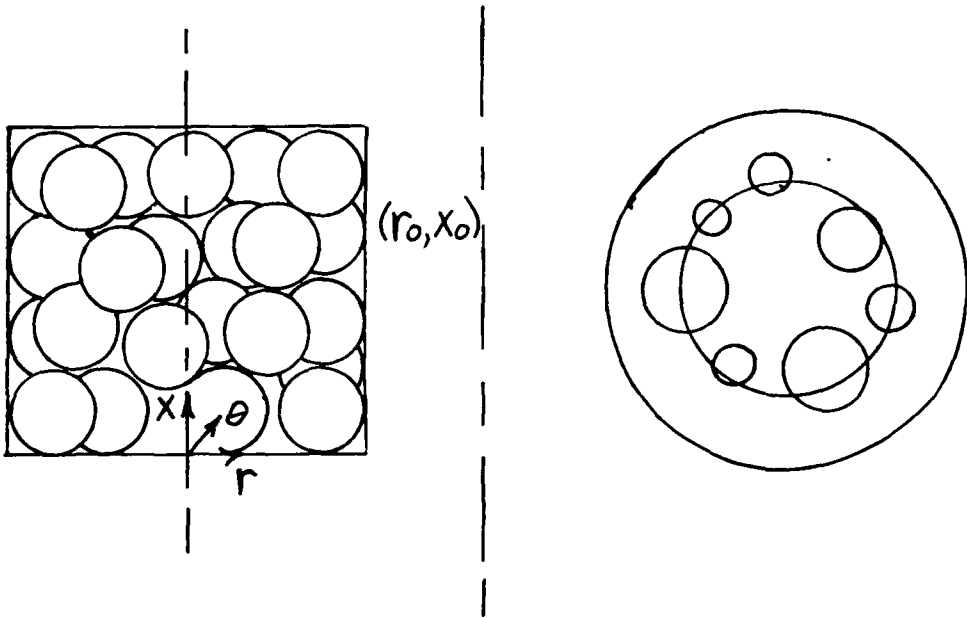


ACTIVE PACKED BED



INCOMING VELOCITY PROFILE

FIGURE 1. ILLUSTRATION OF
ACTIVE PACKED BED



$$\begin{aligned}
 \epsilon(r_0, x_0) &= \sum_i (r_0 \cdot d\theta_i) / (2 \cdot \pi \cdot r_0) \\
 &= \sum_i d\theta_i / (2 \cdot \pi) \\
 &\approx 0.56 \quad \text{FOR THE ABOVE EXAMPLE}
 \end{aligned}$$

FIGURE 2. ϵ AS A CONTINUOUS
FUNCTION OF X
AND r.

$$\begin{bmatrix}
 \begin{array}{ccc|c}
 x & x & & 0 \\
 x & x & x & \\
 x & x & x & \\
 \dots & \dots & \dots & \\
 0 & x & x & x \\
 x & x & &
 \end{array}
 \end{bmatrix} \cdot \begin{bmatrix}
 \begin{array}{ccc|c}
 x & x & & 0 \\
 & x & & \\
 & & x & \\
 & & & \ddots \\
 0 & & & x \\
 & & & x
 \end{array}
 \end{bmatrix} \cdot \begin{bmatrix}
 T_{i2} \\
 \vdots \\
 \vdots \\
 T_{iN-1}
 \end{bmatrix} = \begin{bmatrix}
 x \\
 x \\
 x \\
 \vdots \\
 x \\
 x
 \end{bmatrix}$$

$$\begin{bmatrix}
 \begin{array}{cc|cc}
 x & & x & x \\
 & x & x & x \\
 x & & x & x \\
 \dots & \dots & \dots & \dots \\
 0 & x & 0 & x \\
 & x & & x
 \end{array}
 \end{bmatrix} \cdot \begin{bmatrix}
 \begin{array}{ccc|c}
 x & x & & 0 \\
 x & x & x & 0 \\
 x & x & x & \\
 \dots & \dots & \dots & \\
 0 & & x & x \\
 & & x & x
 \end{array}
 \end{bmatrix} \cdot \begin{bmatrix}
 \theta_{i2} \\
 \vdots \\
 \vdots \\
 \theta_{iN-1}
 \end{bmatrix} = \begin{bmatrix}
 x \\
 x \\
 x \\
 \vdots \\
 x \\
 x
 \end{bmatrix}$$

FIGURE 3. FORM OF MATRIX EQUATION

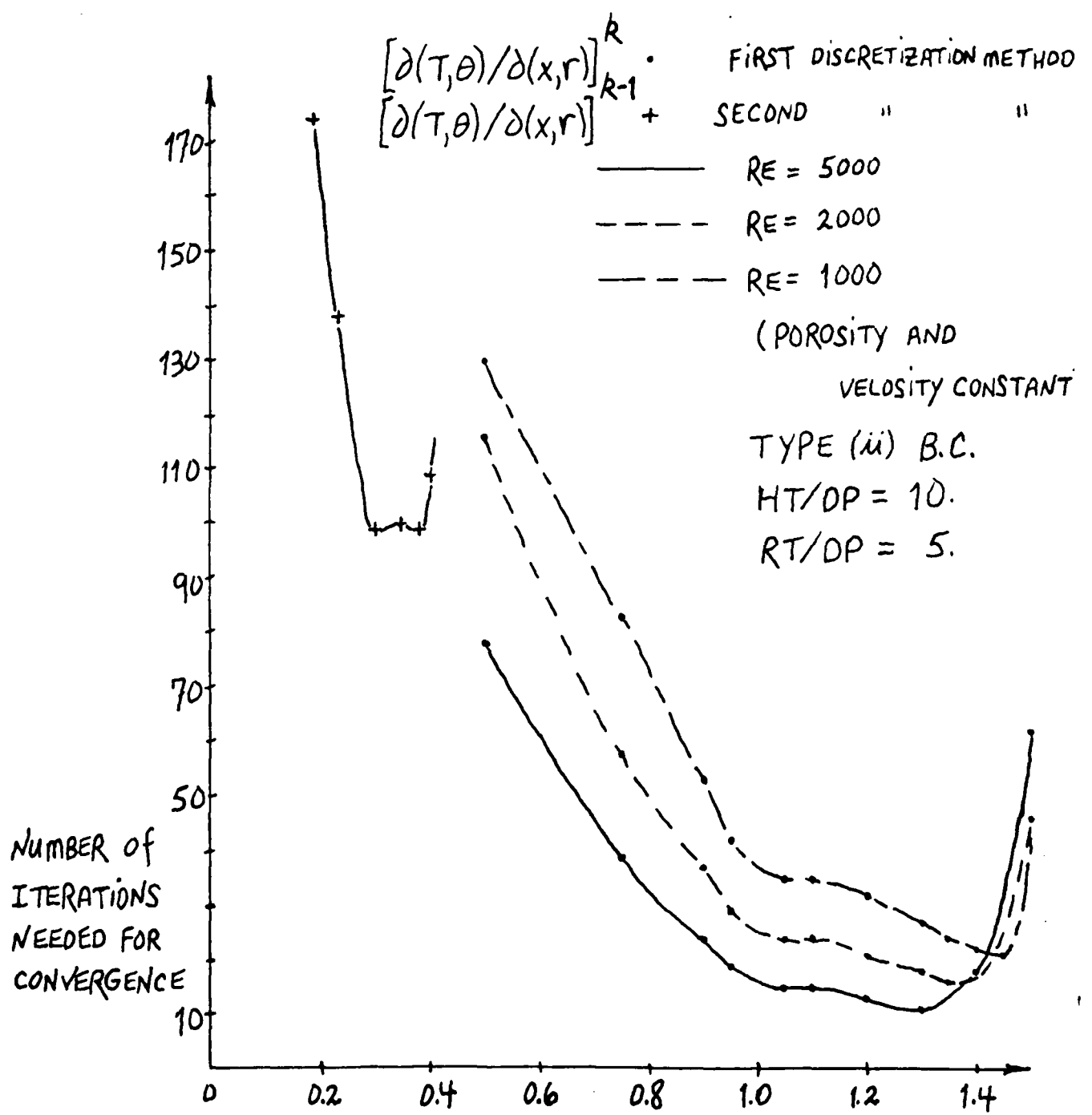


FIGURE 4. RELAXATION COEFFICIENT ws
OPTIMIZATION OF NUMERICAL PROCEDURE

UNIFORM VELOCITY ; TYPE (i) B.C.

$\epsilon = 0.4$

$RE = 5000$.

$T_0 = 15^\circ\text{C}$

$T_w = 20^\circ\text{C}$

$HT/DP = 10$.

$RT/DP = 5$.

- NUMERICAL SOLUTION
WITH AXIAL CONDUCTION
- + NUMERICAL SOLUTION
WITHOUT AXIAL CONDUCTION
- △ THEORETICAL SOLUTION

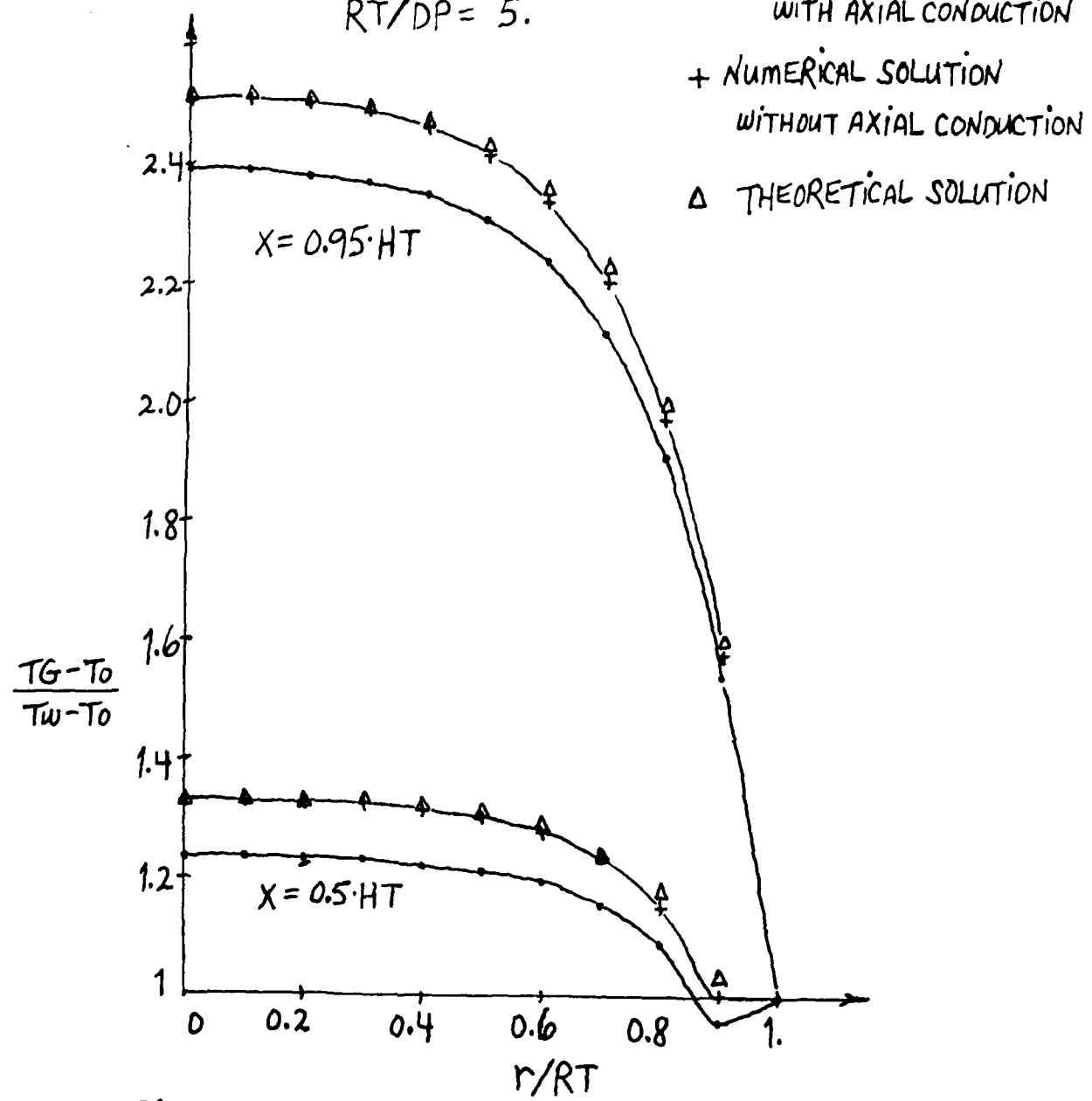
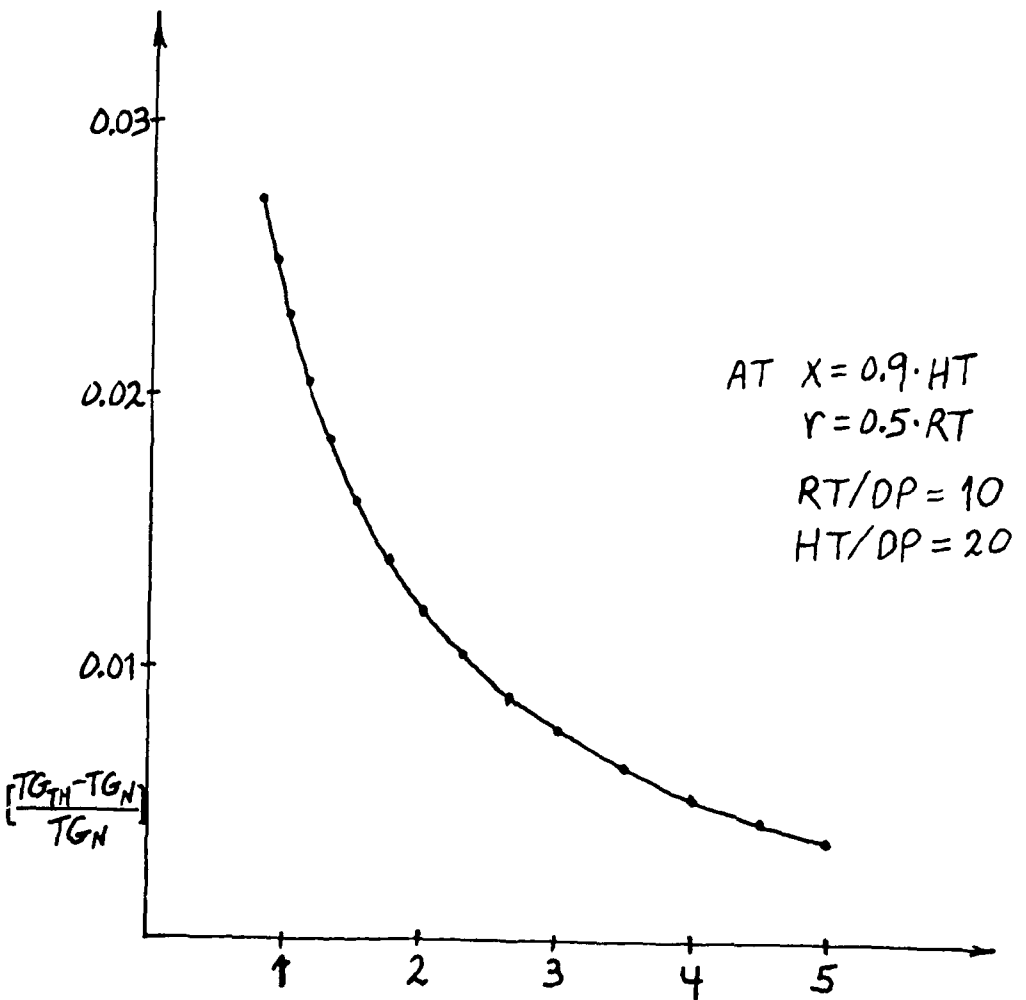
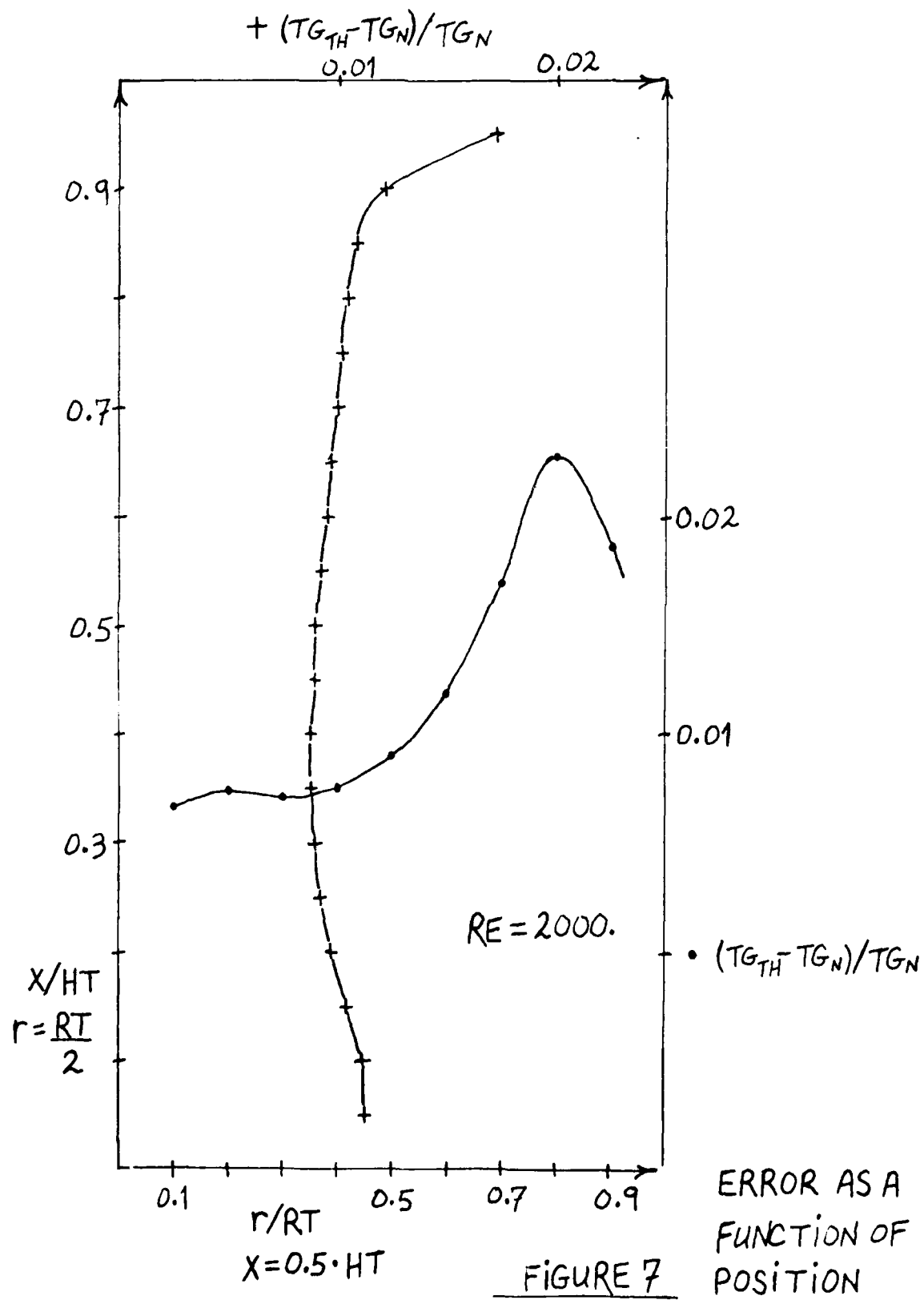


FIGURE 5. COMPARISON OF NUMERICAL PROCEDURES



$$RE = \frac{\bar{u} \cdot RT}{\nu} \cdot 10^3$$

FIGURE 6. RE DÉPENDANCE
OF RELATIVE ERROR



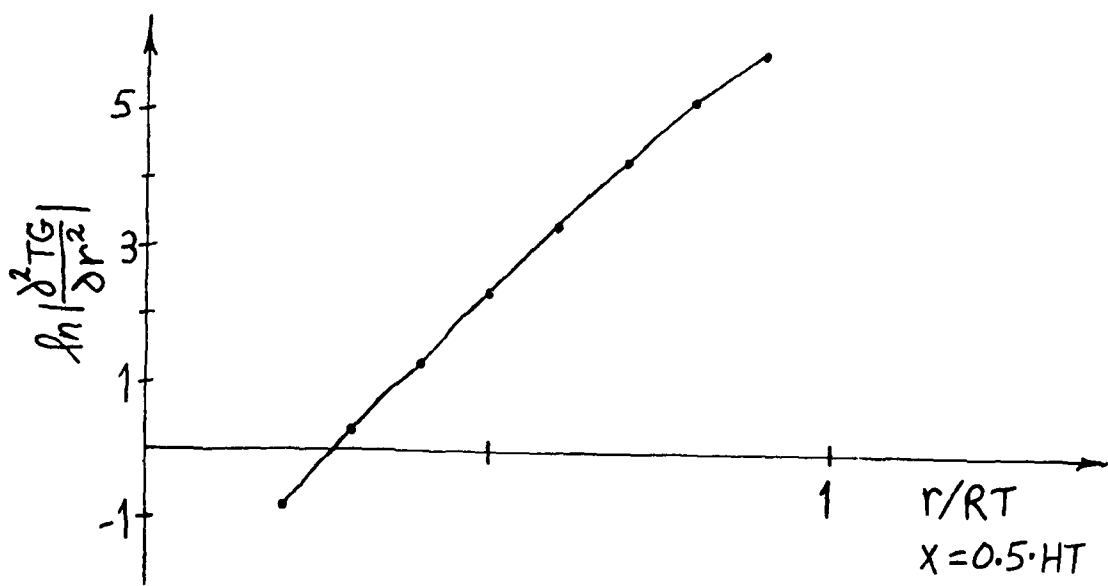
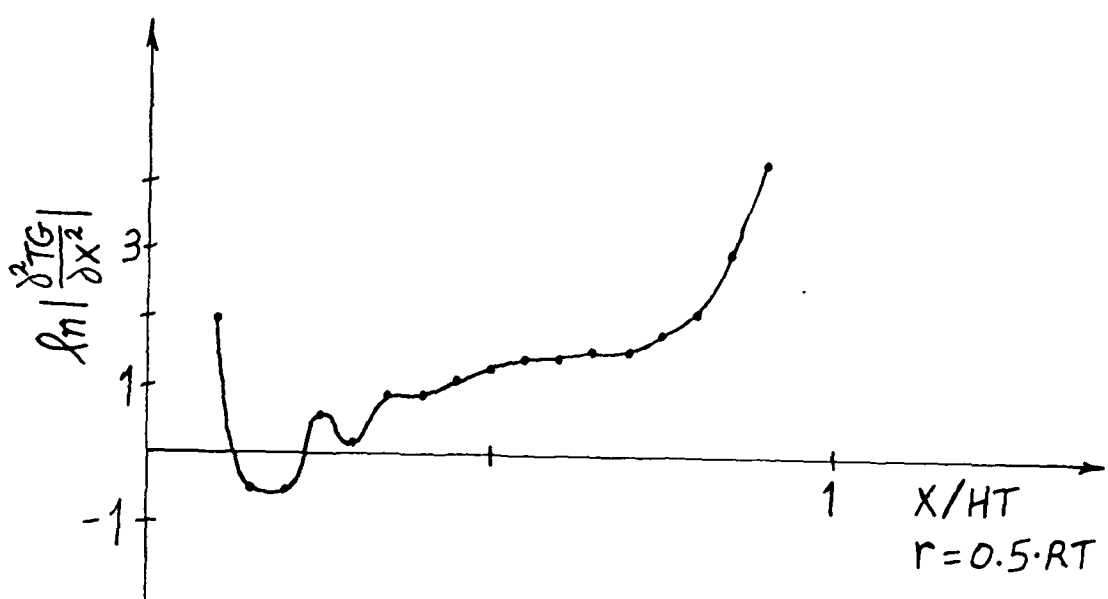
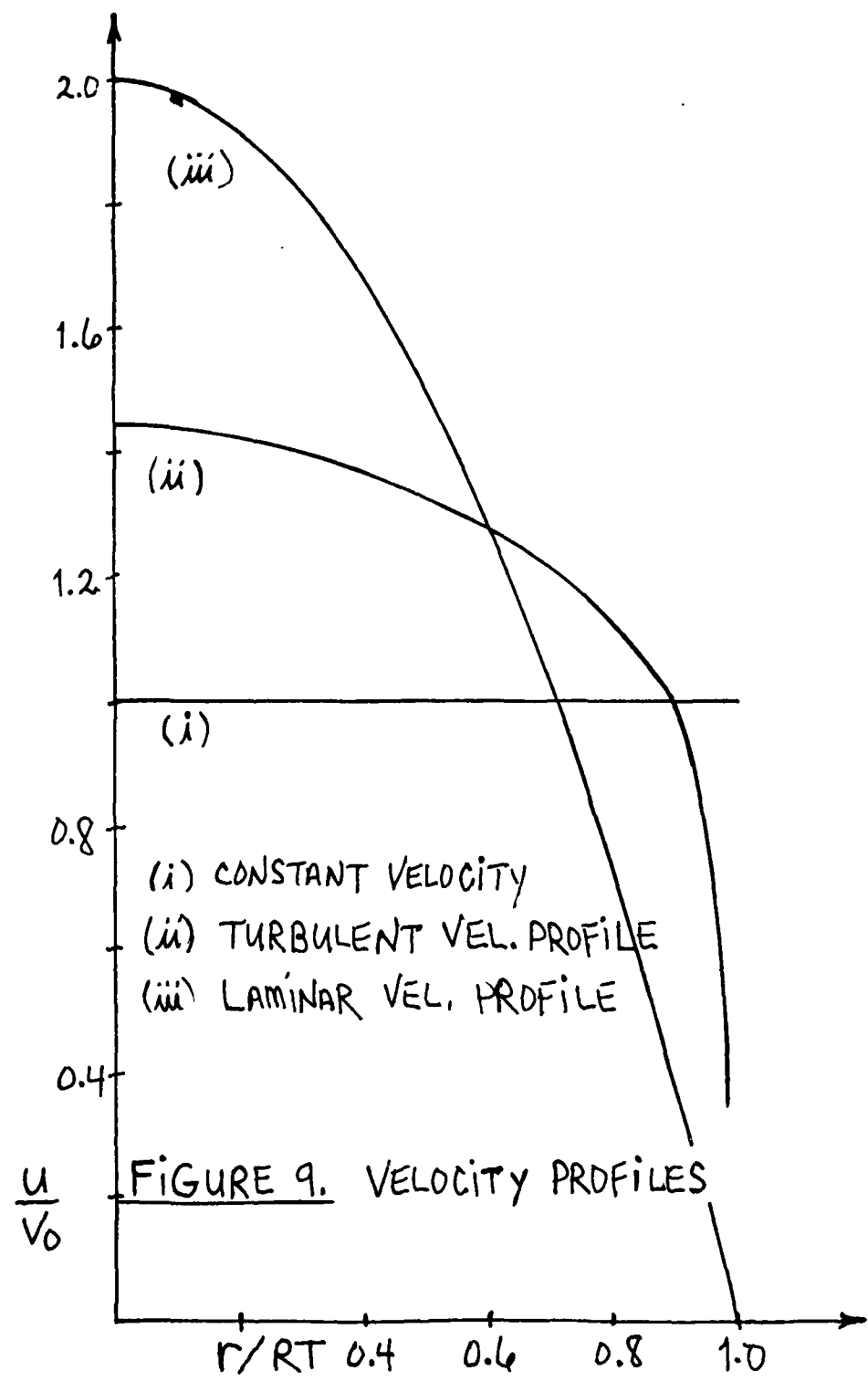
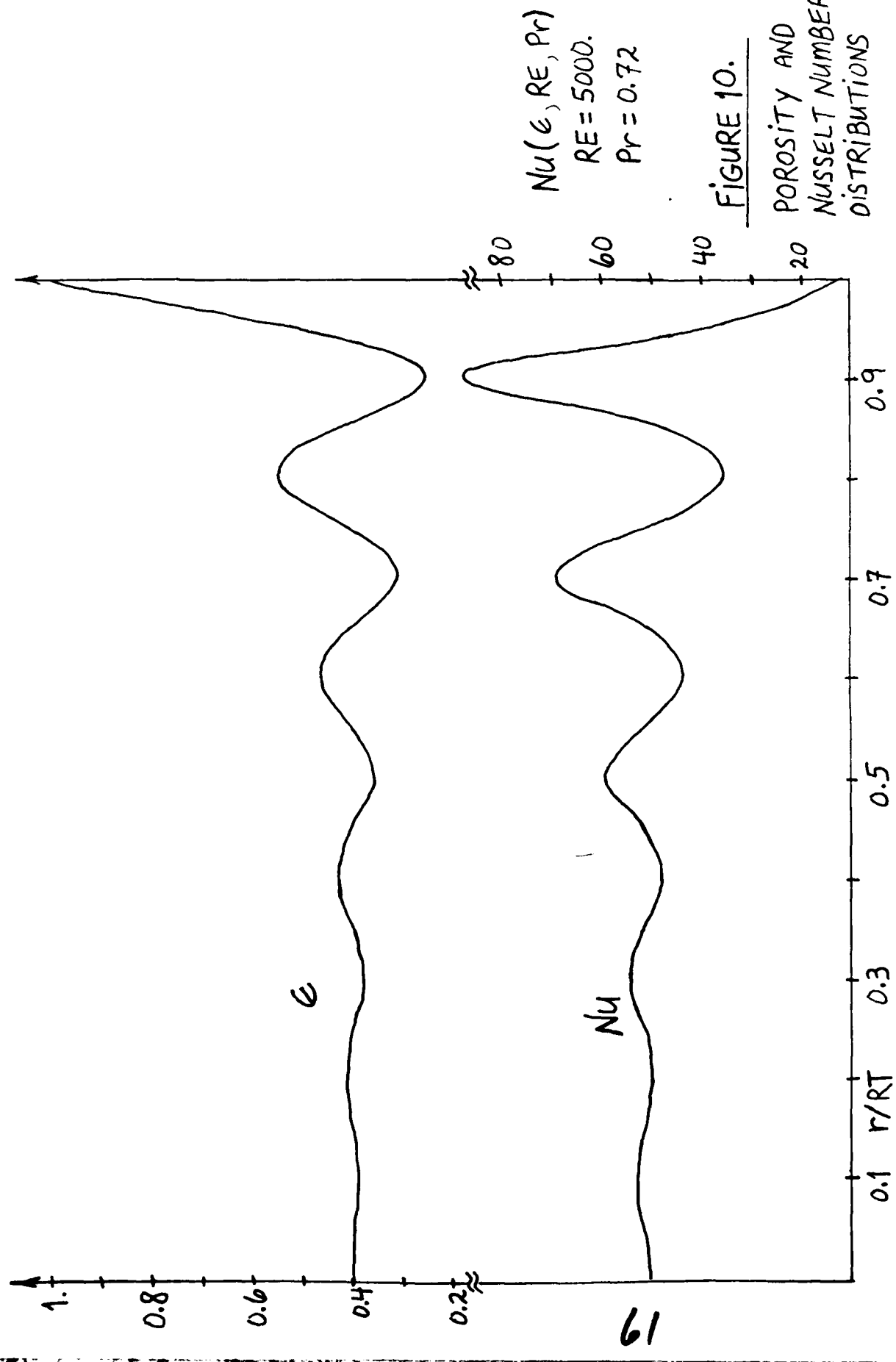


FIGURE 8. SECOND DERIVATIVES AS A FUNCTION OF POSITION





— CORRESPONDING NUMERICAL SOLUTION
WITHOUT AXIAL CONDUCTION
• CONSTANT SUPERFICIAL VELOCITY

2.0

RE = 4000.

PE \gg 1

Nu based on AVERAGE RE

X = HT

HT/DP = 20

RT/DP = 5

T_W = 20 °C

T₀ = 15 °C

1.8

1.6

1.4

$\frac{(T_G - T_0)}{(T_W - T_0)}$

1.2

1

1. r/RT

FIGURE 11. EFFECT OF α ON
TEMPERATURE PROFILE I

— — — CORRESPONDING NUMERICAL SOLUTION
WITHOUT AXIAL CONDUCTION
• TURBULENT SUPERFICIAL VELOCITY

$RE = 4000.$

$PE \geq 1$

Nu BASED ON AVERAGE RE

$X = HT$

$HT/DP = 20.$

$RT/DP = 5.$

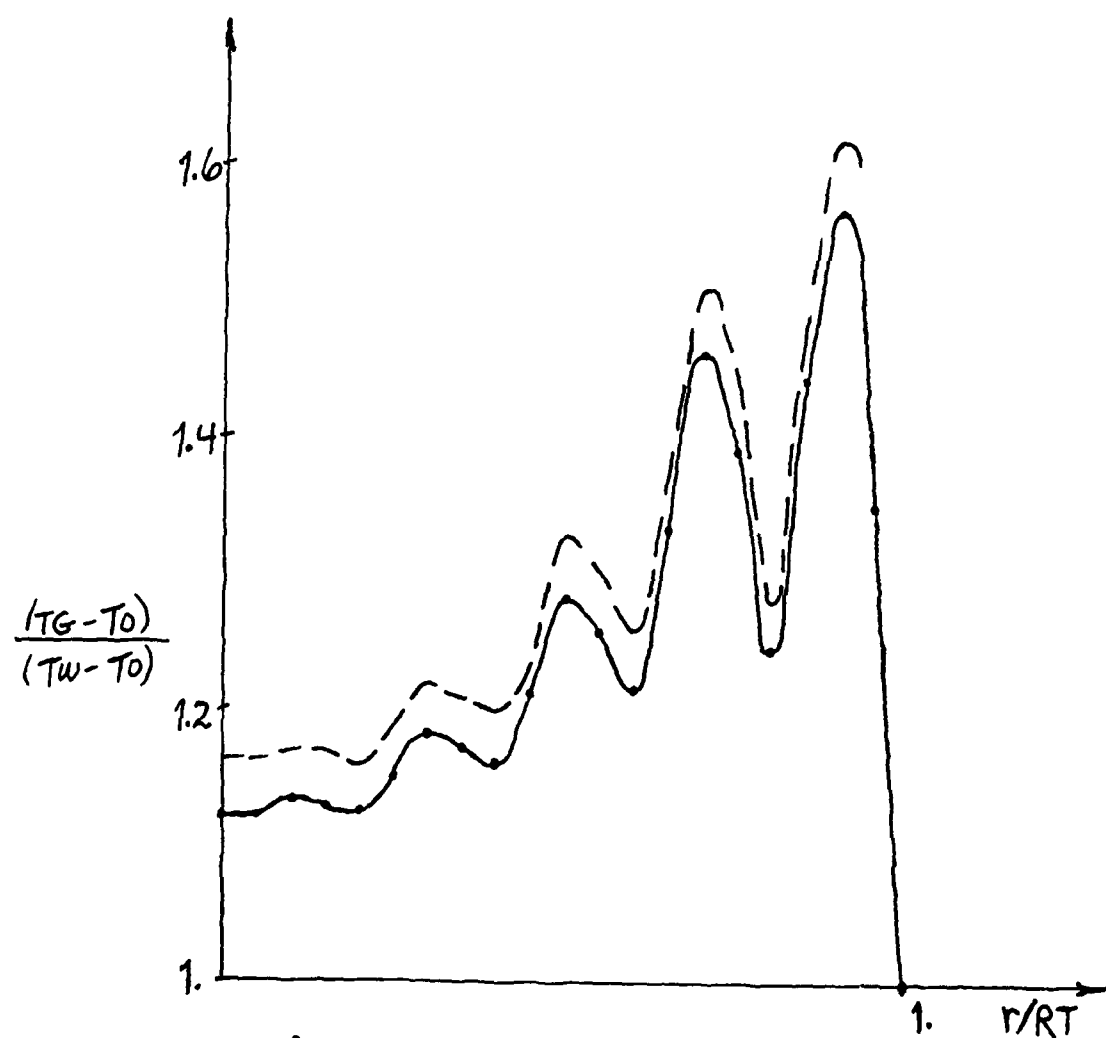


FIGURE 12. TEMPERATURE PROFILE II

- PARABOLIC SUPERFICIAL VELOCITY

$RE = 4000.$

$PE \gg 1$

NU BASED ON AVERAGE RE

$X = HT$

$RT/DP = 5.$

$HT/DP = 20.$

— CORRESPONDING
NUMERICAL SOL'N
WITHOUT AXIAL
CONDUCTION

$$\frac{T_G - T_0}{T_W - T_0}$$

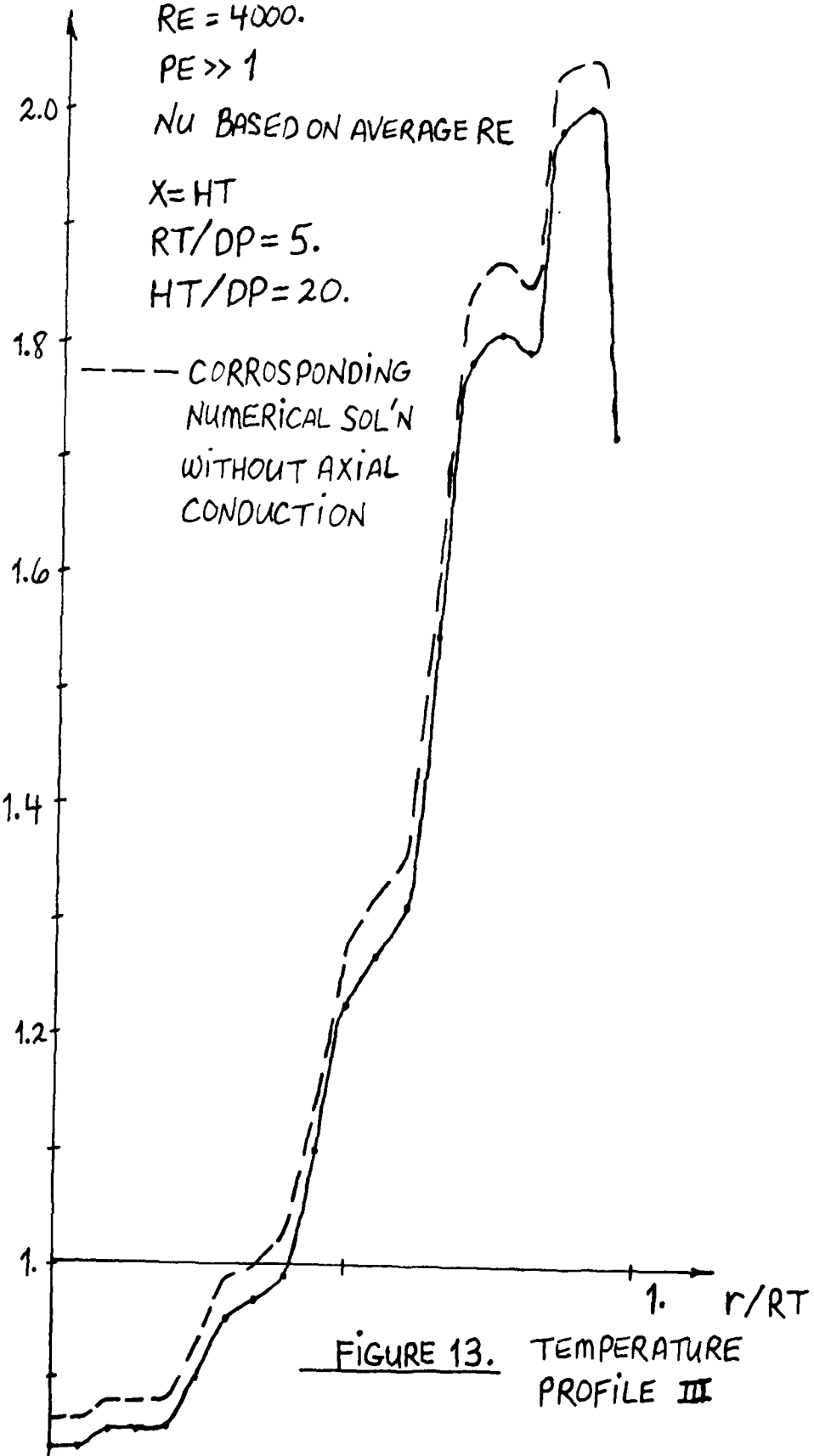
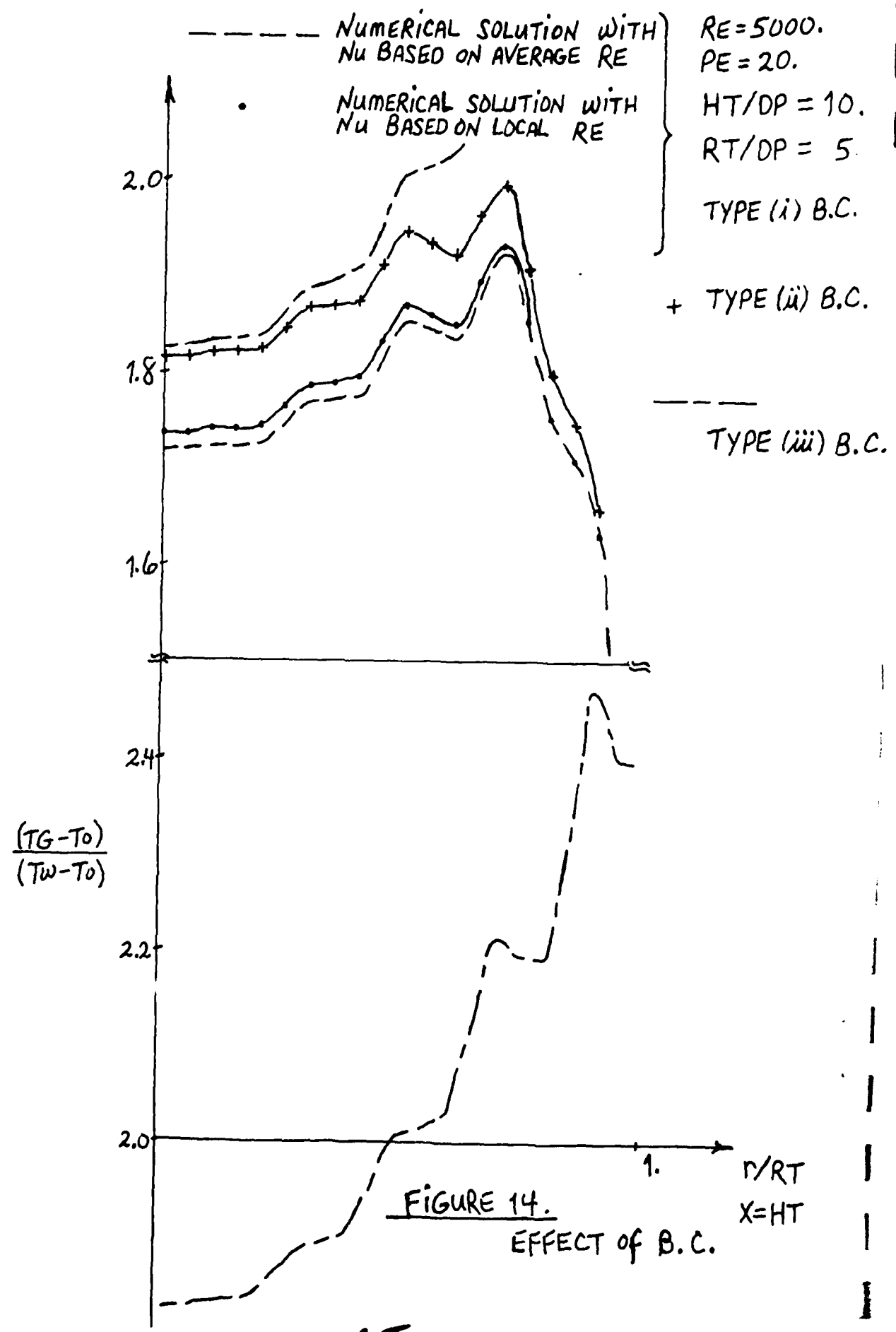


FIGURE 13. TEMPERATURE PROFILE III



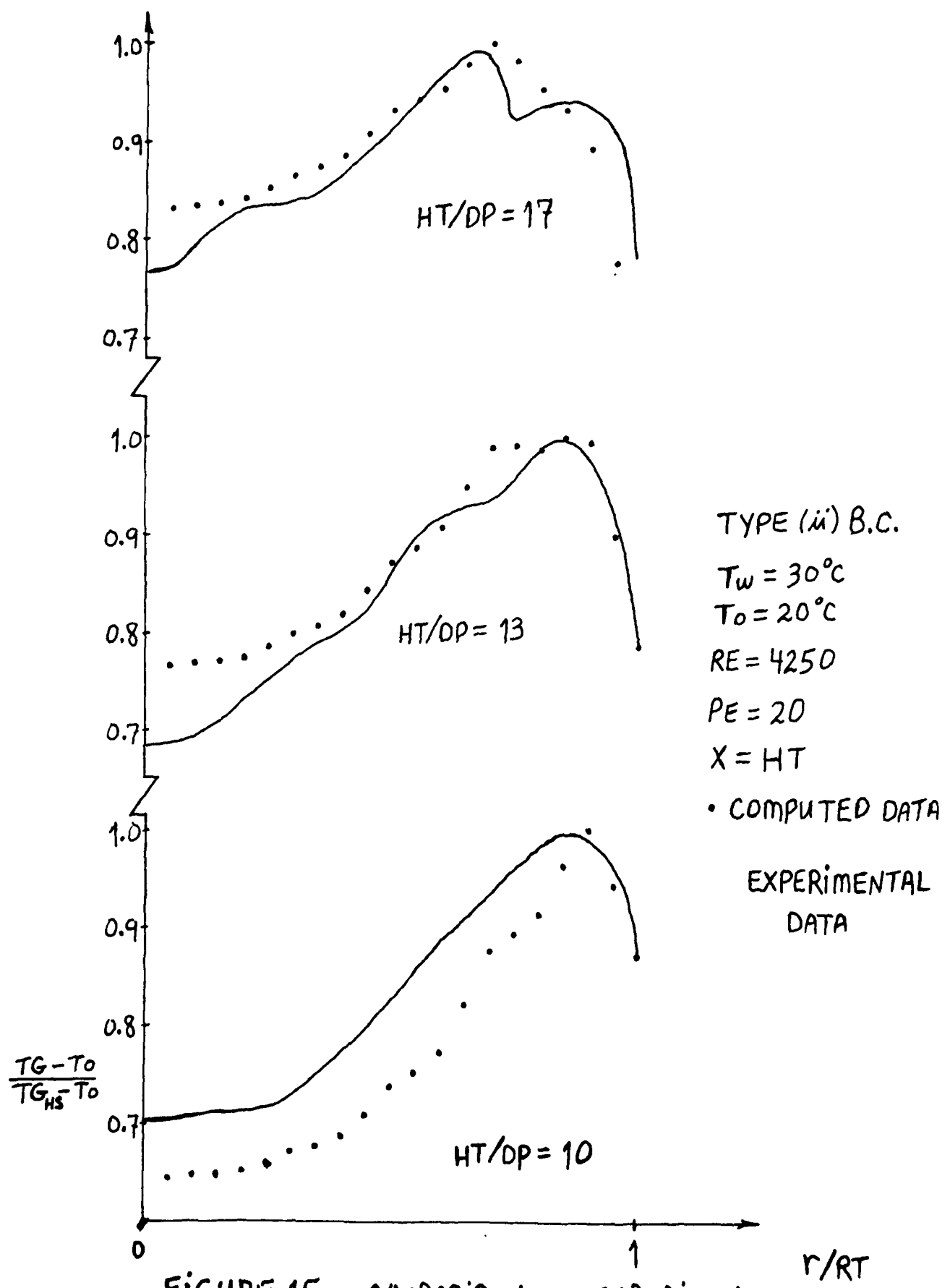


FIGURE 15. COMPARISON TO EXPERIMENTAL RESULTS

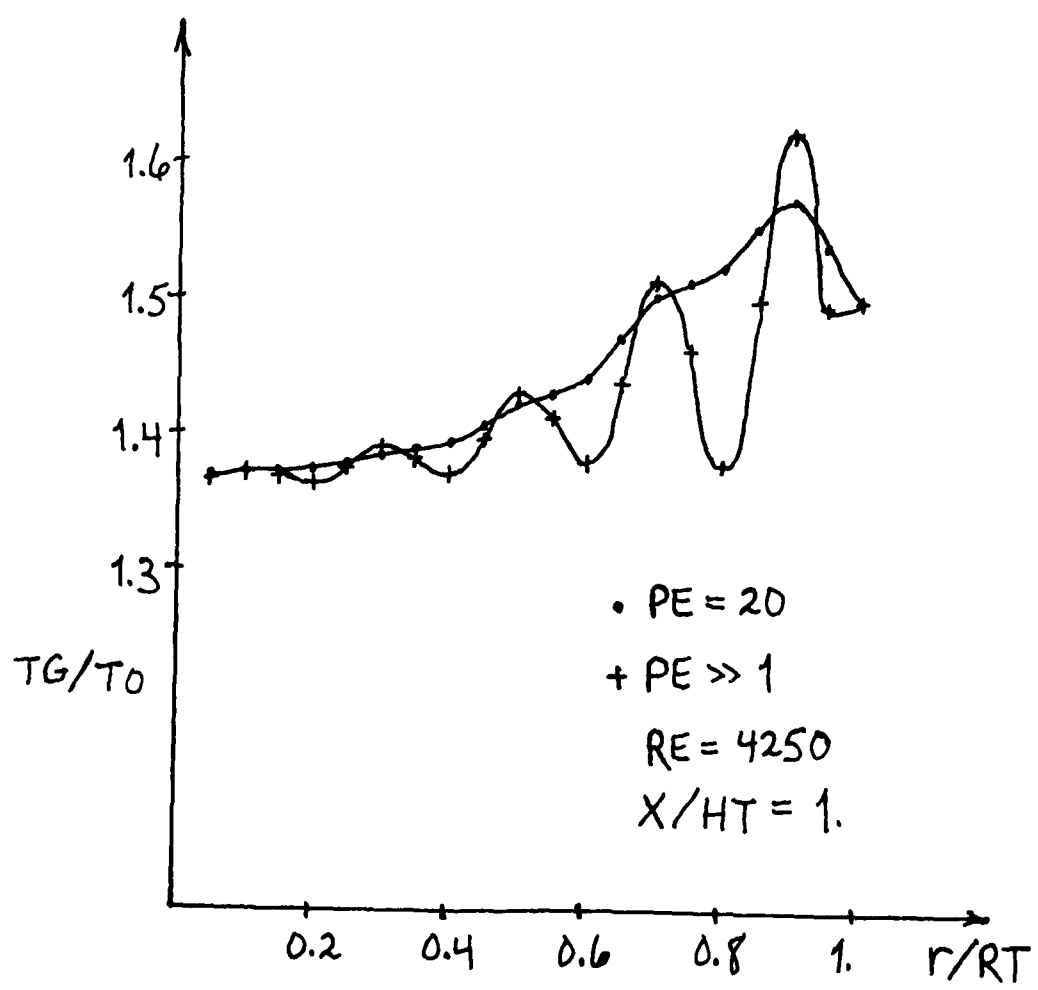
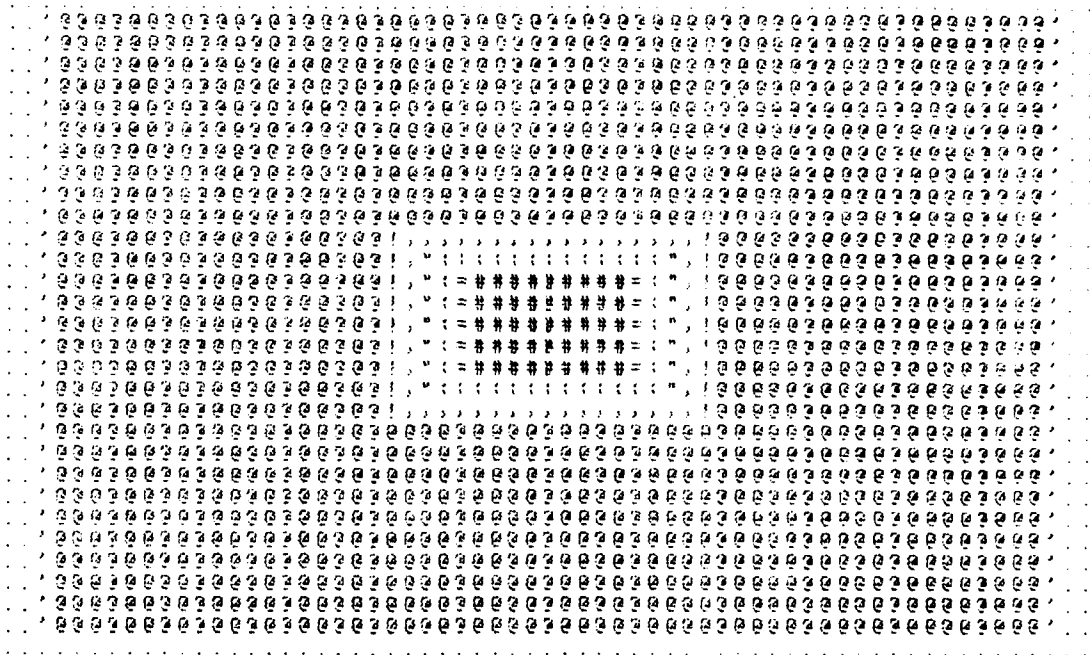


FIGURE 16. EFFECT OF PE

ISO-FRACTION DE VIDE



MINIMUM = 0.00000E+01 MAXIMUM = 4.00000E+01 CLASSES = 2.000

.	.LT.	2.000E-02	*	.LT.	2.200E-01
+	.LT.	4.000E-02	%	.LT.	2.400E-01
-	.LT.	6.000E-02	"	.LT.	2.600E-01
*	.LT.	8.000E-02	0	.LT.	2.800E-01
/	.LT.	1.000E-01	.	.LT.	3.000E-01
#	.LT.	1.200E-01	?	.LT.	3.200E-01
=	.LT.	1.400E-01	,	.LT.	3.400E-01
\$.LT.	1.600E-01	M	.LT.	3.600E-01
:	.LT.	1.800E-01	!	.LT.	3.800E-01
X	.LT.	2.000E-01	e	.LT.	4.000E-01

$RE = 4000,$

$HT/DP = 20,$

$RT/DP = 10,$

FIGURE 16.5

E DISTRIBUTION
FOR BLOCKAGE

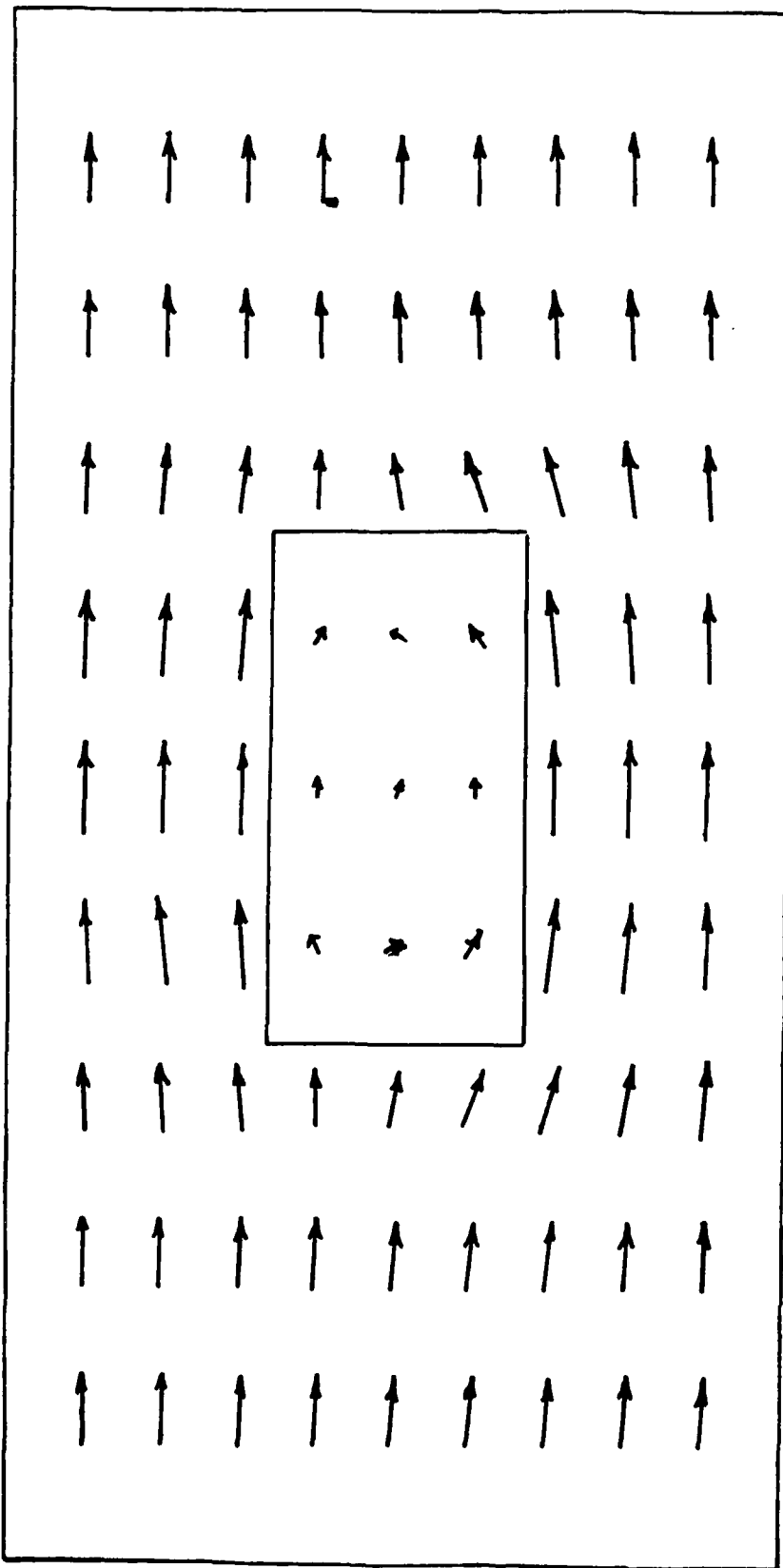


FIGURE 17. VELOCITY FIELD FOR BLOCKAGE

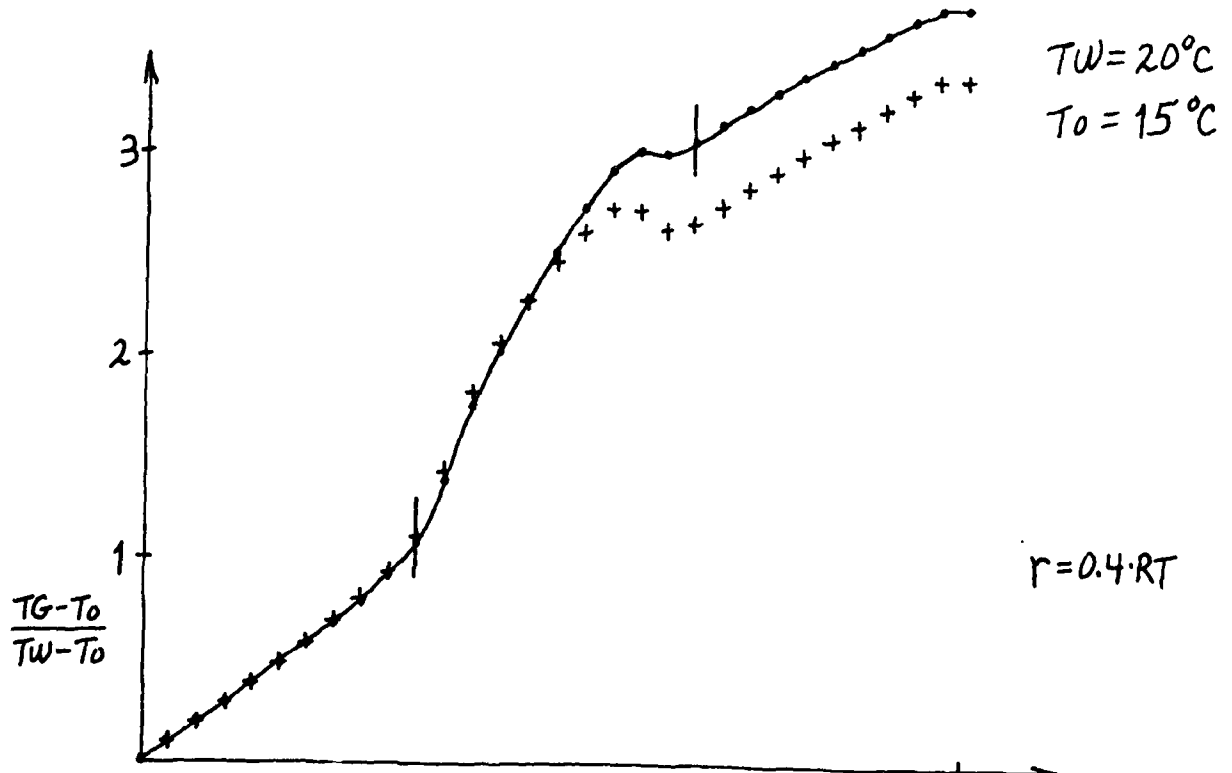
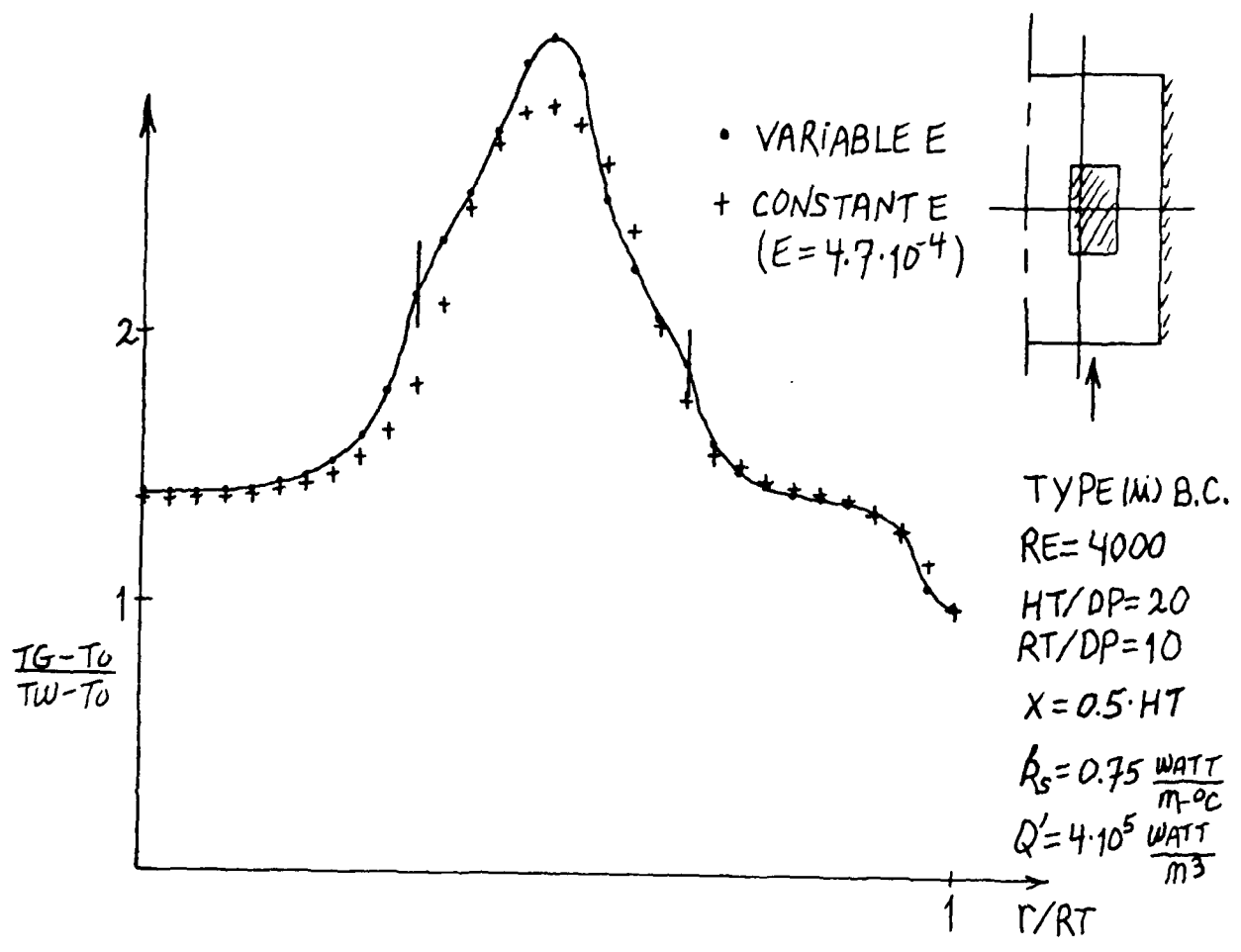


FIGURE 18. RADIAL AND AXIAL TEMP. PROFILES

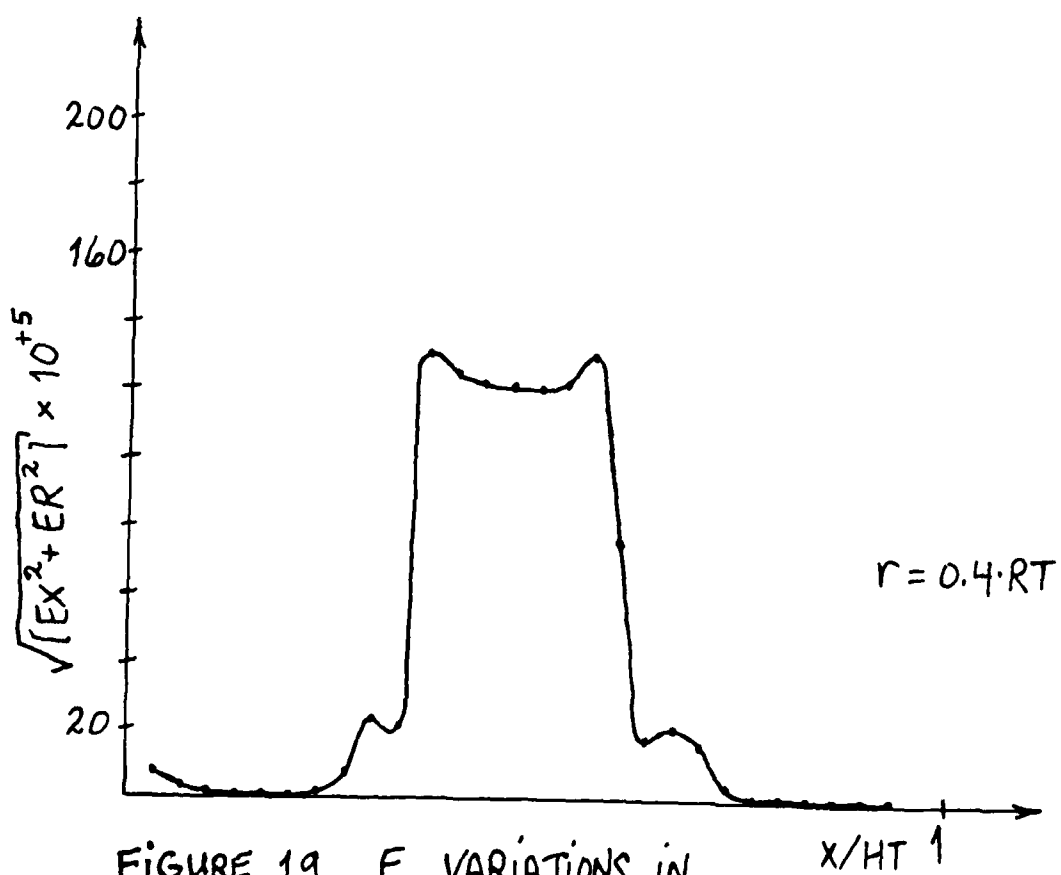
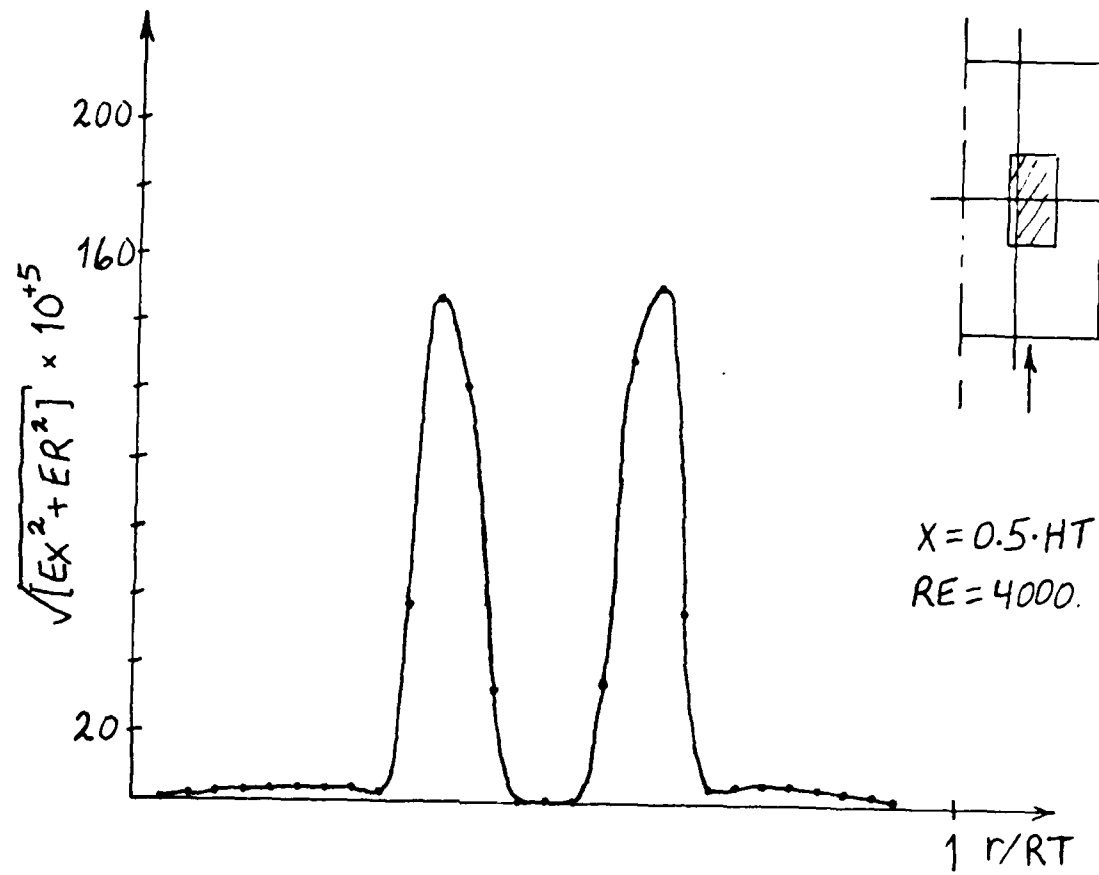
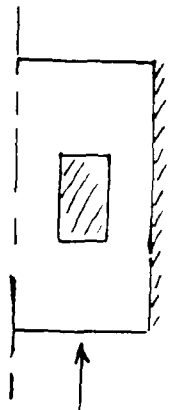


FIGURE 19. E VARIATIONS IN
X AND r



TYPE(ii) B.C.

$RE = 4000$.

$HT/DP = 20$.

$RT/DP = 10$.

$X = HT$

• $k_s = 0.75 \frac{\text{WATT}}{\text{m} \cdot ^\circ\text{C}}$

+ $k_s = 0.6$

○ $k_s = 0.4$

△ $k_s = 0.2$

VARIABLE E

$Q' = 4 \cdot 10^5 \frac{\text{WATT}}{\text{m}^3}$

$T_w = 20^\circ\text{C}$

$T_0 = 15^\circ\text{C}$

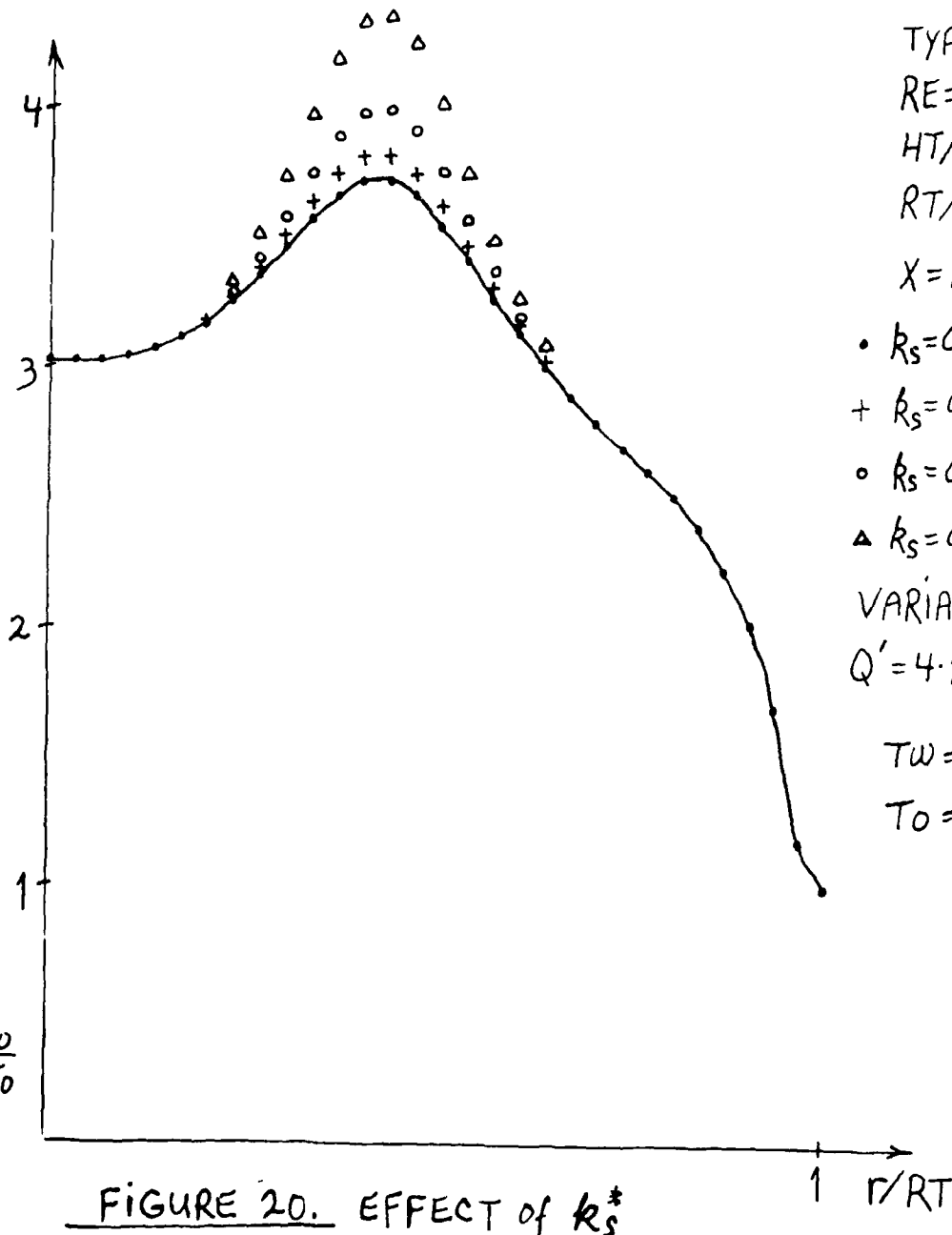


FIGURE 20. EFFECT of k_s^*

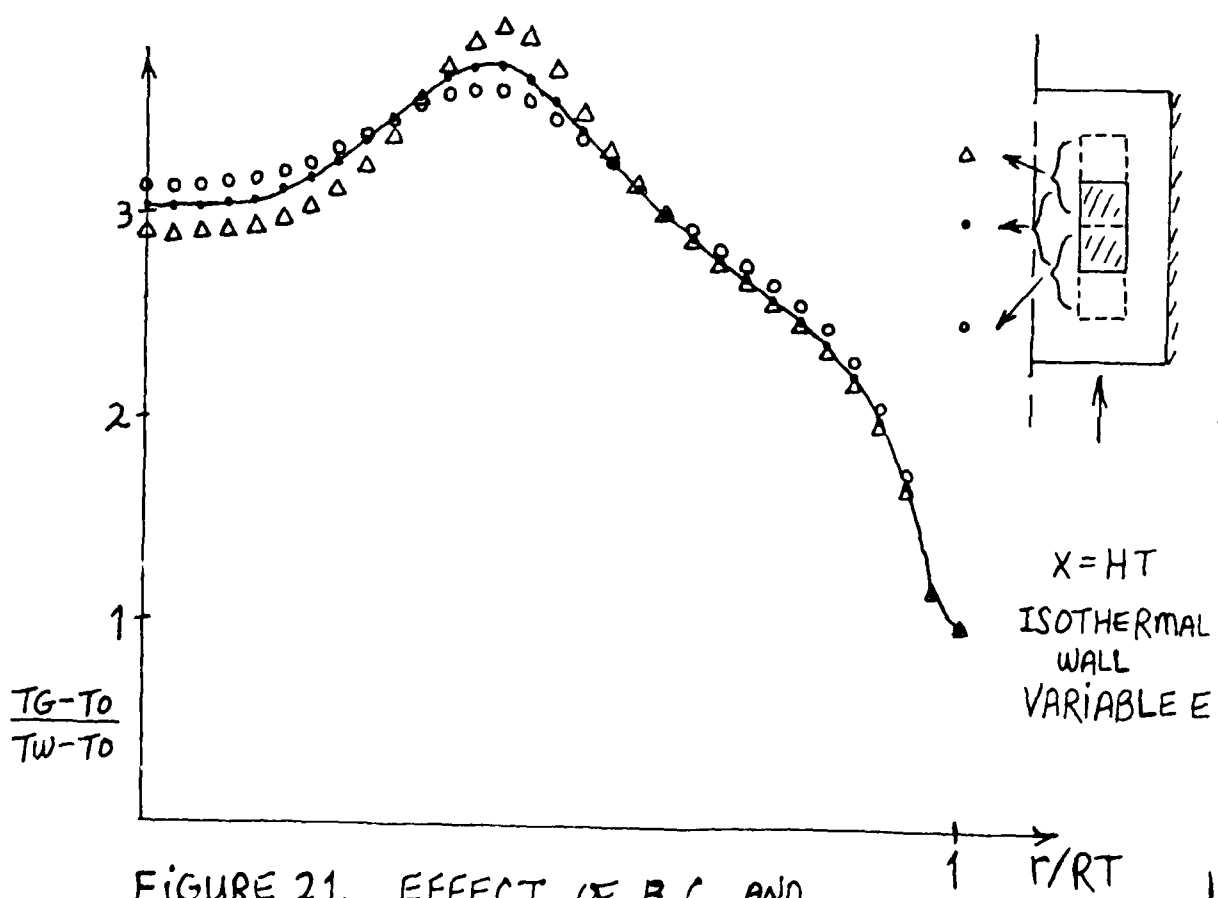
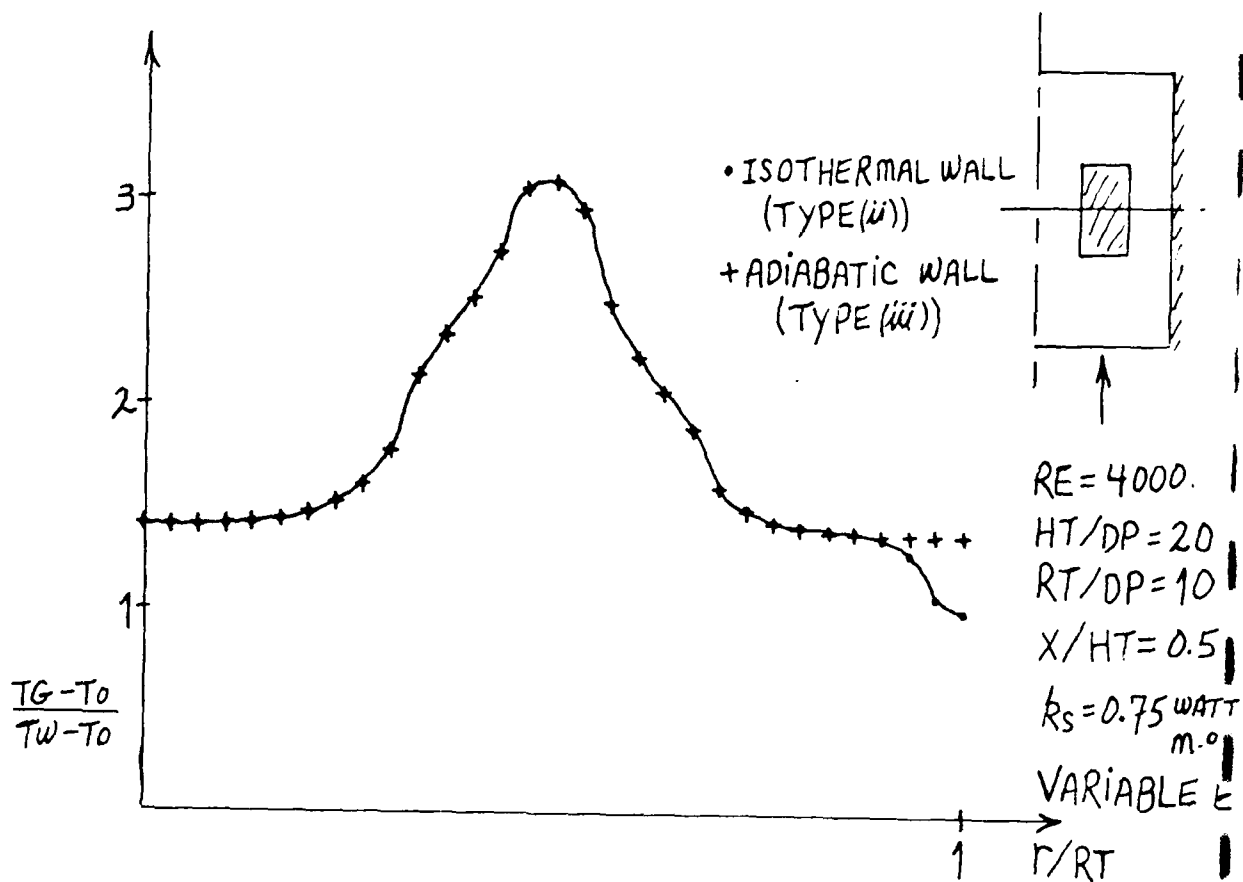


FIGURE 21. EFFECT OF B.C. AND POSITION OF BLOCKAGE.

END

DATE
FILMED

8-80

DTIC